Pedro Filipe Barros Silva

Development of a System for Automatic Plant Species Recognition

Departamento de Matemática
Faculdade de Ciências da Universidade do Porto
2013

Pedro Filipe Barros Silva

Development of a System for Automatic Plant Species Recognition

Tese submetida à Faculdade de Ciências da Universidade do Porto para obtenção do grau de Mestre em Engenharia Matemática

Departamento de Matemática
Faculdade de Ciências da Universidade do Porto
2013

”Es ist nicht genug zu wissen - man muss auch anwenden. Es ist nicht genug zu wollen - man muss auch tun.”, Johann Wolfgang von Goethe

Acknowledgments

This thesis was proposed by Prof. Doutor André R. S. Marçal in the context of the Master Programme in Mathematical Engineering of the Faculty of Science of University Porto and was developed under his supervision in the academic year 2012/2013.

I would like to thank Prof. Doutor André R. S. Marçal from the Mathematics Department of the Faculty of Science of University Porto for his support in the preparation of the paper "Evaluation of features for leaf discrimination", accepted to publication in the proceedings of the "International Conference on Image Analysis and Recognition".

I would also like to thank Prof. Doutor Rubim Manuel Almeida da Silva from the Biology Department of the Faculty of Science of University Porto for his help with the construction of the leaf database presented in this thesis, without which this entire work would not have been possible.

A further acknowledgement goes to Prof. Doutor Joaquim Fernando Pinto da Costa for his remarks on some aspect of the statistical analysis presented in this thesis.

At last but not less important, I thank my closest family members for their comprehension and support, not only during the writing of this thesis, but also along these five years of superior studies.

Abstract

The present work, titled "Development of a System for Automatic Plant Species Recognition", was developed in the academic year 2012/2013 in the context of the Master degree in Mathematical Engineering of the Faculty of Science, University of Porto.

Traditionally, the identification of plants has been done by specialized technicians called taxonomers. However, recent years have seen a growing trend in task automation, motivated by the development of increasingly competent information processing platforms, as well as ever more efficient algorithms.

The possibility of being able to identify plants through the automatic extraction of morphometric information from digital images of plant leaves is a matter of growing interest not only among specialists like biologists but also among laymen.

The development of a computer tool with these features is desirable in many contexts like for instance robotic agriculture. However, there are many other possible contexts and particular interest on the development of applications, which can be used on mobile devices, allowing for the in loco recognition of plant species by non necessarily skilled users, exists.

The main objectives of this thesis are to provide a general description of the problem of plant recognition through automatic extraction of morphometric information from leaf images, using of image and signal processing techniques, as well as to discuss the statistical properties of some of these methods in the context of a real database implementation.

This thesis ends with the presentation of a prototype system developed in Matlab® for the automatic identification of plants. A critical analysis of the main limitations of this kind of systems and the indication of future work possibilities is also provided.

Resumo

A presente dissertação, intitulada "Desenvolvimento de um Sistema para o Reconhecimento Automático de Espécies de Plantas", foi desenvolvida no ano letivo de 2012/2013 no âmbito do curso de mestrado em Engenharia Matemática da Faculdade de Ciências da Universidade do Porto.

Tradicionalmente, a identificação de plantas tem sido realizada por técnicos especializados chamados taxonomistas. Contudo, nos últimos anos, tem-se assistido a uma tendência crescente para a automação de tarefas, fruto do desenvolvimento de plataformas de processamento de informação cada vez mais competentes, bem como de algoritmos cada vez mais eficientes.

A possibilidade de poder reconhecer plantas com base em informação morfométrica obtida de forma automática através de imagens digitais de folhas é um assunto que motiva interesse junto de técnicos como biólogos, mas também junto de leigos. O desenvolvimento de uma ferramenta computacional com estas capacidades é desejável em variados contextos como, por exemplo, a agricultura robótica.

Contudo, diversos outros contextos existem, havendo nomeadamente interesse no desenvolvimento de atlas de plantas que possam ser carregados para dispositivos móveis, permitindo a identificação in loco de espécies vegetais por utilizadores que não necessitam inclusivamente de ser dotados de conhecimentos técnicos.

Este trabalho visa fornecer uma perspectiva global sobre o estado de arte do desenvolvimento de sistemas para o reconhecimento automático de plantas com base em técnicas de processamento de sinal e imagem, bem como analisar e discutir as propriedades estatísticas dos métodos mais utilizados para este fim no contexto de uma base de dados real.

A dissertação conclui com a apresentação de um protótipo em Matlab® para a identificação automática de plantas, com uma avaliação crítica das principais limitações deste tipo de sistemas, bem como com a indicação de possibilidades de trabalho futuro.

Zusammenfassung

Diese Abschlussarbeit mit dem Titel "Entwicklung eines Systems zur automatischen Erkennung von Pflanzenarten" wurde im akademischen Jahr 2012/2013 im Rahmen des Masterstudiengangs "Mathematische Ingenieurwissenschaft" der Wissenschaftlichen Fakultät der Universität Porto entwickelt.

Herkömmlich wurde die Pflanzenerkennung von Spezialisten ausgeführt. In den letzten Jahren sah man jedoch eine zunehmende Tendenz zur Automatisierung von menschlichen Tätigkeiten auftauchen, die von der Entwicklung ständig wachsender Informationsverarbeitungsplattformen und immer effizienteren Algorithmen vorangetrieben wird.

Die Möglichkeit, Pflanzen durch morphometrische Information zu erkennen, die automatisch von digitalen Bildern ihrer Blätter gesammelt worden ist, interessiert nicht nur Spezialisten wie Biologen sondern auch Laien. Die Entwicklung eines Computersystems mit diesen Funktionalitäten ist in verschiedenen Kontexten erwünscht wie z.B. in dem der robotischen Landwirtschaft.

Es gibt andere Zusammenhänge, in denen die Entwicklung von so einem System erwünscht ist - nämlich die Erstellung eines Pflanzenatlas, der als Anwendungssoftware in Smartphones benutzt werden kann. Dies könnte Benutzern, die nicht notwendigerweise fachspezifische Kenntnisse besitzen müssen, die Identifizierung von Pflanzenarten vor Ort ermöglichen.

Die Ziele dieser Arbeit bestehen darin, einen Überblick zum gegenwärtigen Forschungsstand der Systeme zur automatischen Erkennung von Pflanzen mit Basis auf Signal- und Bildverarbeitungstechniken zu geben, genauso wie eine Analyse und Diskussion der statistischen Eigenschaften der bedeutendsten Methoden durchzuführen.

Diese Masterarbeit schließt mit der Darstellung eines in Matlab entwickelten Prototypen zur automatischen Pflanzenerkennung, mit der kritischen Auswertung der wichtigsten Hindernisse und mit der Angabe möglicher künftiger aufbauender Arbeiten ab.

Contents

Abstract **II**

Resumo **III**

Zusammenfassung **IV**

List of Tables **VII**

List of Figures **IX**

Acronyms **X**

1 Introduction **1**

2 State of the Art **3**

2.1 Leaf shape analysis 3

2.1.1 Elliptic Fourier Descriptors 5

2.1.2 Contour signatures 18

2.1.3 Landmarks 20

2.1.4 Shape features 21

2.1.5 Polygon fitting and fractal dimensions 24

2.2 Venation extraction and analysis 25

2.3 Leaf margin analysis 26

2.4 Leaf texture analysis 27
2.5 Other methods 28
2.6 Automatic Classification Systems 29
2.7 Overview 31

3 Plant Recognition System **32**

3.1 Database 35
3.2 Statistical Analysis 37
3.2.1 Elliptic Fourier Analysis 37
3.2.2 Shape features 45
3.2.3 Texture features 50
3.3 Conclusions 53

4 Computational tool in Matlab **54**

4.1 Creating a new database 55
4.2 Classifying a new observation 57
4.3 Limitations 58

5 Conclusions **63**

5.1 Contributions 63
5.2 Future Work 64

References **65**

List of Tables

2.1 Common shape features for leaf shape analysis. 23

2.2 Common texture analysis features based on statistical moments. 27

3.1 Leaf database: plant species (class) and number of specimens available (#). . 36

3.2 EFA: Summary of classification results. 43

3.3 EFD: Confusion matrix for Linear Discriminant Analysis. 44

3.4 Shape features: Pearson's correlation. 45

3.5 Shape features: Summary of classification results. 48

3.6 Shape features: Confusion matrix for Linear Discriminant Analysis. 49

3.7 EFA and texture features: Summary of classification results. 51

3.8 Shape and texture features: Summary of classification results. 51

3.9 Shape and texture Features: Confusion matrix for Linear Discriminant Analysis. 52

List of Figures

2.1 Example of shape variation in specimens of *Quercus suber*. 4

2.2 Example of different leaf shapes (10 classes). 4

2.3 Illustration of the grid intersection quantization method. 5

2.4 Chain code link labels. 7

2.5 Example of chain code codification. 7

2.6 Illustration of the Elliptic approximation of a contour. 13

2.7 Reconstruction of a specimen of *acer palmatum* using EFD. 17

2.8 Centroid distance signature of a leaf of *acer palmatum*. 18

2.9 Problem of self-intersection in a leaf of *populus alba*. 19

3.1 Diagram of an automatic plant recognition system. 32

3.2 Example of good image acquisition practice. 33

3.3 Example of a segmented image. 34

3.4 Leaf database overview - 40 class types. 35

3.5 EFA: Cumulative explained variability by principal components. 39

3.6 EFA: Principal Component Analysis Weights. 40

3.7 EFA: Class mean in the principal component space. 41

3.8 EFA: Hierarchical Clustering with Ward's Linkage. 41

3.9 Shape features: Cumulative explained variability by principal components. . 46

3.10 Shape features: Class mean in the principal component space. 47

3.11 Shape features: Hierarchical Clustering with Ward's Linkage. 47

4.1 Computational Tool: Main Window. 54

4.2 Computational Tool: New Database Window. 55

4.3 Computational Tool: Classifying a new leaf (good result). 58

4.4 Computational Tool: Classifying a new leaf (wrong result). 59

4.5 Computational Tool: Classifying a new leaf (wrong result). 60

4.6 Computational Tool: Classifying a leaf of a plant not present in the database. 61

4.7 Computational Tool: Classifying a leaf of a plant not present in the database. 61

Acronyms

CDS Centroid Distance Signature

EFA Elliptic Fourier Analysis

EFD Elliptic Fourier Descriptors

KNN K-Nearest Neighbours

LDA Linear Discriminant Analysis

PCA Principal Component Analysis

Chapter 1

Introduction

Plant recognition has traditionally been done by specialized taxonomists, who use several plant attributes like the general shape of plant leaves, the colour of flowers and the shape and colour of fruits, among other criteria, to distinguish between different species.

The development of computer technologies and image and signal processing techniques has been motivating a growing trend to automation and traditional methodologies are being increasingly replaced by novel methods both in industry, applied research and other sectors of society. The problem of plant recognition is not an exception.

Currently, there is a shortage on taxonomists and the financial expenditure of this kind of specialized services has been raising [5]. On the other hand, increasingly more sophisticated mobile phones are becoming a commonplace in many people's lives and interest in the development of plant identification applications has been reported. The development of an automatic system for plant recognition through leaf images could provide both specialists and non-specialists with a valuable tool with reduced or no costs.

Such a system would have many advantages over the traditional approaches, namely: it could avoid subjective errors done by human operators, as such a system would only use quantitative analysis; it could provide with a very inexpensive way of studying and identifying leaves, as no special hardware besides a regular camera and computer processing technology, nowadays ubiquitous, would be required and it could allow for the maintenance of large and possibly specialized leaf databases with reduced effort.

On the other hand, the digital approach to leaf classification creates many challenges related with the effectiveness of the available image processing algorithms and with the complexness of the problem itself. Deformed specimens, problems with contour definition, intersection problems arising by either inappropriate digitalization or complex leaf geometry, alterations

in leaf aspect, occurring for instance in consequence of contamination by diseases, insect's actions or generic mechanical damage are among some of them [5].

Some of these problems are yet to be overcome and will probably be around for a long time, if they are ever to be solved completely. However, despite their existence, good results on the use of automatic techniques for plant recognition system have been systematically reported along the years.

The main objective of this thesis is to provide a thorough review of the current state of image-based plant recognition techniques and systems. Further objectives are to provide an empirical statistical analysis of some of these methods in a real world setting using an image database of collected leaves and to compare two of the most used techniques. The last objective consists of the creation of a working prototype for plant leaf recognition with use of Matlab ®.

This thesis is organized in five chapters:

- Chapter 1 is this introduction.
- Chapter 2 provides a brief but insightful discussion of the state of the art of the different methods for leaf analysis based in shape, venation, margin and texture properties, referring also some of the most recent automatic classification systems presented to the scientific community.
- Chapter 3 presents the results of the application of the techniques discussed in Chapter 2 in a real world setting.
- Chapter 4 documents a fully computational tool for automatic plant recognition.
- Chapter 5 is the conclusion of this thesis and it includes a general overview of the work done and the presentation of possible guidelines for future work.

The development of the present thesis lead to the publication of the paper "*Evaluation of features for leaf discrimination*" in the proceedings of the "International Conference on Image Analysis and Recognition" (ICIAR 2013).

Chapter 2

State of the Art

In this chapter, the state of the art for automatic plant classification using image processing techniques is presented, starting with a general, yet brief discussion of leaf analysis methods according to different leaf properties, focusing on particularly relevant techniques. Familiarity with key concepts of digital image processing, Fourier analysis, vector analysis and linear algebra is assumed.

Over the past few decades, several methods for leaf analysis have been developed which gathered different levels of attention considering their scope of application and their ability of computer implementation. Some of those are here presented, using for this purpose the information collected on the most recent review article on this subject to provide the reader with an overview of each existent technique and its applicability [5].

Human operators (botanists) use many different plant and leaf characteristics in their morphological and taxonomical research. It is generally considered that the most useful characteristics for plant recognition are the two-dimensional outline shape of either leaves or petals, as well as the leaf's vein network structure and the leaf margin's characters. Automatic systems for plant classification using digital image processing techniques are generally based in one or more of these characteristics.

2.1 Leaf shape analysis

The outline of leaf shape is the leaf analysis method which has been by far receiving the most attention when applying computational techniques to botanical image processing. In fact, researchers believe that leaf shape contains the most discriminant power, given that most plants exhibit a characteristic leaf shape [5]. That is, although considerable high variation

may be found in detail among the leaves of a certain plant, the concept of average leaf shape can be used to distinguish a particular plant from another plant. This belief is also related with the fact that differences in margin characters or vein structure are more subtle and of more difficult automatic computer processing than differences in shape. Figures 2.1 and 2.2 show leaves retrieved from the database constructed in the context of this thesis (see Chapter 3) to illustrate these assumptions.

Figure 2.1: Example of shape variation in specimens of *Quercus suber*.

Figure 2.2: Example of different leaf shapes (10 classes).

In terms of automatic computer processing, many factors are in favour of the use of leaf shape analysis, namely the existence of several shape analysis techniques which have been successfully used in various contexts and which can be straightforwardly implemented.

Some different methods for leaf shape analysis based on Fourier analysis, contour signatures, landmark analysis, shape features, fractal dimension and texture analysis are next presented and discussed.

2.1.1 Elliptic Fourier Descriptors

One of the most well-known frequency domain based representations of closed contours in digital image processing are the Elliptic Fourier Descriptors (EFD). This technique was first introduced in 1982 by Kuhl and Giardina [19] and uses the concept of chain code, which was originally proposed in 1974 by Freeman [10]. The objective of both chain codes and EFD is to provide an adequate approximation of a certain shape which can be easily processed in digital computers.

Firstly, the mathematical details of this shape analysis method are presented. Secondly, an overview of its use in the context of plant automatic classification systems is provided.

Consider a simple curve in two dimensions and superimpose a uniform, square grid, like depicted in Figure 2.3.

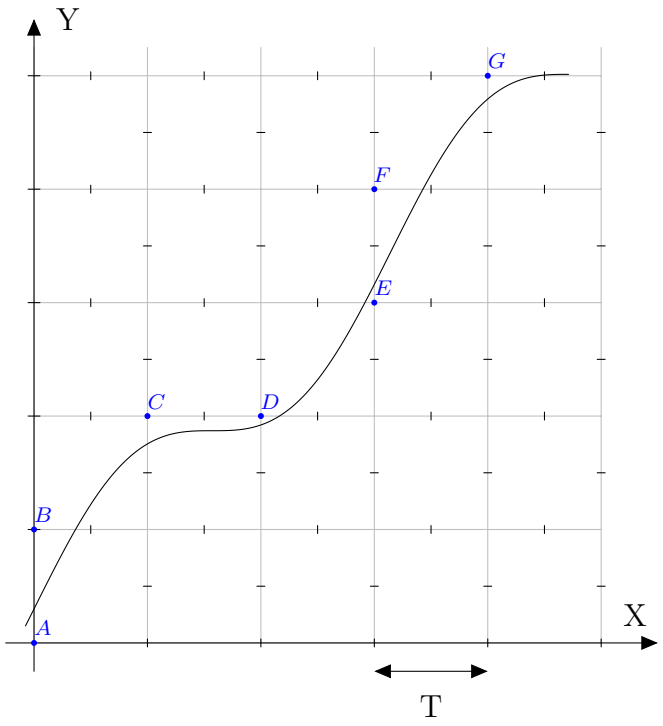

Figure 2.3: Illustration of the grid intersection quantization method.

It is possible to identify an X-Y coordinate system with the considered grid, such that every node on the grid can be given in terms of discrete coordinates (mT, nT), where $m, n \in \mathbb{Z}$ and T is the distance between adjacent grid lines. The parameter T can in this context be understood as a mere scale factor, meaning that the coordinates of the nodes can be simplified to (m, n). Given this coordinate system, an approximation to the given curve can now be derived by selecting any sequence of grid nodes, which are considered to lie

the closest with respect to some criterion, to the given curve. There are several criteria to determine which grid nodes lie the closest to a curve. The scheme associated with the chain code system is known as *intersection quantization*.

Intersection quantization establishes the following rule for node selection: trace the curve from its initial point to its endpoint and whenever t and m verify $x(t) - mT = 0$, select n such that $(n - \frac{1}{2})T < y(t) \leq (n + \frac{1}{2})T$; analogously, whenever $y(t) - nT = 0$, select m such that $(m - \frac{1}{2})T < x(t) \leq (m + \frac{1}{2})T$.

Geometrically, this methods means that one should identify any point on the curve which x or y coordinate is an integer multiple of T, i.e., consider all intersections of the curve with all the lines parallel to $x = T$ and $y = T$. For each of these intersection points, let us say $P = (\hat{x}, \hat{y})$, if $\hat{x}$ is an integer multiple of T, determine the grid node $N = (m, n)$ such that $\hat{x} \in \mathcal{V}_{\frac{1}{2}}(n)$; and if $\hat{y}$ is an integer multiple of T, determine the grid node $N = (m, n)$ such that $\hat{y} \in \mathcal{V}_{\frac{1}{2}}(m)$, where $\mathcal{V}_\alpha$ designates the usual notion of unidimensional neighbourhood of radius α.

The geometric explanation given above clearly shows why this approximation method is called *intersection quantization*. The nodes generated by the application of this method to the curve depicted in Figure 2.3, labeled as A, B, C, D, E, F and G, provide us now with a path (linear piecewise continuous function), ABCDEFG, which approximates the given curve.

Let us analyse some properties of any path derived with the intersection quantization method. It is obvious that any link in such a path can only have two possible lengths, either T or $T\sqrt{2}$, respectively if the link traverses the grid horizontally/vertically or diagonally. On the other hand, for each internal node, i.e., excluding endpoints, both its successor and predecessor are one of its eight possible neighbours (adjacent grid nodes).

These properties motivate the definition of chain code. A chain code V of length K is a path $V = a_1\, a_2\, a_3\, \ldots\, a_K$, where each link a_i is codified as an integer number between 0 and 7. Considering an usual Cartesian referential, each link a_i describes an angle of $\frac{a_i \pi}{4}$ radians with Ox. Like previously remarked, T is just a scale factor, so each link's length can be normalized to be 1 or $\sqrt{2}$, depending, respectively, on whether a_i is an even or an odd number. Figure 2.4 presents the codification dictionary given by a chain code contour approximation and Figure 2.5 illustrates the concept of contour approximation using Freeman's chain code considering the curve depicted in Figure 2.3.

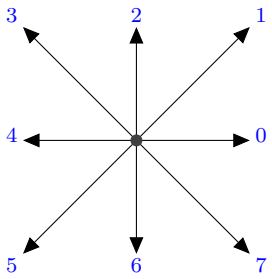

Figure 2.4: Chain code link labels.

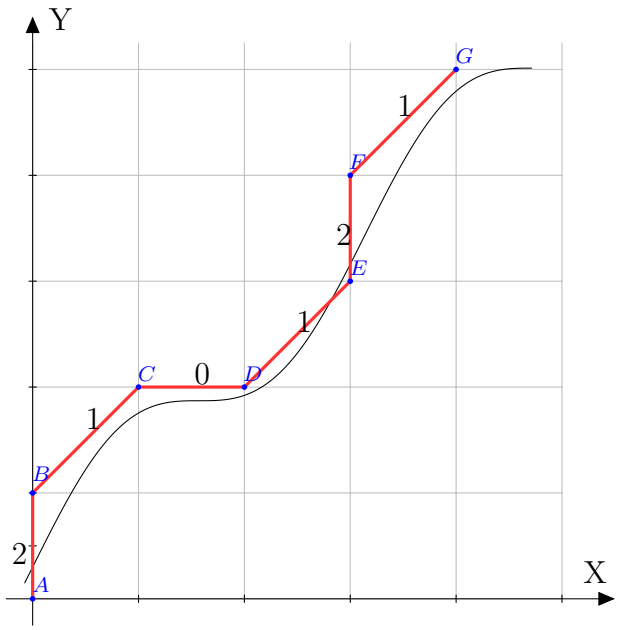

Figure 2.5: Example of chain code codification.

According to Figure 2.5, the chain code for the curve in Figure 2.3 is $V = 210121$ (assuming A as starting point and time increasing to the right side).

Now, imagining a point running through a **closed contour** in an infinite cycle, it is easy to acknowledge that a chain code can be suitably represented as a Fourier series, given the fact that the code repeats itself on successive traversals of the contour. Assuming that the point traverses the contour at constant speed, the time needed to traverse a particular link a_i is then

$$\Delta t_i = 1 + \left(\frac{\sqrt{2}-1}{2}\right)(1-(-1)^{a_i}).$$

With this in mind, the necessary time to traverse the first p links in the chain code can be defined as

$$t_p = \sum_{i=1}^{p} \Delta t_i.$$

According to this definition, the basic period of a chain code of length K is $T = t_K$. The changes in x and y coordinates projections of the chain code as the link a_i is being traversed are defined as

$$\Delta x_i = \text{sgn}(6 - a_i) \cdot \text{sgn}(2 - a_i)$$
$$\Delta y_i = \text{sgn}(4 - a_i) \cdot \text{sgn}(a_i),$$

where sgn stands for the *signal function*, i.e., $\text{sgn}(\mathbb{R}^+) = 1$, $\text{sgn}(\mathbb{R}^-) = -1$ and $\text{sgn}(0) = 0$. Locating the starting point of the chain code arbitrarily at the origin, the projections on x and y of the first p traversed links of the chain are respectively given by

$$x_p = \sum_{i=1}^{p} \Delta x_i \qquad \text{and} \qquad y_p = \sum_{i=1}^{p} \Delta y_i.$$

The Fourier series expansion of both x and y projections of the chain code of the entire contour can now be considered. Considering, for example, the x projection, its Fourier series expansion may be written as

$$x(t) = A_0 + \sum_{n=1}^{+\infty} a_n \cos\left(\frac{2n\pi t}{T}\right) + b_n \sin\left(\frac{2n\pi t}{T}\right),$$

where $A_0 = \frac{1}{T}\int_0^T x(t)\text{dt}$, $a_n = \frac{2}{T}\int_0^T x(t)\cos\left(\frac{2n\pi t}{T}\right)\text{dt}$ and $b_n = \frac{2}{T}\int_0^T x(t)\sin\left(\frac{2n\pi t}{T}\right)\text{dt}$.

As $x(t)$ is a piecewise linear and continuous function $\forall t$, the Fourier coefficients corresponding to the nth harmonic can be easily found.

Let us consider the time derivative $\dot{x}(t)$ of $x(t)$. This function consists of the sequence of piecewise constant derivatives $\frac{\Delta x_p}{\Delta t_p}$ associated with each time interval $]t_{p-1}, t_p[$ for $p \in \{1, \ldots, K\}$. The time derivative function is itself a periodic function with period T, which means that it can also be represented as a Fourier series

$$\dot{x}(t) = \sum_{n=1}^{+\infty} \alpha_n \cos\left(\frac{2n\pi t}{T}\right) + \beta_n \sin\left(\frac{2n\pi t}{T}\right), \tag{2.1}$$

where $\alpha_n = \frac{2}{T}\int_0^T \dot{x}(t)\cos\left(\frac{2n\pi t}{T}\right)\text{dt}$ and $\beta_n = \frac{2}{T}\int_0^T \dot{x}(t)\sin\left(\frac{2n\pi t}{T}\right)\text{dt}$.

Given the fact that $\dot{x}(t)$ is a piecewise constant function, α_n and β_n can be written as

$$\alpha_n = \frac{2}{T}\sum_{p=1}^{K}\frac{\Delta x_p}{\Delta t_p}\int_{t_{p-1}}^{t_p}\cos\left(\frac{2n\pi t}{T}\right)\mathrm{dt} = \frac{1}{n\pi}\sum_{p=1}^{K}\frac{\Delta x_p}{\Delta t_p}\left[\sin\left(\frac{2n\pi t_p}{T}\right)-\sin\left(\frac{2n\pi t_{p-1}}{T}\right)\right]$$

$$\beta_n = \frac{2}{T}\sum_{p=1}^{K}\frac{\Delta x_p}{\Delta t_p}\int_{t_{p-1}}^{t_p}\sin\left(\frac{2n\pi t}{T}\right)\mathrm{dt} = \frac{1}{n\pi}\sum_{p=1}^{K}\frac{\Delta x_p}{\Delta t_p}\left[\cos\left(\frac{2n\pi t_p}{T}\right)-\cos\left(\frac{2n\pi t_{p-1}}{T}\right)\right].$$

On the other hand, $\dot{x}(t)$ can be obtained by its definition as the time derivative of $x(t)$ and be written as

$$\dot{x}(t) = \sum_{n=1}^{\infty} -\frac{2n\pi}{T}a_n\sin\left(\frac{2n\pi t}{T}\right)+\frac{2n\pi}{T}b_n\sin\left(\frac{2n\pi t}{T}\right). \tag{2.2}$$

Considering equations 2.1 and 2.2 for $\dot{x}(t)$, the following equalities must hold

$$a_n = \frac{T}{2n^2\pi^2}\sum_{p=1}^{K}\frac{\Delta x_p}{\Delta t_p}\left[\cos\left(\frac{2n\pi t_p}{T}\right)-\cos\left(\frac{2n\pi t_{p-1}}{T}\right)\right]$$

$$b_n = \frac{T}{2n^2\pi^2}\sum_{p=1}^{K}\frac{\Delta x_p}{\Delta t_p}\left[\sin\left(\frac{2n\pi t_p}{T}\right)-\sin\left(\frac{2n\pi t_{p-1}}{T}\right)\right].$$

An analogous process leads to the conclusion that for the y projection the following equations hold

$$y(t) = C_0 + \sum_{n=1}^{+\infty} c_n\cos\left(\frac{2n\pi t}{T}\right)+d_n\sin\left(\frac{2n\pi t}{T}\right)$$

$$c_n = \frac{T}{2n^2\pi^2}\sum_{p=1}^{K}\frac{\Delta y_p}{\Delta t_p}\left[\cos\left(\frac{2n\pi t_p}{T}\right)-\cos\left(\frac{2n\pi t_{p-1}}{T}\right)\right]$$

$$d_n = \frac{T}{2n^2\pi^2}\sum_{p=1}^{K}\frac{\Delta y_p}{\Delta t_p}\left[\sin\left(\frac{2n\pi t_p}{T}\right)-\sin\left(\frac{2n\pi t_{p-1}}{T}\right)\right].$$

The DC components of these Fourier series can be obtained by direct computation. The following equalities hold

$$A_0 = \frac{1}{T}\sum_{p=1}^{K}\left[\frac{\Delta x_p}{2\Delta t_p}\left(t_p^2-t_{p-1}^2\right)+\xi_p\left(t_p-t_{p-1}\right)\right]$$

$$C_0 = \frac{1}{T}\sum_{p=1}^{K}\left[\frac{\Delta y_p}{2\Delta t_p}\left(t_p^2 - t_{p-1}^2\right) + \delta_p\left(t_p - t_{p-1}\right)\right]$$

where

$$\xi_p = \sum_{j=1}^{p-1}\Delta x_j - \frac{\Delta x_p}{\Delta t_p}\sum_{j=1}^{p-1}\Delta t_j$$

$$\delta_p = \sum_{j=1}^{p-1}\Delta y_j - \frac{\Delta y_p}{\Delta t_p}\sum_{j=1}^{p-1}\Delta t_j$$

and $\xi_1 = \delta_1 = 0$.

Shape analysis methods need to verify certain properties for the sake of automatic pattern recognition and automatic classification systems. Desirable properties include translation invariance, rotation invariance and scale invariance. In the following, some of the properties of the EFD will be analysed.

Given a closed contour codified as a Freeman code, its Fourier truncated approximation for digital processing can be written as

$$x(t) = A_0 + \sum_{n=1}^{N} X_n \qquad \text{and} \qquad y(t) = C_0 + \sum_{n=1}^{N} Y_n,$$

where the components of the projections X_n and Y_n are for $n \in \{1, \ldots, N\}$ given by

$$X_n(t) = a_n \cos\left(\frac{2n\pi t}{T}\right) + b_n \sin\left(\frac{2n\pi t}{T}\right)$$

$$Y_n(t) = c_n \cos\left(\frac{2n\pi t}{T}\right) + d_n \sin\left(\frac{2n\pi t}{T}\right).$$

Consider a fixed value of $n \in \mathbb{N}$. Kuhl [11] has proven that the set of points $(X_n(t), Y_n(t))$ for each constant harmonic n describes an elliptic locus (the case $n = 0$ corresponds to a single point) by showing that the following formula holds

$$\frac{(c_n^2 + d_n^2)X_n(t)^2 + (a_n^2 + b_n^2)Y_n(t)^2 - 2(a_n c_n + b_n d_n)X_n(t)Y_n(t)}{(a_n d_n - b_n c_n)^2} = 1. \tag{2.3}$$

Recall from Analytic Geometry that the canonical equation of an ellipsis centred at the origin is $\frac{x^2}{e_1^2} + \frac{y^2}{e_2^2} = 1$ for $e_1, e_2 \in \mathbb{R}\backslash\{0\}$. Recall also from the general classification of quadratic forms, that if the ellipsis axis are rotated in relation to the usual Cartesian referential axis, an xy term appears in this equation. This said, it is easy to acknowledge that Equation 2.3 corresponds to an elliptic locus.

The designation "Elliptic Fourier Descriptors" can now be easily understood. Kuhl showed as well that the Fourier approximation of the original contour can be thought in terms of a sum of rotating phasors verifying a proper phase relationship (cf. Figure 2.6). These phasors are defined by the previously introduced projections. As shown, each rotating phasor has an elliptic focus and it will rotate faster than the first harmonic by its harmonic number n (cf. Figure 2.6).

Kuhl's argument to prove that the same elliptic loci $(X_n(t), Y_n(t))$ are obtained independently of the starting point on the contour is now presented. Nonetheless, phasors take different orientations in their approximation process.

Consider the Fourier coefficients $a_n, b_n, c_n, d_n, n \geq 1$ of an arbitrary starting point t and the coefficients $a_n^*, b_n^*, c_n^*, d_n^*, n \geq 1$ corresponding to a new starting point t^*, which is displaced λ units around the contour in relation to the original starting point $(t = t^* + \lambda)$.

The projections from the new starting point are

$$\begin{aligned} X_n^*(t^*) &= a_n^* \cos\left(\frac{2\pi t^*}{T}\right) + b_n^* \sin\left(\frac{2\pi t^*}{T}\right) \\ Y_n^*(t^*) &= c_n^* \cos\left(\frac{2\pi t^*}{T}\right) + d_n^* \sin\left(\frac{2\pi t^*}{T}\right). \end{aligned} \tag{2.4}$$

A difference in starting points in the contour corresponds to a phase-shift in terms of the projections, i.e.,

$$X_n^*(t^*) = X_n(t^* + \lambda) \qquad \text{and} \qquad Y_n^*(t^*) = Y_n(t^* + \lambda). \tag{2.5}$$

This means that a starting point displaced λ units in the direction of rotation around the contour has the following projections from the original starting point

$$X_n^*(t^*) = a_n \cos\left(\frac{2n\pi(t^* + \lambda)}{T}\right) + b_n \sin\left(\frac{2n\pi(t^* + \lambda)}{T}\right)$$

$$Y_n^*(t^*) = c_n \cos\left(\frac{2n\pi(t^* + \lambda)}{T}\right) + d_n \sin\left(\frac{2n\pi(t^* + \lambda)}{T}\right).$$

Using the formulae for the cosine and the sin of two angles, it follows that

$$\begin{aligned} X_n(t^*) &= a_n \cos\left(\frac{2n\pi t^*}{T}\right)\cos\left(\frac{2n\pi\lambda}{T}\right) - a_n \sin\left(\frac{2n\pi t^*}{T}\right)\sin\left(\frac{2n\pi\lambda}{T}\right) \\ &\quad + b_n \sin\left(\frac{2n\pi t^*}{T}\right)\cos\left(\frac{2n\pi\lambda}{T}\right) + b_n \cos\left(\frac{2n\pi t^*}{T}\right)\sin\left(\frac{2n\pi\lambda}{T}\right) \\ Y_n^*(t^*) &= c_n \cos\left(\frac{2n\pi t^*}{T}\right)\cos\left(\frac{2n\pi\lambda}{T}\right) - c_n \sin\left(\frac{2n\pi t^*}{T}\right)\sin\left(\frac{2n\pi\lambda}{T}\right) \\ &\quad + d_n \sin\left(\frac{2n\pi t^*}{T}\right)\cos\left(\frac{2n\pi\lambda}{T}\right) + d_n \cos\left(\frac{2n\pi t^*}{T}\right)\sin\left(\frac{2n\pi\lambda}{T}\right). \end{aligned} \tag{2.6}$$

Equations 2.4 and 2.6 allow to write the following relationship between the Fourier coefficients of the original and the displaced contour starting points by means of a rotation matrix as

$$\begin{bmatrix} a_n^* & b_n^* \\ c_n^* & d_n^* \end{bmatrix} = \begin{bmatrix} a_n & b_n \\ c_n & d_n \end{bmatrix} \begin{bmatrix} \cos\left(\frac{2n\pi\lambda}{T}\right) & -\sin\left(\frac{2n\pi\lambda}{T}\right) \\ \sin\left(\frac{2n\pi\lambda}{T}\right) & \cos\left(\frac{2n\pi\lambda}{T}\right) \end{bmatrix}.$$

Using Equations 2.3 and 2.5, it follows that

$$\frac{(c_n^2+d_n^2)X_n^*(t^*)^2 + (a_n^2+b_n^2)Y_n^*(t^*)^2 - 2(a_nc_n+b_nd_n)X_n^*(t^*)Y_n^*(t^*)}{(a_nd_n-b_nc_n)^2} = 1. \tag{2.7}$$

This shows that the same elliptic foci are obtained for different starting points.

Consider now the case of a counter-clockwise rotation of ψ degrees of the coordinate axis X-Y. Let us designate the new rotated axis system as U-V. This relation can again be expressed by a rotation matrix as follows

$$\begin{bmatrix} U \\ V \end{bmatrix} = \begin{bmatrix} \cos\psi & \sin\psi \\ -\sin\psi & \cos\psi \end{bmatrix} \begin{bmatrix} X \\ Y \end{bmatrix}.$$

Writing Equation 2.4 in matrix form, the following identity for its U_n and V_n projections on the U-V coordinate system may be derived as

$$\begin{bmatrix} U_n \\ V_n \end{bmatrix} = \begin{bmatrix} \cos\psi & \sin\psi \\ -\sin\psi & \cos\psi \end{bmatrix} \begin{bmatrix} X_n^*(t^*) \\ Y_n^*(t^*) \end{bmatrix} = \begin{bmatrix} \cos\psi & \sin\psi \\ -\sin\psi & \cos\psi \end{bmatrix} \begin{bmatrix} a_n^* & b_n^* \\ c_n^* & d_n^* \end{bmatrix} \begin{bmatrix} \cos\left(\frac{2\pi nt^*}{T}\right) \\ \sin\left(\frac{2\pi nt^*}{T}\right) \end{bmatrix}.$$

Using this equation, a set of axially rotated Fourier coefficients, designated as $a_n^{**}, b_n^{**}, c_n^{**}, d_n^{**}$, can be defined as

$$\begin{bmatrix} a_n^{**} & b_n^{**} \\ c_n^{**} & d_n^{**} \end{bmatrix} = \begin{bmatrix} \cos\psi & \sin\psi \\ -\sin\psi & \cos\psi \end{bmatrix} \begin{bmatrix} a_n^{*} & b_n^{*} \\ c_n^{*} & d_n^{*} \end{bmatrix}.$$

The joint effect of axial rotation and displacement of starting point may now be written in matrix form in terms of the original Fourier coefficients (of the original starting point) as

$$\begin{bmatrix} a_n^{**} & b_n^{**} \\ c_n^{**} & d_n^{**} \end{bmatrix} = \begin{bmatrix} \cos\psi & \sin\psi \\ -\sin\psi & \cos\psi \end{bmatrix} \begin{bmatrix} a_n & b_n \\ c_n & d_n \end{bmatrix} \begin{bmatrix} \cos\left(\frac{2n\pi\lambda}{T}\right) & -\sin\left(\frac{2n\pi\lambda}{T}\right) \\ \sin\left(\frac{2n\pi\lambda}{T}\right) & \cos\left(\frac{2n\pi\lambda}{T}\right) \end{bmatrix}. \tag{2.8}$$

Figure 2.6 represents and summarizes the process of elliptic approximation of a contour.

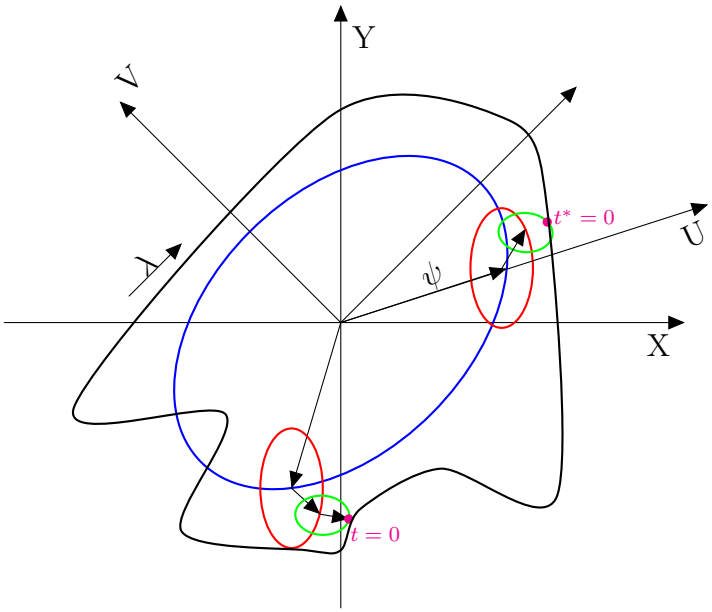

Figure 2.6: Illustration of the Elliptic approximation of a contour.

One of the main objectives of any shape analysis methods is to derive a proper digital representation of some shape in order to allow pattern recognition. That means in this case, using the Fourier coefficients $a_n, b_n, c_n, d_n, \forall n \in \mathbb{N}$ of the truncated Fourier approximation of any given closed contour for the purpose of shape recognition and identification (e.g. template matching).

Equation 2.8 provides a relationship between Fourier coefficients before and after axial rotation and translation, which clearly shows how the coefficients vary accordingly to spatial rotation, magnitude and translation of the contour, as well as the initial starting point.

For the sake of pattern recognition based on EFD, a normalization for the coefficients $a_n, b_n, c_n, d_n, \forall n \in \mathbb{N}$ must be derived.

As claimed by Kuhl and Giardina [19], the rotating phasors provide a most convenient basis for normalization when the locus of the first harmonic phasor is elliptic. They yield two related *classifications*, corresponding to the points at either end of the major axis of the elliptic locus. When the locus of the first harmonic is circular, useful *classifications* are the coefficients for those places on the original contour, which are at a specified distance from the contour center point (A_0, C_0).

The case of an elliptic locus associated with the first harmonic shall be considered first. For this case, a process consisting of two steps allows normalization. Initially, the first harmonic phasor is rotated until it becomes aligned with the semi-major axis of its elliptic locus. Secondly, the original coordinate system X-Y in which the contour was originally oriented, is rotated into the new U-V coordinate system, which is defined by the major and minor axis of the elliptic locus, such that the positive part of the X axis coincides with the semi-major axis located in the phasor rotation (cf. Figure 2.6).

In order to determine the relationship between the only two possible *classifications*, consider that the *classification* associated with one semi-major axis was obtained through starting-point and axial rotations of $\theta_1 = \frac{2\pi\lambda_1}{T}$ and ψ_1 radians, respectively. In this context, λ_1 stands for the contour starting point displacement. According to Equation 2.8, the *classification* for the semi-major axis is

$$\begin{bmatrix} a^{**}_{n\,1} & b^{**}_{n\,1} \\ c^{**}_{n\,1} & d^{**}_{n\,1} \end{bmatrix} = \begin{bmatrix} \cos\psi_1 & \sin\psi_1 \\ -\sin\psi_1 & \cos\psi_1 \end{bmatrix} \begin{bmatrix} a_n & b_n \\ c_n & d_n \end{bmatrix} \begin{bmatrix} \cos(n\theta) & \sin(n\theta) \\ -\sin(n\theta) & \cos(n\theta) \end{bmatrix}. \tag{2.9}$$

The *classification* for the other semi-major axis of the ellipsis can be obtained considering a second rotation of both the starting point and the spatial angle by π radians as follows

$$\begin{bmatrix} a^{**}_{n\,2} & b^{**}_{n\,2} \\ c^{**}_{n\,2} & d^{**}_{n\,2} \end{bmatrix} = \begin{bmatrix} \cos(\psi_1+\pi) & \sin(\psi_1+\pi) \\ -\sin(\psi_1+\pi) & \cos(\psi_1+\pi) \end{bmatrix} \begin{bmatrix} a_n & b_n \\ c_n & d_n \end{bmatrix} \begin{bmatrix} \cos(n(\theta_1+\pi)) & \sin(n(\theta_1+\pi)) \\ -\sin(n(\theta_1+\pi)) & \cos(n(\theta_1+\pi)) \end{bmatrix}.$$

Using trigonometric identities and Equation 2.9 it is possible to conclude that

$$\begin{bmatrix} a^{**}_{n\,2} & b^{**}_{n\,2} \\ c^{**}_{n\,2} & d^{**}_{n\,2} \end{bmatrix} = (-1)^{n+1} \begin{bmatrix} a^{**}_{n\,1} & b^{**}_{n\,1} \\ c^{**}_{n\,1} & d^{**}_{n\,1} \end{bmatrix}.$$

This shows that the odd harmonics of the two *classifications* remain unchangeable, but even harmonics change sign. The starting point angular rotation θ_1 can be determined from

the phasor $(x_1, y_1) = (a_1 \cos\theta + b_1 \sin\theta, c_1 \cos\theta + d_1 \sin\theta)$, where $\theta = \frac{2\pi t}{T}$, by calculating the derivative of the magnitude of the first harmonic phasor $E = \sqrt{x_1^2 + y_1^2}$. Doing the calculations it is possible to show that

$$\theta_1 = \frac{1}{2} \arctan \frac{2(a_1 b_1 + c_1 d_1)}{a_1^2 + c_1^2 - b_1^2 - d_1^2}$$

The first semi-major axis moves away from the starting point in the direction of rotation about the contour, as the sign of the second derivative of E is always negative for $0 \leq \theta_1 < \pi$.

The spatial rotation ψ_1 is determined from the Fourier coefficients a_1^* and c_1^*, which are correct for the starting point displaced θ_1 radians, i.e.

$$a_1^* = a_1 \cos\theta_1 + b_1 \sin\theta_1$$
$$c_1^* = c_1 \cos\theta_1 + d_1 \sin\theta_1$$

When the first harmonic phasor is aligned with the semi-major axis ϕ_1, $t^* = 0$ so $X_1(t^*) = X_1(0) = a_1^*$ and $Y_1(t^*) = Y_1(0) = c_1^*$ and therefore

$$\psi_1 = \arctan \frac{Y_1^*(0)}{X_1^*(0)} = \arctan \frac{c_1^*}{a_1^*},\ 0 \leq \psi_1 < 2\pi.$$

The magnitude of the semi-major axis can now be computed as

$$E^*(0) = \sqrt{x_1^*(0)^2 + y_1^*(0)^2} = \sqrt{a_1^{*2} + c_1^{*2}}.$$

It is now possible to make the *classification* independent of size by dividing each coefficient by the magnitude of the semi-major axis. Independence from translation effects is achieved by ignoring the bias terms A_0 and C_0. For the case of size-normalized classification, the harmonic content of the first harmonic is always $a_1^{**} = 1$, $b_1^{**} = 0$, $c_1^{**} = 0$ and $|d_1^{**}| < 1$.

Consider now the case in which the first harmonic locus is circular. This is the case if and only if $a_1^2 + b_1^2 + c_1^2 + d_1^2 = 2(a_1 d_1 - b_1 c_1)$ holds. The normalization process is derived in a similar fashion, but in this case, both the starting point and the spatial rotations cannot be made to match the semi-major axis. The rotations are made in this case from the bias point (A_0, C_0) to its most distant point on the contour. If more than one such points exist, more than one *classifications* will also exist.

Recalling the chain code representation, the candidate distances E_p are given as

$$E_p = \sqrt{(A_0 - x_p)^2 + (C_0 - y_p)^2}, p \in \{1, \ldots, K\}.$$

These are among the bias point and the starting point of each link a_p (cf. Figure 2.5).

The *classification* for each chain code link a_p, corresponding to a point of equally maximum distance from the bias point, must now be computed. The starting point rotation θ_p for a *classification* of such a link a_p is

$$\theta_p = \frac{2\pi t_p}{T}, 0 < \theta_p \leq 2\pi$$

and the spatial rotation angle ψ_p is

$$\psi_p = \arctan \frac{y_p - C_0}{x_p - A_0}, \; 0 \leq \psi_p < 2\pi.$$

The *classification* for index p is

$$\begin{bmatrix} a^{**}_{n\ p} & b^{**}_{n\ p} \\ c^{**}_{n\ p} & d^{**}_{n\ p} \end{bmatrix} = \begin{bmatrix} \cos(\psi_p) & \sin(\psi_p) \\ -\sin(\psi_p) & \cos(\psi_p) \end{bmatrix} \begin{bmatrix} a_n & b_n \\ c_n & d_n \end{bmatrix} \begin{bmatrix} \cos(n\theta_p) & \sin(n\theta_p) \\ -\sin(n\theta_p) & \cos(n\theta_p) \end{bmatrix}.$$

Size normalization is now achieved diving each Fourier coefficient by the radius of the circle associated with the first harmonic. It is obvious that, if a contour can be rotated $\frac{2\pi}{m}$ rad with $m \in \mathbb{N}, m \geq 3$, it will have a circular first harmonic locus and just one *classification*. Any regular polygon with more than 3 sides is an example of such a contour. This normalization procedure can substitute the elliptic-case procedure if a different method for size normalization is employed, i.e., instead of dividing each coefficient by the length of the semi-major axis, the maximal distance E_p is to be employed.

This mathematical discussion concludes with the indication that a bounding for the empirical error of the enunciated EFD approximation method exists and was presented in the original article of Kuhl and Giardina [19]. This part of the discussion was not presented here, because the number of EFD needed for a certain Elliptic Fourier Analysis (EFA), i.e. the application of EFD to describe or compare shape outlines in the context of morphometric studies and pattern recognition applications, heavily depends on the objective of the application.

A contextualization of this mathematical technique to leaf analysis is presented next. One of the biggest advantages of this method is that it provides a succession of increasingly accurate approximations to a given contour. Moreover, it also allows reconstruction of the original contour from the Fourier harmonics computed with arbitrary precision. This concept is illustrated in Figure 2.7 using a leaf from *acer palmatum*.

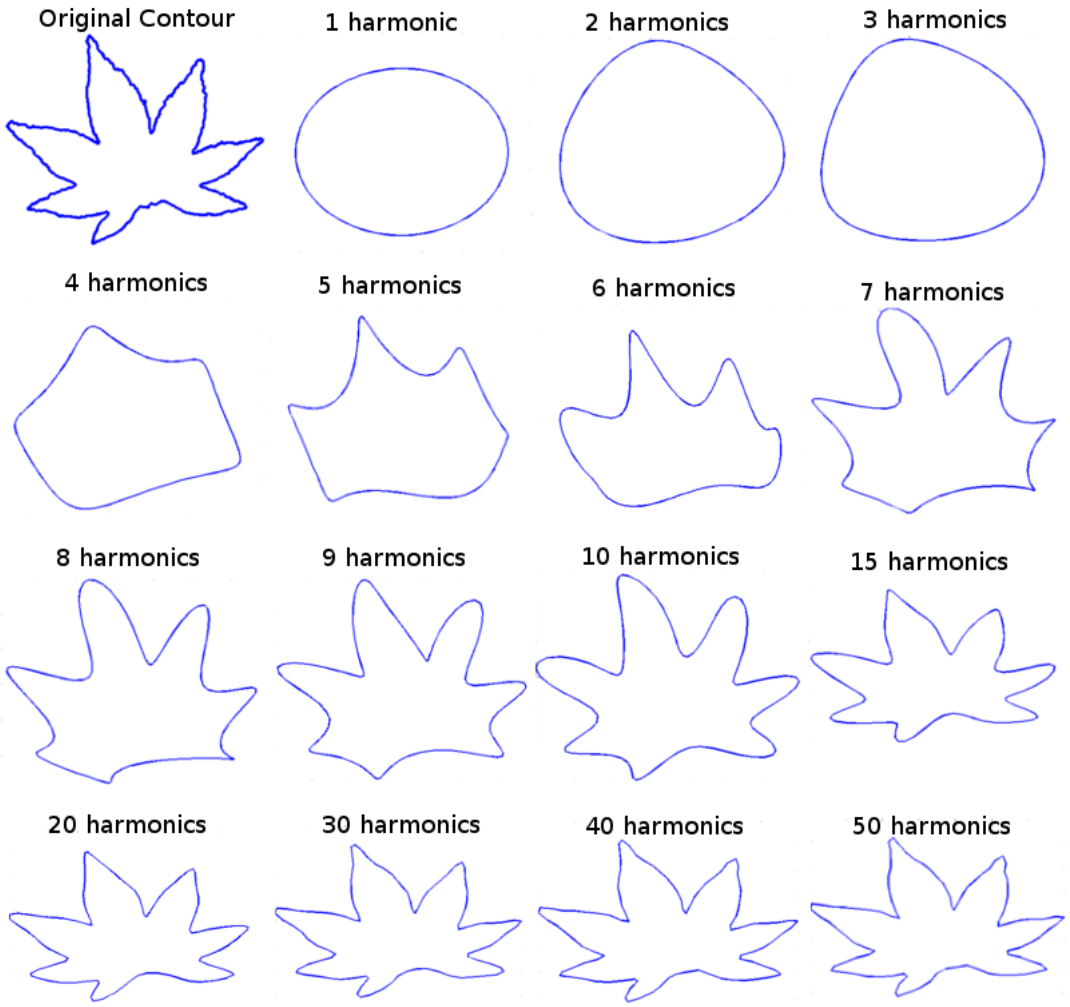

Figure 2.7: Reconstruction of a specimen of *acer palmatum* using EFD.

A study from 2009 completed by Hearn [14], suggests that 10 harmonics are sufficient for accurate leaf shape representation and distinction between leaf shapes. Hearn used 151 species of plants and EFA with 10 harmonics over an initial leaf shape approximation with 100 boundary points samples. An overall accuracy of automatic classification of 72% was reported.

A study from McLellan and Endler [20] provides a comparison between leaf shape analysis methods based on Fourier analysis. The conclusions of this study point out that EFD are capable of adequate leaf shape description and discrimination although their performance was not greatly superior to the other methods considered.

Leaf shape analysis through Elliptic Fourier Descriptors remains an active topic of both fundamental and applied research. This technique is still one of the most used in morpho-

metrics for its straightforward implementation, its generally accurate results and versatility. Some of the most recent publications using EFD include [2], [13], [22] and [35].

This discussion concludes with the presentation of some disadvantages and problems of EFA, namely the lack of universal criteria on how to select the number of harmonics to use in an analysis (this is generally empirically and subjectively chosen by eye inspection in most morphometric studies), how to decide which harmonics convey interesting information and how to avoid the curse of dimensionality when considering feature spaces for automatic pattern recognition. Some further remarks about these issues are presented in Chapter 3.

2.1.2 Contour signatures

Another leaf shape analysis technique consists of the use of contour signatures. A contour signature is, generally speaking, a sequence of values calculated using sampled points on some closed contour considering a clockwise or counterclockwise orientation and an arbitrary starting point. One of the most typical examples of a contour signature is the Centroid Distance Signature (CDS), which consists of the sequence of distances between some shape's centroid and its outline points according to some sampling scheme (see Figure 2.8). The objective of this technique is somewhat similar to that of EFD, as both want to reduce a bidimensional contour to some vector form which is independent of orientation, location and scale.

Figure 2.8 illustrates this concept using a binary image of a specimen of *acer palmatum*. The blue dot in the binary image represents the centroid of the object and the red dot the contour starting point. The CDS was obtained considering a clockwise orientation of the contour.

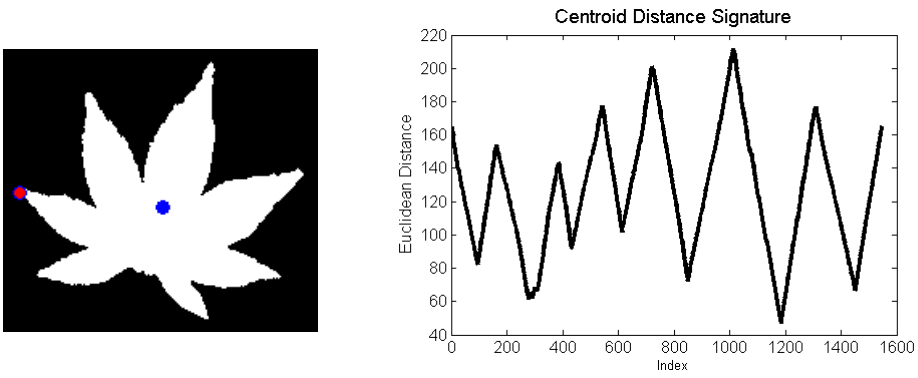

Figure 2.8: Centroid distance signature of a leaf of *acer palmatum*.

One of the biggest problems with this shape analysis approach in the context of automatic leaf classification is self-intersection. Self-intersection happens when a certain leaf part

overlaps another leaf part. This happens frequently in morphometric studies given several different factors, such as the effect of digitalization (the process of getting an image of some leaf represents a geometric projection from a tridimensional object into a bidimensional space, which can carry shape deformations) or even as a consequence of normal leaf anatomy.

In fact, this problem arises particularly often with lobed leaves, i.e., leaves with deeply indented margins. Mathematically, a lobed leaf can be understood as a non-convex set, considering the leaf area as a set in $\mathbb{R}^2$. Figure 2.9 illustrates the referred intersection problems. Green dots indicate regions of possible leaf overlap in consequence of 3D-2D projection and red dots indicate effects derived from the bad conservation status of the specimen.

Figure 2.9: Problem of self-intersection in a leaf of *populus alba*.

Mokhtarian and Abbasi [21] proposed in 2004 a method to try to overcome the problem of self-intersection with application to leaf recognition. The assumption of their method is that darker regions will appear in photographed or digitized leaves in which self-intersection occurred. This information is used to try to obtain the real leaf outline. However this method just works well when sufficient light passes through the leaf margins, otherwise darker areas will not be visible.

Another concern with contour signatures is that they are not immediately comparable after their extraction from a given object. This demands a lot of effort in the normalisation process as the number of points in each signature must be the same and the signatures must be referenced in relation to one comparable starting point. Landmarks can be of use for selecting a comparison point, but they are, as known, not consistent between species. In general, the results might be highly dependent on the comparison method chosen. Ye et. al [34] proposed very recently a method to try to overcome some of these problems with relative success.

Despite these problems, some studies with contour signatures in the context of leaf recognition have been published [30], [31]. In general, contour signatures are not a good method for the sake of plant leaf recognition based on leaf images, because as explained earlier, the method's main concern is to obtain a real-valued function codifying the boundary and leaf outlines frequently cannot be rendered as one-dimensional real function because of the described self-intersection problems. Considering the CDS for instance, it is easy to think of a certain direction from a given leaf shape centroid to the leaf boundary such that the spanned segment crosses the leaf outline in more than one point. In these cases, special attention must be given.

2.1.3 Landmarks

Another branch of leaf shape analysis, namely the identification of landmarks, shall be here briefly referred more for the sake of completeness and given its interest in the context of comparative biology applications than for its importance in this thesis.

Very roughly defined, a landmark is a biologically identifiable point of an organism which can (theoretically) be compared between different organisms. Considering for example a human hand, the knuckles may be understood as landmarks and they can be used for geometric comparison between hands of several individuals. In the case of leaves some points, which are usually taken as landmarks, are the peciole and apex.

Landmarks are not very adequate for the development of an automatic plant identification system. Many factors contribute to this situation: technical knowledge is usually required for the proper selection of landmarks; the automatic extraction of landmark points is very difficult in practice and there is no guarantee that a given landmark found in one species is comparable with an equivalent landmark in another species (it might not be present or it might not be found without a retuning of the analysis algorithm).

These techniques are however heavily used in comparative biology and morphometric studies, where both traditional (using traditional variables such as leaflet width and length) and geometric-based techniques (focusing on the shape of the leaf outline) are applied. They can be used to compare and quantify the effects on leaf expansion and growth of plants in different environments, to study genetic mutations and to analyse specific intra-species variability of key-points in leaves, among other biological parameters.

2.1.4 Shape features

Shape features consist, generally speaking, of a set of measurements that describe a certain shape according to some of its fundamental geometric properties. Commonly used features for the description of a certain shape are for example its aspect ratio, rectangularity, circularity, solidity, compactness and convexity. The nomenclatures may vary considerably but the general definition of these measures is very consistent and they are presented in any introductory book on image processing, such as for instance [12]. Shape features are intensively used in image processing and many times not necessarily in classification contexts.

One of the most interesting aspects of shape analysis through shape features is that this technique is very intuitive, i.e., shape features are easy to understand as they quantify basic geometric properties which match the human visual perception. Even if a thorough description of the calculation process of some of the already mentioned shape features would not have been provided, the reader could easily guess what is meant for instances under a feature's name like for example rectangularity.

Another big advantage of this approach is the ease of implementation and automatic extraction of these features from a given shape, which can generally be done with relatively low computational expense. This happens to be also one of the dangers of this technique. Given the simplicity of these features, the analyst might be tempted to include just a few measures, oversimplifying the analysis.

On the other hand, these features tend to be very correlated among each other, so it is important to chose a good set of features to include in a given analysis in order to avoid multicollinearity. This can be a difficult task [20]. In some cases though, the inclusion of redundant features can be used as a classification technique, as reported by Perner [23].

Shape features are somewhat similar to linear measurements and in general equally limited in terms of the analysis of shape outline, depending on the size of groups to distinguish from. They are nonetheless side by side with EFD the most used techniques for automatic plant identification.

The main disadvantage of this technique in relation to EFD is that contour reconstruction from collected features is not possible. This is not particularly important in the case of automatic pattern recognition, but plays a great role in morphometric studies. Shape features are for instance not particularly useful in terms of understanding leaf shape variation, something that is in general successfully achieved with EFA reconstruction.

Some of the most noticeable and recent studies on the use of shape features in the context of leaf shape recognition include [8], [16], [24], [29], [32] and [33]. They invariably report good results in the application of shape features to leaf shape analysis. A comparison between all these papers is hardly achievable because different shape features are used in conjunction with different classification schemes.

This discussion concludes with the presentation in Table 2.1 of a set of shape features considered by the author of this thesis in the analysis published in [27]. These constitute a slightly modified version of the work of Pauwels et al. [24] and similarly to the EFD have desirable translation, rotation and scale invariance.

Let I denote an object of interest in a binary image, ∂I its border, $D(I)$ its diameter, i.e., the maximum distance between any two points in ∂I and $A(I)$ its area. Let $A(H(I))$ denote the area of the object's convex hull (i.e. any 'optimal' inscribing convex polygon) and $L(\partial I)$ the object's contour length. Assume that the operator $d(.)$ stands for the Euclidean distance.

Shape feature	**Description**
Eccentricity	Eccentricity of the ellipse with identical second moments to I. This value ranges from 0 to 1.
Aspect Ratio	Consider any $X, Y \in \partial I$. Choose X and Y such that $d(X,Y) = D(I)$. Find $Z, W \in \partial I$ maximizing $D^{\perp} = d(Z,W)$ on the set of all pairs of ∂I that define a segment orthogonal to $[XY]$. The aspect ratio is defined as the quotient $D(I)/D^{\perp}$. Values close to 0 indicate an elongated shape.
Elongation	Compute the maximum escape distance $d_{\max} = \max_{X \in I} d(X, \partial I)$. Elongation is obtained as $1 - 2d_{\max}/D(I)$ and ranges from 0 to 1. The minimum is achieved for a circular region. Note that the ratio $2d_{\max}/D(I)$ is the quotient between the diameter of the largest inscribed circle and the diameter of the smallest circumscribed circle.
Solidity	The ratio $A(I)/A(H(I))$ is computed, which can be understood as a certain measure of convexity. It measures how well I fits a convex shape.
Stochastic Convexity	This variable extends the usual notion of convexity in topological sense, using sampling to perform the calculation. The aim is to estimate the probability of a random segment $[XY]$, $X, Y \in I$, to be fully contained in I.
Isoperimetric Factor	The ratio $4\pi A(I)/L(\partial I)^2$ is calculated. The maximum value of 1 is reached for a circular region. Curvy intertwined contours yield low values.
Maximal Indentation Depth	Let $C_{H(I)}$ and $L(H(I))$ denote the centroid and arclength of $H(I)$. The distances $d(X, C_{H(I)})$ and $d(Y, C_{H(I)})$ are computed $\forall X \in H(I)$ and $\forall Y \in \partial I$. The indentation function can then be defined as $[d(X, C_{H(I)}) - d(Y, C_{H(I)})]/L(H(I))$, which is sampled at one degree intervals. The maximal indentation depth $\mathfrak{D}$ is the maximum of this function.
Lobedness	The Fourier Transform of the indentation function above is computed after mean removal. The resulting spectrum is normalized by the total energy. Calculate lobedness as $F \times \mathfrak{D}^2$, where F stands for the smallest frequency at which the cumulated energy exceeds 80%. This feature characterizes how lobed a leaf is.

Table 2.1: Common shape features for leaf shape analysis.

2.1.5 Polygon fitting and fractal dimensions

Another shape analysis method which has been applied to leaf shape analysis is the so-called fractal dimension analysis. Briefly speaking, fractal dimension analysis consists in the development of a measure (real number) that quantifies how completely the outline of a given leaf fills the dimensional space to which it belongs. This can be understood as a measure of contour complexity and relates in this sense to the shape feature *lobedness* introduced in Table 2.1.

Several variations for the calculation of fractal dimensions exist and one of the most well-known methods is the Minkowski-Bouligand's method.

McLellan and Endler [20] showed, using fractal dimension alongside other descriptors, that fractal dimension tends to be highly correlated with perimeter to area ratios (dissection indexes), suggesting that this measurement does not bring a higher benefit than traditional shape features, like those discussed in Section 2.1.1.4. Nonetheless, several authors have been developing and using fractal dimension related techniques in the context of leaf shape analysis, among which [4] and [9] are specially relevant. High recognition rates have been reported on small databases.

The attempt to use only fractal dimension as a single descriptor for the problem of leaf recognition seems inadequate given the enormous variety of leaf shapes (cf. Figure 2.2). In certain cases, the use of fractal dimension as an auxiliary measure might be of use, although the referred conclusions of McLellan's and Endler's study [20] should be kept in mind.

Comparison of these techniques with other described methods is difficult, given the small size of the until now used databases in fractal dimension related studies.

2.2 Venation extraction and analysis

Leaf veins are structures somewhat similar to human veins. Their function is to provide leaves with a transport mechanism for important liquids like mineral-enriched water, sugar and other substances. As in many other aspects of leaf biology, there is a great variability in detail, but general vein structures can in some cases be comparable between specimens of a given species. Under some conditions, leaf veins exhibit a different colouration in relation to the rest of the leaf lamina.

Leaf venation extraction can be extremely easy or extremely difficult, depending on what is aimed for. If a high contrast is injected into the leaf venation system for example, extracting the leaf venation will require a very simple segmentation algorithm. Another situation that could lead to effortless extraction would be the use of proper radiometric equipment in image acquisition.

Considering the development of an automatic leaf recognition system, it would be desirable to be able to extract venation from regular RGB images without too much exigence on the image acquisition process. This would necessarily lead to complicated algorithms, which probably would not bring a considerable gain, but instead would cause a huge computational load.

If databases are collected under good conditions (controlled illumination), simple mathematical morphology and the Otsu binarization algorithm may provide very good results in leaf venation extraction like reported by Zheng and Wang [39]. These databases are however not generally available, mostly because in the context of the development of a complete automatic plant recognition system it is desirable to conserve high variability in the original data (data acquisition without controlled settings) in order not to inflate the accuracy of the employed method's results.

Other authors have been considering more sophisticated techniques like frequency domain filters and neural networks [5]. At present, fully automated venation extraction is still giving its first steps.

2.3 Leaf margin analysis

Leaf margin analysis remains one the of less explored computer-based leaf analysis methods. The following factors contribute to this situation: on one hand, not all leaves exhibit teeth on the margin, i.e., a serration pattern is not present in all species (in fact some leaves exhibit a very smooth margin), which makes automatic comparison between specimens hardly feasible; on the other hand, as claimed by Royer et. al. [26], "no computer algorithm can reliably detect leaf teeth'.

Nonetheless, leaf teeth are an important feature for leaf discrimination and many botanists use them in morphological studies and manual plant species identification [5]. For example, the number and size of teeth are generally used in studies on the relation between climate and growth patterns in plants.

Considering the case in which just plant species exhibiting teeth pattern are being studied, manually quantifying the area of the tooth margin region and the size and number of teeth may give discriminant variables, which can always be combined with other leaf shape analysis methods. For plant species not possessing any teeth patterns on the margin, other techniques must be applied.

For the sake of a complete automated plant classification system, leaf margin analysis is somewhat limited. It can be very important to discriminate on a particular level between plant species which are very similar in all characteristics but the margin. However, it cannot be used alone in a general global classification scheme. This technique is therefore limited to ecological and biological studies on particular species and is usually applied in research papers focusing on plant properties and morphometrics in general, rather than on automated leaf classification systems.

2.4 Leaf texture analysis

Leaf texture analysis consists of the application of common image texture analysis techniques to leaf images in plant classification systems. This can be of use if texture exhibits consistent properties within a certain species and especially if used in combination with other leaf analysis methods like leaf shape techniques. Several authors have reported good results of the inclusion of texture analysis techniques in leaf classification systems, but given the different sizes of the databases employed as well as the nature of the employed methods, no consistent results about the quality of this approach are available [5].

Table 2.4 shows some of the most common and simple general texture analysis variables as presented in [12]. Texture analysis based on statistical properties of the intensity histogram is generally used in image processing applications. A class of methods of this type use statistical moments. If Z is a random variable indicating image intensity, its nth moment around the mean is $\mu_n = \sum_{i=0}^{L-1} (z_i - m)^n p(z_i)$, where m is the mean of Z, $p(.)$ its histogram and L is the number of intensity levels.

Texture feature	**Description**
Average Intensity	Average intensity is defined as the mean of the intensity image, m.
Average Contrast	Average contrast is the the standard deviation of the intensity image, $\sigma = \sqrt{\mu_2(z)}$.
Smoothness	Smoothness is defined as $R = 1 - 1/(1 + \sigma^2)$ and measures the relative smoothness of the intensities in a given region. For a region of constant intensity, R takes the value 0 and R approaches 1 as regions exhibit larger disparities in intensity values. σ^2 is generally normalized by $(L-1)^2$ to ensure that $R \in [0, 1]$.
Third moment	μ_3 is a measure of the intensity histogram's skewness. This measure is generally normalized by $(L-1)^2$ like smoothness.
Uniformity	Defined as $U = \sum_{i=0}^{L-1} p^2(z_i)$, uniformity's maximum value is reached when all intensity levels are equal.
Entropy	A measure of intensity randomness.

Table 2.2: Common texture analysis features based on statistical moments.

2.5 Other methods

There are several other papers published on leaf recognition which do not fit in any of categories referred until now. Some, because they use other aspects of leaf biology like lamina-based methods; others, because they use other mathematical techniques besides those mentioned so far. A very brief summary on these alternative methods is presented here.

Among the most classic approaches those using curvature spaces and Procrustes analysis must be obligatorily referred. Curvature space analysis is an outline analysis technique related with both EFA and landmarks, but which like the name indicates focus on local curvature properties of leaf outline. Procrustes analysis is a morphometric method, which is generally applied with the purpose of comparing shapes. The idea of the method is to find the best space transformation that deforms one shape into another to quantify similarity.

More recently, some distance matrices and graph-theory based methods were proposed [3], [17]. Some other approaches have been tried with a special focus on statistical methods directly applied to leaf recognition. While traditionally the aim was to effectively describe shape and/or other leaf attributes and then use available pattern recognition theory to perform classification, in these specialized approaches methods of pattern recognition for this specific problem are being developed. Some of these include [36], [37] and [38].

It is hard to understand whether these methods contribute to real advances in the state of the art, as the experimental parts are in general not compatible between studies (different databases, classification schemes and criteria). Very high recognition results are invariably reported, but with limited testing conditions.

2.6 Automatic Classification Systems

An overview of the current state of availability of automatic plant classification systems is presented now. Generically speaking, the systems proposed so far may be classified in three categories: systems for generic plant species identification, systems for agricultural purposes and systems for the study of intra-specific variation, geographical distribution and climate effects.

Many system have been developed and proposed in the last few years aiming for the general purpose of automatic plant recognition. One of these systems was proposed in 2006 by Du et al. [7]. This system was based on local shape properties, arguing that any global shape-based approach is risky, as it does not deal well with damaged or overlapped leaves. The shape analysis technique used, involved a combination of polygon fitting with Fourier descriptors and dynamic programming. The authors reported a good accuracy rate on the considered database and tolerance to damaged specimens.

The recent revolution on mobile phone devices has been changing the aim of the development of such plant recognition systems and is leading to the appearance of prototypes on smartphone. There is a general interest on allowing users (both specialists and non-specialists) to go out in the field and use their mobile phones to identify plants.

One of the largest ongoing projects to fulfil this objective is concerned with the development of a field guide of plants in the United States of America [1]. This systems allows the user to feed in an image of a leaf on a simple background and outputs the twenty closest leaves to the input query in the sense of shape matching. Another large project is the CLOVER system [18], which has a very similar philosophy but uses other shape analysis techniques.

Both projects have reported good results on at least a small number of species and under some conditions. Nonetheless, there is so far no general purpose system for everyday use and the until now developed systems are generally confined to the flora of a particular geographic region.

In the context of agricultural application the interest is often not identifying a plant but to determine whether this plant is desirable or not. One of the oldest papers on the use of image processing analysis techniques to the identification of weeds in crops was presented in 1989 by Petry et al. [25]. The general interest on distinction between weed and crop is connected with the optimization of agricultural techniques and the reduction of their impact in the environment (e.g. targeted application of fertilizers or pesticides).

More recent approaches include Hemming et al. in 2001 [15]. They used a system with controlled luminescence to distinguish between two crop species and weed plants (any plant

not fitting in the crop group). Several other research papers followed on aiming at the constant improvement of recognition rates and the loosening of the demanded conditions.

The last but not least important common application concerns intra-specific variation studies. This includes the application of some of the already introduced leaf analysis to morphometric studies. The general aim is to quantify variables of plant biology in order to understand for instance the correlation between environment and plant growth or to clear out taxon boundaries between several species. These applications are generally computer based and designed for use in laboratory.

2.7 Overview

A broad discussion on leaf analysis methods was provided. It seems that researchers agree upon the fact that leaf discrimination is best achieved using shape analysis methods. This belief is connected with the human visual experience, as shape is the main feature that humans use to access similarity and differences between objects, but also with the easiness of its computer treatment.

Considering the introduced leaf shape methods, Elliptic Fourier Descriptors and shape features seem to be the most adequate for the development of an automatic system, given their versatility and the good results they generally provide. Contour signatures, like remarked, are inadequate for the general problem of automatic leaf recognition and landmarks, although adequate and providing good results, generally require technical knowledge, which is a limiting factor.

The strict use of leaf shape methods without giving attention to other leaf properties is likely to perform worse than a combination of several features. However, like reported, although leaf margin and leaf venation analysis could provide a good contribution for the improvement of leaf species recognition with use of automatic image processing techniques, it is very difficult to develop automatic algorithms which can efficiently extract and classify both leaf margin and leaf veins. Moreover, not all leafs exhibit a pattern on their margin which could create difficulties on the statistical processing of data and leaf vein extraction would require a light controlled setting for image acquisition.

This said, considering the development of a general purpose plant identification system, the most promising techniques seem to be the Elliptic Fourier Descriptors and the shape textures. The inclusion of leaf texture may improve classification in a given database but can inhibit good approximate results for the classification of unknown plants. A statistical analysis of the use of both EFD and shape features is addressed in Chapter 3.

Chapter 3

Plant Recognition System

In this chapter, a plant recognition system is proposed and discussed using some of the techniques presented in Chapter 2. In the following, the different necessary steps for the creation of such an image processing system are analysed. Generally speaking, an image processing system with the purpose of pattern recognition requires the following steps: image acquisition, image segmentation and noise removal, feature extraction and classification. This information is summarized in the diagram of Figure 3.1. Each of these steps will be explained in detail in this chapter.

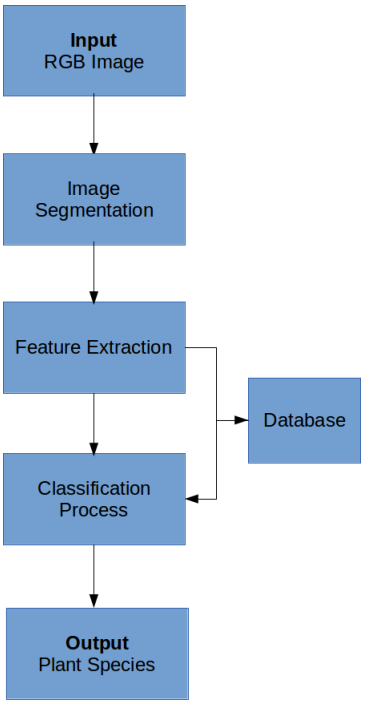

Figure 3.1: Diagram of an automatic plant recognition system.

RGB images obtained with regular cameras are considered. No special light conditions are required but general favourable conditions must be fulfilled (e.g. strong shadows shall not be being cast on the leaf in the moment of image acquisition). For convenience centring the image on the leaf can be done but this is not strictly necessary. The leaf shall not be however in the corners of the image, as this would interfere with the image segmentation algorithm applied.

Image segmentation is a very context depending process, which can be either very easy or very hard. Ideally, no special care in the moment of image acquisition should be required. Not setting any restriction at this level though, would create a myriad of situations, which not even the most competent and actual image segmentation algorithm could possibly solve in all cases.

As this would compromise the accuracy of the entire system, the problem must be simplified. An easy way to guarantee good results in the segmentation process is to impose the condition that pictures of leaves are taken in a contrasting background (see Figure 3.2).

Figure 3.2: Example of good image acquisition practice.

The algorithm chosen for image segmentation is a mixture of colour slicing with Otsu's algorithm. Initially, it requires the calculation of the mean H, S and V values of four small rectangles near each corner of the digital image. Secondly, a deviation matrix resulting from the comparison between each image pixel and the mean H, S and V values of the background is computed. The Otsu's algorithm is finally applied to obtain a global threshold of the deviation histogram.

A noise removal process (morphological operations) can be afterwards applied in order to ensure that there is only one object on the image. Figure 3.3 presents an example of a correctly segmented image.

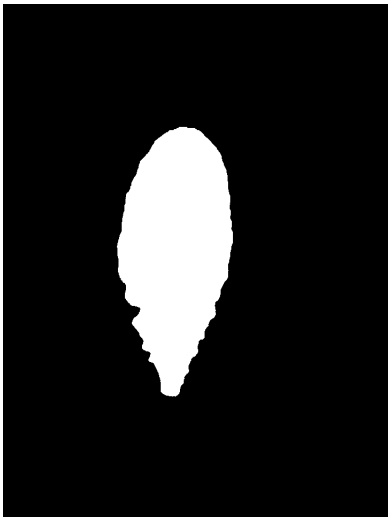

Figure 3.3: Example of a segmented image.

Given the fact that there is a high level of spurious variation introduced by the form and size of the petioles in leaves, they are removed through morphological operations prior to feature extraction. This process ensures statistically more stable results.

Feature extraction concerns the process of acquiring variables to use in classification schemes and is perhaps the most delicate step in the entire process, requiring a careful statistical analysis of results. Several features are analysed in Chapter 3.2 and a comparison between two of the most important approaches for leaf analysis is provided.

Prior to the classification of a new and unknown specimen, it is necessary to possess a database of features for all the different specimens in each species to train statistical classifiers. This numeric database is derived from an image database (see Chapter 3.1).

The process ends with the application of a classification process to the features extracted from the specimen to be classified. These are compared to references in the database and an output with the probable species to which the input leaf belongs is given.

In the rest of this chapter, a database with leaf images from different plants as well as a comparison between Elliptic Fourier Descriptors and shape and texture features for the automatic recognition of plant species are presented. These results are used in Chapter 4 to propose a computational tool implementing the discussed scheme.

3.1 Database

A database of images of plant leaves was constructed. 40 different species of plants were considered, harvesting an average number of 10 leaf specimens from each plant. A total number of 443 images was collected. Each leaf specimen was photographed using two different devices, a Canon EOS 40D reflex camera and an Apple iPAD2 tablet. For the development of the system proposed in this thesis the focus was on the 720 × 920 pixel, 24-bit RGB images taken with the Apple iPAD2 device.

The collected leaves were photographed over a contrasting background. For green leaves, a reddish colour was used. For the special case of the *acer palmatum* leaves, a gray background was used. The choice of colours was arbitrary, respecting solely the previously indicated condition of acquiring leaf image over a contrasting background.

Figure 3.4 provides an overview of the aspect of the different leaves considered and Table 3.1 synthesizes the information on plant species and number of specimens.

Figure 3.4: Leaf database overview - 40 class types.

Class	Scientific Name	#	Class	Scientific Name	#
1	Quercus suber	12	21	Fraxinus sp.	10
2	Salix atrocinera	10	22	Primula vulgaris	12
3	Populus nigra	10	23	Erodium sp.	11
4	Alnus sp.	8	24	Bougainvillea sp.	13
5	Quercus robur	12	25	Arisarum vulgare	9
6	Crataegus monogyna	8	26	Euonymus japonicus	12
7	Ilex aquifolium	10	27	Ilex perado ssp. azorica	11
8	Nerium oleander	11	28	Magnolia soulangeana	12
9	Betula pubescens	14	29	Buxus sempervirens	12
10	Tilia tomentosa	13	30	Urtica dioica	12
11	Acer palmatum	16	31	Podocarpus sp.	11
12	Celtis sp.	12	32	Acca sellowiana	11
13	Corylus avellana	13	33	Hydrangea sp.	11
14	Castanea sativa	12	34	Pseudosasa japonica	11
15	Populus alba	10	35	Magnolia grandiflora	11
16	Acer negundo	10	36	Geranium sp.	10
17	Taxus bacatta	5	37	Aesculus californica	10
18	Papaver sp.	12	38	Chelidonium majus	10
19	Polypolium vulgare	13	39	Schinus terebinthifolius	10
20	Pinus sp.	12	40	Fragaria vesca	11

Table 3.1: Leaf database: plant species (class) and number of specimens available (#).

According to leaf complexity two large groups can be identified in this database: leaves from class 1 to 15 and 22 to 36 are simple and leaves from class 16 to 21 and 37 to 40 are complex. Only simple leaves will be considered for the development of the present system, as the explored techniques would be inadequate for the shape description and analysis of complex leaves. EFD can describe any closed contour but the shape variability in the specimens of any of these classes would yield senseless results. On the other hand, it would be impossible to compare the results of EFA with other techniques, as for instance shape features are formulated for one object with a single connected component.

These complex leaves were collected in the perspective of future work and aiming the construction of a complete leaf database, which could be made freely available to the scientific community.

A detailed overview of the images obtained with the Apple iPAD2 device is provided in appendix to this thesis.

For the sake of completeness it is important to refer here as well that some other leaf image databases exist, which are publicly available. These were discovered in a rather late phase of the development of this thesis. Examples of such databases include the Swedish leaf dataset [28], the Flavia dataset [32] and the ICL leaf database assembled in the Institute of Intelligent Machines, Chinese Academy of Sciences. The first two databases have a similar number of plants to the database presented here. The third database has a very large number of plants (220) but offers many challenges in terms of pre-processing (many images are contaminated and many leaves exhibit complex geometry and self-intersection problems).

3.2 Statistical Analysis

In this section, the statistical results of the leaf shape and texture analysis methods as introduced in Chapter 2 are explored considering the simple leaves of database presented in Section 3.1. The performance of EFD and shape features methods is compared using a parametric and a non-parametric classifier and multivariate analysis techniques.

The set of the 340 simple leaves has been randomly split in 70% training and 30% test, assuring that at least one element of each species is represented in each subset and respecting the class structure. The test set contains on average 3 leaves from each plant and it will be used for comparisons among models. Moreover, 10-fold cross validation is used for model accuracy testing.

Familiarity with Principal Component Analysis, Linear Discriminant Analysis, the KNN Algorithm, multivariate statistical analysis and pattern recognition is assumed.

3.2.1 Elliptic Fourier Analysis

Like previously remarked, EFA consists in the use of EFD to perform morphometric analysis. The general methodology of EFA includes: image segmentation, boundary extraction, boundary codification as chain code and calculation of EFD. The tool presented in Section 4.1 was used to create a database of EFD.

The first question arising in an EFA is related with the number of harmonics to include in the analysis. It is generally difficult to associate harmonics with particular features in the boundary of a given shape like already observed. The general criterion seems to be choosing a number of harmonics correctly depicting the overall aspect of the shapes in analysis. It is nonetheless true that high order harmonics are generally related with high frequency variations which can be noise or a leaf margin pattern. As a pattern is not commonly found

between different leaves, the best practice is to fix a number of harmonics and keep with that decision. There are some formulas to calculate the power contained in each harmonic in order to decide how many harmonics and possibly which harmonics to include in the analysis but generally Principal Component Analysis (PCA) is preferred. In this analysis 10 harmonics in combination with PCA are considered.

PCA is a transformation from the original feature space into another space with more desirable properties. When analysing data it is frequently the case that, even though special care is taken in the selection process, the selected variables exhibit very frequently high correlation. PCA is a method to overcome this problem, as it provides a set of new variables which are linear combinations of each original feature, but unlike the original features, the principal components are not correlated among each other.

On the other hand, PCA verifies a very important property: the new principal axes successfully maximize the variance in the data with respect to themselves and they are naturally ranked by data variability, i.e., the first principal axis explains the most data variability and each successive axis explains less and less data variability. These properties make PCA a valuable tool, helping to avoid the dimensionality curse and allowing effective dimensionality reduction.

Another interesting feature of principal components is that they are the continuous solution of the cluster membership indicators of the K-means clustering method, i.e., the PCA transformation automatically performs data clustering according to the K-means objective function [6].

A data matrix with the first 10 harmonics from each leaf image was constructed using normalized EFA, i.e., a_1, b_1 and c_1 were not included as their values do not carry any information (recall that in this case $a_1 = 1$ and $b_1 = c_1 = 0$), meaning that our original feature space had 37 variables. Some authors argue that the normalization given by the EFD process is not the best, but it was used in our study, given its simplicity compared with some alternatives that would require the use of landmarks or for instances techniques demanding further technical knowledge like Procrustes analysis.

The decision whether to include or remove d_1 can be problematic. This term is associated with the harmonic eccentricity which is approximately the width to length ratio (*aspect ratio*) of the object being analysed. It is often the case, that this coefficient carries the most variation. As all Elliptic Fourier coefficients are normalized, it is safe to include d_1 in the analysis. This leads to another problem: it is necessary to choose whether PCA shall be performed with scaled or unscaled data.

This problem must be addressed considering the information about the data being anal-

ysed. When the variables in analysis exhibit very different variances or are measured in incommensurable units, they should generally be scaled to ensure that principal component weights remain stable and that differences in scale and variance will not bias each variable's importance. Unscaled (or raw) data should be used in all other situations.

Considering the randomized training set and the 37 variables corresponding to d_1 and all the other coefficients associated with the harmonics 2 to 10, it is possible to conclude that variances range from the orders 10^{-4} to 10. Although it is easy to accept that d_1 constitutes a discriminant feature, there is no aprioristic reason to assume that this variable should be more important than any other, especially as the relation between geometric aspects and harmonics is generally unknown. PCA with scaled data shall be used. Figure 3.5 shows the explained data variability by the first n principal components.

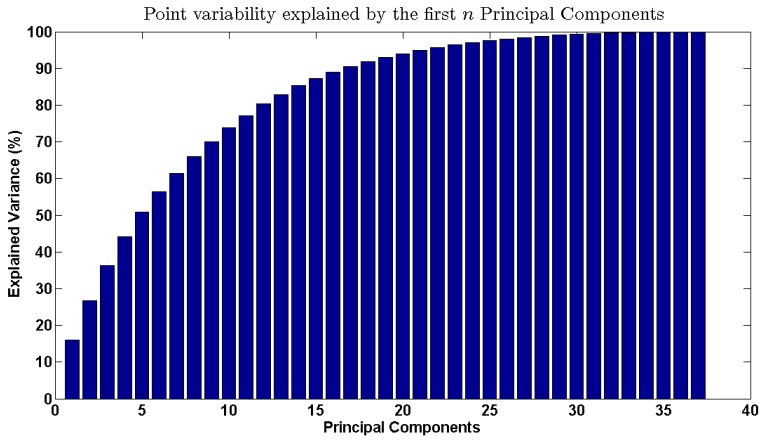

Figure 3.5: EFA: Cumulative explained variability by principal components.

Given the fact that 34 is an excessive number of variables for a pattern classification problem with 30 classes and 340 observations, the information in Figure 3.5 shall be used to perform dimensionality reduction. According to this figure, 17 principal components are sufficient to explain over 90% of data variability. This value is generally considered as a mark in common applications of PCA. It is then possible to reduce the dimension of the original feature set from 37 to 17, a more acceptable number.

This graph makes clear that each principal component brings a small increment of total explained data variability. This suggests that the explaining power might be split upon the input variables or that the input variables do not explain the dynamics in the data.

Figure 3.6 represents the absolute value of the weights of each principal component as a colour matrix (rows represent input variables, columns represent principal components).

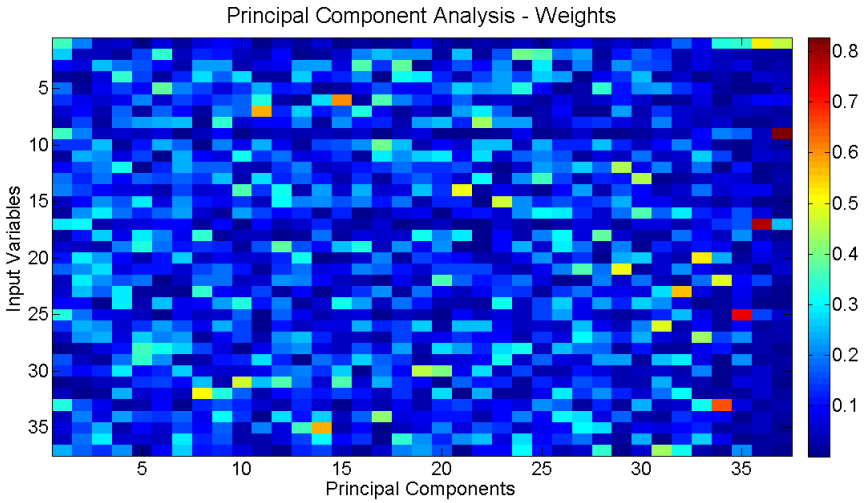

Figure 3.6: EFA: Principal Component Analysis Weights.

The interpretation of the weights of PCA can be risky but it is useful as an exploratory tool. The d_1 coefficient has a high weight in the first principal component, confirming our previous remark about the effect of this variable in point variability. Other harmonics contribute to the first principal component with lower absolute weight.

The second and third principal components exhibit higher weights for harmonic content with orders between 4 and 6. In the third principal component, one coefficient from the 10th harmonic has high weight. This migration of weight importance in terms of harmonic content is related with the nature of the method, which provides an approximation continuously increasing in detail.

It is dangerous to comment on principal components of higher order, as the explained variance is very small (cf. Figure 3.5). The fact that the first principal component alone explains just approximately 15% of point variability and many weights having low absolute values indicates that the input variables may do not describe the data well.

Figure 3.7 represents the mean of the principal component scores of the considered classes in the space spanned by the first three principal components (around 37% of explained point variability).

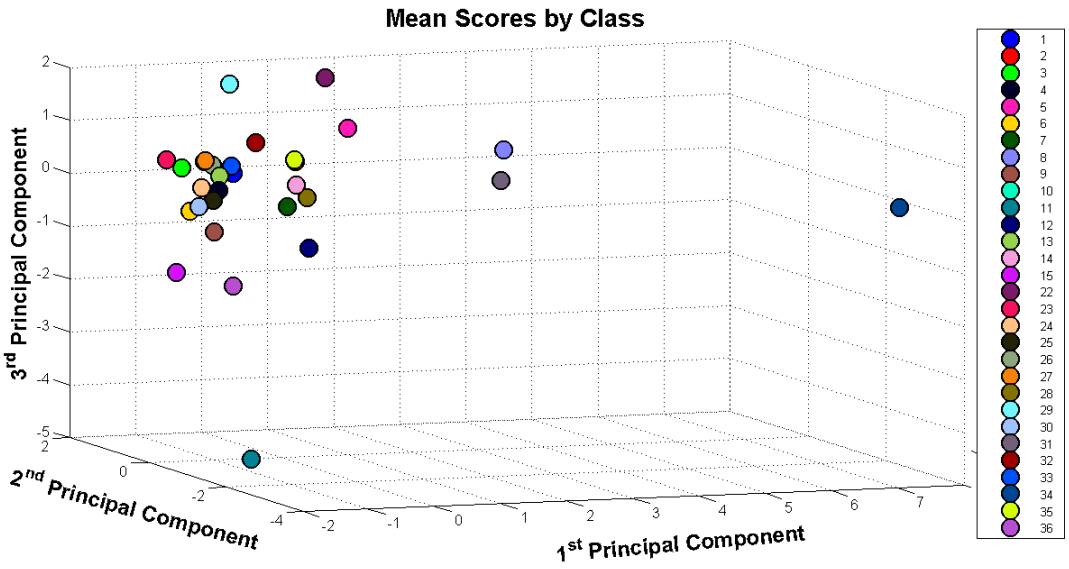

Figure 3.7: EFA: Class mean in the principal component space.

Figure 3.7 reinforces our suspect that these variables may lack discriminant power. The point cloud is very dense and poor separability between different classes was achieved. This can possibly indicate poor classification accuracy. It is necessary to keep in mind though that these results are confined to three principal components, explaining just around 37% of data variability.

Figure 3.8 represents the result of an hierarchical clustering of the mean scores of each class in principal component space (17 variables) using the Ward's method and euclidean distance.

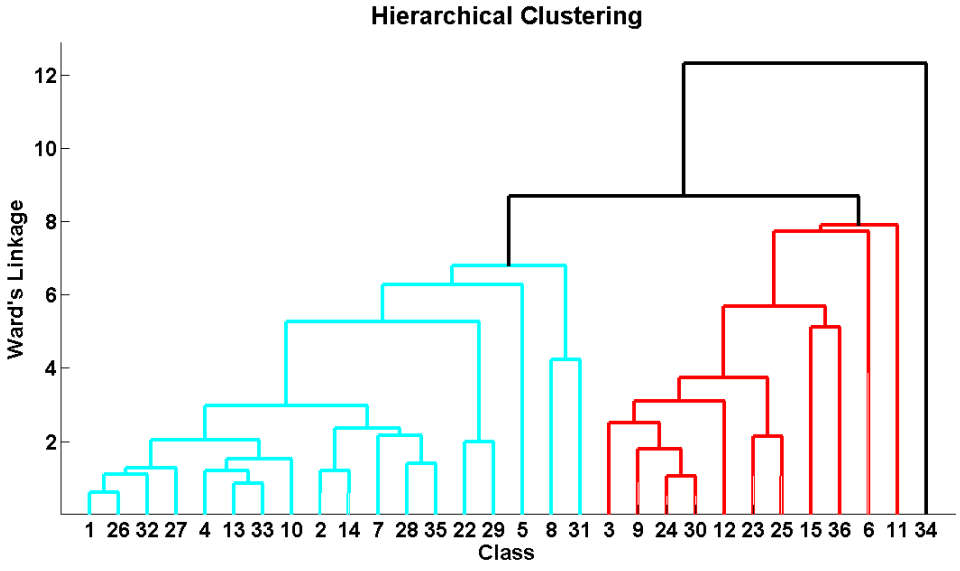

Figure 3.8: EFA: Hierarchical Clustering with Ward's Linkage.

The results of the hierarchical clusterings are satisfactory, as the aggregation seems to reasonably match the human concept of visual shape resemblance. The division in three big groups is difficult to explain. The fact that class 34 was united with the other clusters at level 12 may be connected with the extremal aspect ratio of these leaves. Although the fresh leaves of this plant have a rather extremal aspect ratio, this value may have been increased by the conservation status of the photographed specimens, which were already somewhat dry and curled up.

The results become more satisfactory as lower levels of the hierarchical clustering are considered. In the blue group the clusterings 1,26,32,27; 4,13,33,10 and 2,14,7,28,35 seem very adequate. Analogously, the cluster 3,9,24,30 seems adequate. Inside both blue and red groups, the clustering is reasonable but it is difficult to explain the division into the blue and red groups. The red group seems to concentrate the most dissimilar leaf shapes (including lobed specimens and teethed leaf margins). In average, EFD with PCA seem to be capable of reasonably identifying similarities between leaves based on shape properties.

The principal component scores (17 variables) are now used as input features to some classifiers. Linear Discriminant Analysis (LDA) and the K-Nearest Neighbours (KNN) classifier shall be considered. There is, besides their simplicity, no specific reason for the choice of these classifiers.

In fact, both LDA and KNN are respectively the simplest parametric and non-parametric classification techniques. Although very simple, LDA is still one of the most used classifiers, scoring well in many benchmarks. It relates to several other statistical techniques like Fisher's linear discriminant analysis or regression analysis, as LDA also attempts to express one dependent variable as a linear combination of input features. It is also similar to PCA, as they both search for a linear combination of input variables to explain data but unlike PCA, LDA focus on explaining class differences. The theoretical hypothesis from LDA - the classes considered are normally distributed and have equal variances - are in practice not considered, as LDA is in fact except for a constant term equivalent to Fisher discriminant analysis which does not assume a particular structure for the data.

KNN is a non-parametric and conceptually simple classification algorithm which classifies each new observation using a majority rule in the feature space considering the class of its K training observation neighbours. To evaluate distances in the feature set using the KNN algorithm, the euclidean distance is used.

The results of the classification analysis performed are presented in Table 3.2.

Method	Cross-validation Error	Classification Error
LDA	50.2%	53.9%
KNN (1)	49.0%	55.1%
KNN (3)	53.1%	56.2%
KNN (5)	53.0%	61.8%

Table 3.2: EFA: Summary of classification results.

Like suggested from the previous discussion, classification results are somewhat poor. Linear Discriminant Analysis performs better in the test set than any considered version of the K-Nearest Neighbours classifier used.

The exploratory analysis carried out suggested already that the EFD did not have sufficient exploratory power to distinguish among the high number of plants considered. Increasing the number of EFD harmonics would not lead to better results.

Some researchers improved the general classification results of EFD using as input features not the harmonic coefficients but the reconstructed boundary points from the harmonic coefficients. This procedure is adequate when the objective of the EFA is morphometric analysis and the specimens in study have been referenced for their position.

Considering the case of a general purpose plant species recognition system, using coordinates instead of harmonics could perform worse, unless special care had been taken in terms of position normalization and boundary smoothing. There is no interest in imposing any position restrictions for image acquisition. Also, deciding the number of points to include in the boundary reconstruction can be difficult. Few points can lead to bad classification results through bad discrimination and many points can lead to underrated correlation results through the inclusion of boundary noise.

Table 3.3 presents the confusion matrix for linear discriminant analysis of the Elliptic Fourier Descriptors.

	1	2	3	4	5	6	7	8	9	10	11	12	13	14	15	22	23	24	25	26	27	28	29	30	31	32	33	34	35	36
1	1	1	0	1	0	0	0	0	0	0	0	0	0	0	0	0	0	0	0	0	0	0	0	0	0	0	0	0	0	0
2	0	2	0	0	0	0	0	0	0	0	0	0	0	0	0	0	0	0	0	0	0	0	0	0	0	1	0	0	0	0
3	0	0	3	0	0	0	0	0	0	0	0	0	0	0	0	0	0	0	0	0	0	0	0	0	0	0	0	0	0	0
4	0	0	0	0	0	0	0	0	0	0	0	0	1	0	0	0	0	0	0	0	0	0	0	0	0	0	1	0	0	0
5	0	0	0	0	1	0	0	0	0	0	0	0	0	0	0	0	0	0	0	0	0	0	1	0	0	0	0	0	0	1
6	0	0	0	0	0	0	0	0	0	0	0	0	0	0	0	0	0	0	0	1	1	0	0	0	0	0	0	0	0	0
7	1	0	0	0	0	0	2	0	0	0	0	0	0	0	0	0	0	0	0	0	0	0	0	0	0	0	0	0	0	0
8	0	0	1	0	0	0	0	2	0	0	0	0	0	0	0	0	0	0	0	0	0	0	0	0	0	0	0	0	0	0
9	0	0	1	0	0	0	0	0	3	0	0	0	0	0	0	0	0	0	0	0	0	0	0	0	0	0	0	0	0	0
10	0	0	0	0	0	0	0	0	0	0	0	0	0	0	0	0	1	0	0	1	0	0	0	0	0	0	1	0	0	0
11	0	0	0	0	0	0	0	0	0	0	1	0	1	0	1	0	0	0	0	0	0	0	0	1	0	0	0	0	0	0
12	0	0	0	0	0	0	0	0	0	0	0	3	0	0	0	0	0	0	0	0	0	0	0	0	0	0	0	0	0	0
13	0	0	0	1	0	0	0	0	0	0	0	0	2	0	0	0	0	0	0	0	0	0	0	0	0	0	0	0	0	0
14	0	0	0	2	0	0	0	0	0	0	0	0	0	1	0	0	0	0	0	0	0	0	0	0	0	0	0	0	0	0
15	0	0	0	0	0	0	0	0	0	0	0	0	0	0	2	0	0	0	0	0	1	0	0	0	0	0	0	0	0	0
22	0	0	1	0	0	0	0	0	0	0	0	0	0	0	0	1	0	0	0	0	0	0	1	0	0	0	0	0	0	0
23	0	0	0	0	0	0	0	0	1	0	0	0	0	0	0	0	1	0	0	1	0	0	0	0	0	0	0	0	0	0
24	0	0	1	0	0	0	0	0	0	0	0	0	0	0	0	0	0	2	0	0	0	0	0	0	0	0	0	0	0	0
25	0	0	0	0	0	0	0	0	0	0	0	0	0	1	0	0	0	0	1	0	0	0	0	0	0	0	0	0	0	0
26	1	0	0	1	0	0	0	0	0	1	0	0	0	0	0	0	0	0	0	0	0	0	0	0	0	0	0	0	0	0
27	0	0	0	0	0	0	0	0	0	0	0	0	0	0	0	0	0	0	0	1	1	0	0	0	0	1	0	0	0	0
28	0	0	0	0	0	0	0	0	0	0	0	0	1	0	0	0	0	0	0	0	0	2	0	0	0	0	0	0	0	0
29	0	0	0	0	0	0	0	0	0	0	0	0	0	0	0	0	0	0	0	0	0	0	3	0	0	0	0	0	0	0
30	0	0	0	0	0	0	0	0	1	0	0	0	0	0	0	0	0	0	0	0	0	0	0	2	0	0	0	0	0	0
31	0	0	1	0	0	0	0	0	0	0	0	0	0	0	0	0	0	0	0	0	0	0	0	0	0	0	0	2	0	0
32	0	0	0	0	0	0	0	0	0	0	0	0	0	0	0	0	0	0	0	0	0	0	0	0	0	2	1	0	0	0
33	0	0	0	0	0	0	0	0	0	0	0	0	2	0	0	0	0	0	0	0	0	0	0	0	0	0	1	0	0	0
34	0	0	1	0	0	0	0	0	0	0	0	0	0	0	0	0	0	0	0	0	0	0	0	0	0	0	0	2	0	0
35	0	0	0	0	0	0	0	0	0	0	0	0	1	0	0	0	0	0	0	0	0	0	0	0	0	1	1	0	0	0
36	0	0	0	0	0	0	0	0	1	0	0	0	0	0	0	1	0	0	0	0	0	0	1	0	0	0	0	0	0	0

Table 3.3: EFD: Confusion matrix for Linear Discriminant Analysis.

The analysis of the confusion matrix shows that the classification results are not only quantitatively poor but also qualitatively poor. It could be the case that although a high classification error was achieved, the misclassified units were visually similar but this is generally not the case. Although some test units from visually similar classes are being misclassified (e.g. class 1 with classes 2 and 4), unacceptable results are also present (e.g. class 4 with classes 13 and 33).

Even though general leaf outline shape seems to be the most discriminating feature when identifying leaves, using a technique like EFD seems to be inadequate. Some of the most obvious limitations of this technique, include the incapacity to deal with shape deformations as in case of badly conserved specimens and the already referred self-intersection problem and the need to control for leaf curvature in different specimens or the incapacity to account for leaf outline variation in specimens of a given plant which were collected in different stages of leaf development. No restrictions in the considered database were made in order to minder the consequences of these problems, as the most diverse and uncontrolled possible setting is desirable.

By construction EFD focus on the description (reconstruction) of any closed boundary, which makes the technique very appropriate for morphometric analysis but not for the

development of a general pattern recognition system, as sensitivity to detail (frequently noise) corrupts the results.

Like pointed out by Du et al. [7] though, global-shape descriptors may be inadequate in a general situation. On the other hand, it is also more likely that a method focusing only on outline shape properties performs worse than techniques considering more stable leaf properties like shape features and other methods.

Combining EFD with other techniques may be difficult, as it is hard to identify the relationship between the harmonic content and the geometric properties of a given contour like already mentioned.

3.2.2 Shape features

A set of input features composed by the shape features introduced in Section 2.1.1.4 is now considered: 1. Eccentricity, 2. Aspect Ratio, 3. Elongation, 4. Solidity, 5. Stochastic Convexity, 6. Isoperimetric Factor, 7. Maximal Indentation Depth and 8. Lobedness. This statistical analysis starts with the inspection of the correlation structure of these variables. Table 3.4 represents the Pearson's correlation matrix of the considered features.

1	2	3	4	5	6	7	8
1	0.54	0.55	0.39	0.39	-0.02	-0.29	-0.25
	1	0.68	0.01	0.08	-0.47	0.08	0.08
		1	-0.4	-0.39	-0.79	0.43	0.39
			1	0.86	0.76	-0.89	-0.83
				1	0.67	-0.77	-0.71
					1	-0.74	-0.62
						1	0.95

Table 3.4: Shape features: Pearson's correlation.

The criterion $|\rho| > 0.7$ is a thumb rule for considering two variables highly correlated in Pearson's sense. According to this rule the following high correlated pairs of variables were identified: 3. Elongation with 6. Isoperimetric Factor; 4. Solidity with 5. Stochastic Convexity, 6. Isoperimetric Factor, 7. Maximal Indentation Depth, 8. Lobedness; 5. Stochastic Convexity with 7. Maximal Indentation Depth and 8. Lobedness; 6. Isoperimetric Factor with 7. Maximal Indentation Depth; 7. Maximal Indentation Depth with 8. Lobedness.

It was clear from the definition of these features that high correlation was expected. In particular, the variables 4. Solidity and 5. Stochastic Convexity as well as 7. Maximal Indentation Depth and 8. Lobedness are by construction necessarily high correlated.

As referred, PCA can, not only provide an effective technique for dimensionality reduction, but also for variable decorrelation. A scaled PCA is used for variable decorrelation. The reason to choose a scaled PCA is similar to the case of EFA. It is necessary to prevent *aspect ratio*, being the feature naturally capturing the most variance, from obscuring the effect of other possibly equally important features. Figure 3.9 shows the explained point variability by the first n principal components.

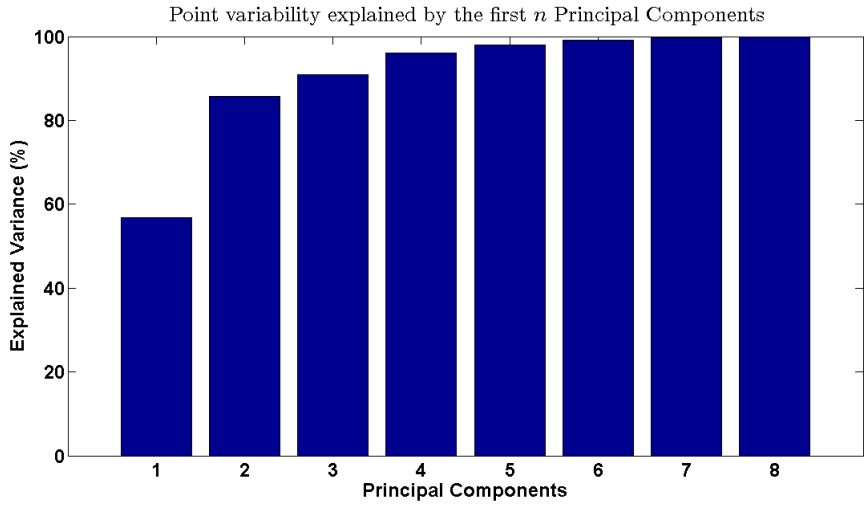

Figure 3.9: Shape features: Cumulative explained variability by principal components.

According to Figure 3.9, the first 3 principal components are enough to explain around 90% of data variability. This is a far fewer number for the same mark as in the case of EFD. The weights of the principal components are in this case difficult to analyse and do not convey any obvious information.

Figure 3.10 represents the mean scores by class using the first three principal components (around 91% of explained data variability). Comparing Figures 3.7 and 3.10, it seems that shape features are more adequate than EFD for the data description. The point cloud is more diffuse in Figure 3.10, indicating better discrimination between classes and consequently higher likelihood for satisfactory classification results than with EFD.

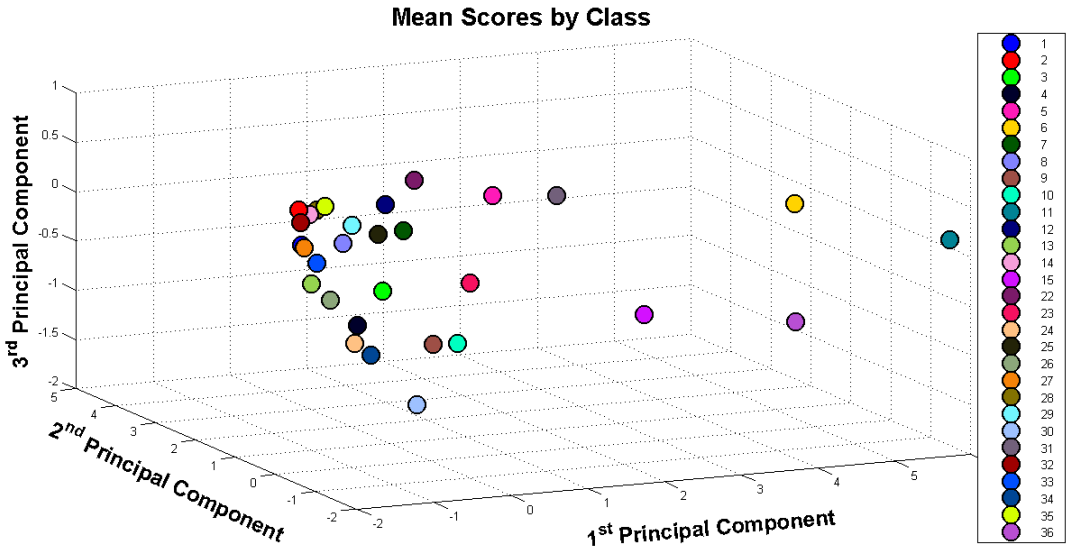

Figure 3.10: Shape features: Class mean in the principal component space.

In the following the results of the hierarchical clustering analysis of the principal components of the considered shape features are presented. Figure 3.11 summarizes the results.

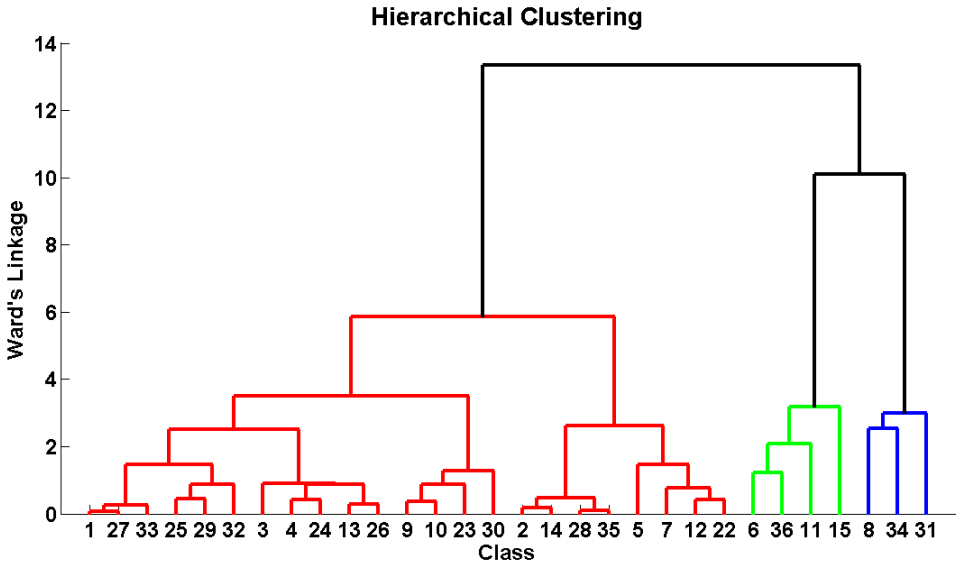

Figure 3.11: Shape features: Hierarchical Clustering with Ward's Linkage.

The results of the hierarchical clustering are very satisfactory. Unlike the case of EFD, in this clustering there is a clear explanation for the division in three different, rather large groups. The blue group is the group of the leaves with extremal aspect ratio. Leaves from classes 8, 31 and 34 are all of linear type and have a disproportionate height to width ratio. The green group is the group of the lobed leaves and the red group contains all the other leaves not fitting into any of these two categories.

The first split in the red group is connected with the general aspect of vertical development of leaves. Notice that all rectangular shapes were agglomerated into the cluster composed by the classes 2, 14, 28, 35, 5, 7, 12 and 22. Considering this cluster, notice the good result obtained by the aggregation of classes 2 - 14 and 28 - 35 and posteriorly the formation of the cluster (2-14)-(28-35).

Considering now the clustering structure on the left, the splitting on the level 4 seems to be isolating cordate leaves (heart-like shape) in the clustering 9, 10, 23, 30. It is however surprising that class 23 is associated in this group and that this class is associated with cluster 9 - 10 prior to the class 30. Finally, the division in two groups around level 3, groups (1, 27, 33, 25, 29, 32) and (3, 4, 24, 13, 26), is difficult to interpret but it is connected with how circular or elliptic a leaf is. In spite of some possible problems, like the association of class 25 with class 29. The results seem consistent, considering the several pairs of good matching results: class 1 with class 27, class 4 with class 24, etc.

The results of automatic classification using all principal components as input features are presented next. Table 3.5 summarizes these results.

Method	Cross-validation Error	Classification Error
LDA	59.4%	39.3%
KNN (1)	63.3%	38.2%
KNN (3)	61.8%	40.4%
KNN (5)	60.7%	42.7%

Table 3.5: Shape features: Summary of classification results.

Similarly to the case of EFD, the parametric classifier generally yields better results than the non-parametric classifier. Although cross-validation errors are higher for shape features than EFD, the classification errors are consistently lower for these features. Considering the LDA classifier, EFD yielded a classification error of 53.9%, whilst shape features yielded a classification error of 39.3%. This represents a significant reduction of 23.3%.

It could be the case that the high values of cross-validation errors would indicate a possible model overfitting. However, this is unlikely as the results do not seem to be significantly different between the parametric and the non-parametric classifiers.

Both the quantitative results of classification analysis and the hierarchical clustering seem to be in favour of shape features as the best analysed method for the development of the aimed system. The results of hierarchical clustering with shape features were empirically more adequate than EFD and yielded unlike EFD biologically interpretable results.

This discussion concludes with the inspection of the confusion matrix for the linear discriminant analysis classifier 3.6.

	1	2	3	4	5	6	7	8	9	10	11	12	13	14	15	22	23	24	25	26	27	28	29	30	31	32	33	34	35	36
1	1	1	0	0	0	0	0	0	0	0	0	0	1	0	0	0	0	0	0	0	0	0	0	0	0	0	0	0	0	0
2	0	1	0	0	0	0	0	0	0	0	0	0	0	0	0	0	0	0	0	0	0	0	0	0	0	2	0	0	0	0
3	0	0	2	0	0	0	0	0	1	0	0	0	0	0	0	0	0	0	0	0	0	0	0	0	0	0	0	0	0	0
4	0	0	0	0	0	0	0	0	0	0	0	0	0	0	0	0	0	1	0	1	0	0	0	0	0	0	0	0	0	0
5	0	0	0	0	3	0	0	0	0	0	0	0	0	0	0	0	0	0	0	0	0	0	0	0	0	0	0	0	0	0
6	0	0	0	0	0	1	0	0	0	0	0	0	0	0	0	0	0	0	0	0	0	0	0	0	0	0	0	0	0	1
7	0	0	0	0	0	0	1	0	0	0	0	0	0	0	0	0	0	0	0	0	0	0	2	0	0	0	0	0	0	0
8	0	0	0	0	0	0	0	3	0	0	0	0	0	0	0	0	0	0	0	0	0	0	0	0	0	0	0	0	0	0
9	0	0	1	0	0	0	1	0	2	0	0	0	0	0	0	0	0	0	0	0	0	0	0	0	0	0	0	0	0	0
10	0	0	0	0	0	0	0	0	0	3	0	0	0	0	0	0	0	0	0	0	0	0	0	0	0	0	0	0	0	0
11	0	0	0	0	0	0	0	0	0	0	4	0	0	0	0	0	0	0	0	0	0	0	0	0	0	0	0	0	0	0
12	0	0	0	0	0	0	0	0	0	0	0	1	0	1	0	1	0	0	0	0	0	0	0	0	0	0	0	0	0	0
13	0	0	0	0	0	0	0	0	0	0	0	0	3	0	0	0	0	0	0	0	0	0	0	0	0	0	0	0	0	0
14	0	0	0	0	0	0	0	0	0	0	0	1	0	2	0	0	0	0	0	0	0	0	0	0	0	0	0	0	0	0
15	0	0	0	0	0	0	0	0	0	0	0	0	0	0	3	0	0	0	0	0	0	0	0	0	0	0	0	0	0	0
22	0	0	0	0	0	0	0	0	0	0	0	0	0	0	0	2	0	0	0	0	0	0	0	0	0	0	0	0	1	0
23	0	0	0	0	0	0	0	0	0	1	0	0	0	0	0	0	2	0	0	0	0	0	0	0	0	0	0	0	0	0
24	0	0	0	0	0	0	0	0	0	0	0	0	0	0	0	0	0	1	0	2	0	0	0	0	0	0	0	0	0	0
25	0	0	0	0	0	0	0	0	0	0	0	0	0	0	0	0	0	0	2	0	0	0	0	0	0	0	0	0	0	0
26	0	0	0	1	0	0	0	0	0	0	0	0	0	0	0	0	0	2	0	0	0	0	0	0	0	0	0	0	0	0
27	1	0	0	0	0	0	0	0	0	0	0	0	1	0	0	0	0	0	0	1	0	0	0	0	0	0	0	0	0	0
28	0	1	0	0	0	0	0	0	0	0	0	0	0	0	0	0	0	0	0	0	0	1	0	0	0	0	0	0	1	0
29	0	0	0	0	0	0	0	0	0	0	0	0	0	0	0	0	0	0	1	0	0	0	2	0	0	0	0	0	0	0
30	0	0	0	0	0	0	0	0	0	0	0	0	0	0	0	0	0	0	0	0	0	0	0	3	0	0	0	0	0	0
31	0	0	0	0	0	0	0	0	0	0	0	0	0	0	0	0	0	0	0	0	0	0	0	0	2	0	0	1	0	0
32	0	0	0	0	0	0	0	0	0	0	0	0	0	1	0	0	0	0	0	0	0	0	0	0	0	2	0	0	0	0
33	0	0	0	1	0	0	0	0	0	0	0	0	2	0	0	0	0	0	0	0	0	0	0	0	0	0	0	0	0	0
34	0	0	0	0	0	0	0	0	0	0	0	0	0	0	0	0	0	0	0	0	0	0	0	0	0	0	0	3	0	0
35	0	0	0	0	0	0	0	0	0	0	0	0	0	2	0	0	0	0	0	0	0	0	0	0	0	0	0	0	1	0
36	0	0	0	0	0	0	0	0	0	0	0	0	0	0	0	0	0	0	0	0	0	0	0	0	0	0	0	0	0	3

Table 3.6: Shape features: Confusion matrix for Linear Discriminant Analysis.

The test units belonging to the classes 5, 8, 10, 11, 13, 15, 25, 30, 34 and 36 were all fully recognized. This is a significant improvement in the number of classes being fully recognized in comparison to the results obtained by EFD, where just classes 3, 12 and 29 were fully recognized.

The classification results seem more reasonable with shape features than with EFD, as most misclassified leaves seem to exhibit shape resemblance with the specimens of the wrongly selected classes (e.g. class 4 with classes 24 and 26), which was not the case with EFD.

In spite of yielding significantly better results than EFD in the test set considered, shape features seem to be insufficient to generally discriminate between leaves, as indicated by the very high cross-validation error of linear discriminant analysis (59.4%). A method to improve this classification results is addressed next.

3.2.3 Texture features

The previous analysis suggests that although generically accepted as the most discriminating leaf attribute, shape on its own may not be able to distinguish between a large number of different types of leaves. This may actually not even be a limitation of any shape analysis method used but just an aspect of the problem itself. Even a trained human operator will have difficulties distinguishing between two resemblant leaves just relying on shape, and in some cases he/she might not even be capable of identifying the plants they came from.

In fact, given a sufficient number of leaf types in analysis, shape will necessarily run out of discriminatory power. A possible "solution" for this problem would be to form clusters and try not to discriminate on the single plant level but on the level of groups of plants sharing common properties. Another solution is the extension of the considered feature set through the inclusion of complementary features. This later solution might be preferable to the first one, as it minimizes the subjective effects of the initial clustering.

In Chapter 2 possible complementary features have been discussed. Some of the most promising features could be either the leaf venation or its margin, but, as mentioned, these create many problems which are not simple to overcome.

One could at first think that a simple alternative to this approach could be colour, as it is well known that different plants have leaves with different colours. Some plants may exhibit for example reddish leaves like *acer palmatum* (cf. Figure 3.4 - 11). However, not only the natural mean colour may vary between species, leaf colour may also vary intra-specifically according to the season of the year in which the leaf specimen was collected and whether the specimen was dry or infected with some fungal disease, just to mention some possible factors.

It is therefore easy to acknowledge that leaf colour is a high volatile feature and that its inclusion in a system with the generic purpose of plant recognition can be dangerous or at least require a particular care according to each situation analysed.

A somewhat related but less volatile leaf aspect is texture. In the following, the results of the repetition of the previous classification analysis are presented, considering now not only shape analysis but also the texture features introduced in Chapter 2.1.4. The original images were converted to grayscale and statistical based texture features were collected.

New data matrices were constructed: the first consisting of the normalized EFD up to order 10 and the texture features and the second consisting of both the shape and texture features. Principal Component Analysis is used mainly with the purpose of dimension reduction in the case of EFD and variable decorrelation in the case of shape features. Analogously to shape

features, texture features exhibit very high correlation values, but this is not an important aspect, as PCA will be used for variable decorrelation.

Tables 3.7 and 3.8 summarize respectively the classification results of EFA and shape features together with texture features.

Method	Cross-validation Error	Classification Error
LDA	41.4%	28.9%
KNN (1)	46.6%	43.8%
KNN (3)	46.2%	47.2%
KNN (5)	51.8%	48.3%

Table 3.7: EFA and texture features: Summary of classification results.

Considering the EFA there was a slight improvement in the cross-validation error for the majority of the classifiers. The results are significantly better for the considered testing set. An improvement of around 20% was registered in the classification error for all classifiers.

Method	Cross-validation Error	Classification Error
LDA	22.3%	15.7%
KNN (1)	31.9%	28.1%
KNN (3)	30.7%	32.6%
KNN (5)	33.8%	27.0%

Table 3.8: Shape and texture features: Summary of classification results.

In the case of the shape features, a dramatic reduction both in the cross-validation and the classification errors was registered. Both parametric and non-parametric classifiers yielded strongly improved results. Considering the LDA, the classification error and the cross-validation error were reduced approximately and respectively by 50% and 40%.

The best classification result was obtained considering a combination of shape features and texture features and using linear discriminant analysis as classifier.

This discussion concludes with the inspection of the confusion matrix for this classifier as presented in Table 3.9.

	1	2	3	4	5	6	7	8	9	10	11	12	13	14	15	22	23	24	25	26	27	28	29	30	31	32	33	34	35	36
1	2	0	0	0	0	0	0	0	0	0	0	0	1	0	0	0	0	0	0	0	0	0	0	0	0	0	0	0	0	0
2	0	3	0	0	0	0	0	0	0	0	0	0	0	0	0	0	0	0	0	0	0	0	0	0	0	0	0	0	0	0
3	0	0	3	0	0	0	0	0	0	0	0	0	0	0	0	0	0	0	0	0	0	0	0	0	0	0	0	0	0	0
4	0	0	0	2	0	0	0	0	0	0	0	0	0	0	0	0	0	0	0	0	0	0	0	0	0	0	0	0	0	0
5	0	0	0	0	3	0	0	0	0	0	0	0	0	0	0	0	0	0	0	0	0	0	0	0	0	0	0	0	0	0
6	0	0	0	0	0	2	0	0	0	0	0	0	0	0	0	0	0	0	0	0	0	0	0	0	0	0	0	0	0	0
7	0	0	0	0	0	0	1	0	0	0	0	1	0	0	0	0	0	0	0	0	1	0	0	0	0	0	0	0	0	0
8	0	0	0	0	0	0	0	3	0	0	0	0	0	0	0	0	0	0	0	0	0	0	0	0	0	0	0	0	0	0
9	0	0	1	0	0	0	0	0	3	0	0	0	0	0	0	0	0	0	0	0	0	0	0	0	0	0	0	0	0	0
10	0	0	0	0	0	0	0	0	1	2	0	0	0	0	0	0	0	0	0	0	0	0	0	0	0	0	0	0	0	0
11	0	0	0	0	0	0	0	0	0	0	4	0	0	0	0	0	0	0	0	0	0	0	0	0	0	0	0	0	0	0
12	0	0	0	0	0	0	0	0	0	0	0	3	0	0	0	0	0	0	0	0	0	0	0	0	0	0	0	0	0	0
13	0	0	0	0	0	0	0	0	0	0	0	0	3	0	0	0	0	0	0	0	0	0	0	0	0	0	0	0	0	0
14	0	0	0	0	0	0	0	0	0	0	0	1	0	1	0	0	0	0	0	0	0	1	0	0	0	0	0	0	0	0
15	0	0	0	0	0	0	0	0	0	0	0	0	0	0	3	0	0	0	0	0	0	0	0	0	0	0	0	0	0	0
22	0	0	0	0	0	0	0	0	0	0	0	0	0	0	0	3	0	0	0	0	0	0	0	0	0	0	0	0	0	0
23	0	0	0	0	0	0	0	0	0	0	0	0	0	0	0	0	3	0	0	0	0	0	0	0	0	0	0	0	0	0
24	0	0	0	0	0	0	0	0	0	0	0	0	0	0	0	0	0	3	0	0	0	0	0	0	0	0	0	0	0	0
25	0	0	0	0	0	0	0	0	0	0	0	0	0	0	0	0	0	0	2	0	0	0	0	0	0	0	0	0	0	0
26	0	0	0	0	0	0	0	0	0	0	0	0	0	0	0	0	0	0	0	2	0	0	0	1	0	0	0	0	0	0
27	0	0	0	0	0	0	0	0	0	0	0	0	0	0	0	0	0	0	0	1	2	0	0	0	0	0	0	0	0	0
28	0	0	0	0	0	0	0	0	0	0	0	0	0	0	0	0	0	0	0	0	0	2	0	0	0	0	0	0	1	0
29	0	0	0	0	0	0	0	0	0	0	0	0	0	0	0	0	0	0	0	0	0	0	3	0	0	0	0	0	0	0
30	0	0	0	0	0	0	0	0	0	0	0	0	0	0	0	0	0	0	0	0	0	0	0	3	0	0	0	0	0	0
31	0	0	0	0	0	0	0	0	0	0	0	0	0	0	0	0	0	0	0	0	0	0	0	0	2	0	0	1	0	0
32	0	1	0	0	0	0	0	0	0	0	0	0	0	0	0	0	0	0	0	0	0	0	0	0	0	2	0	0	0	0
33	0	0	0	0	0	0	0	0	0	0	0	0	0	0	0	0	0	0	0	0	0	0	0	0	0	0	3	0	0	0
34	0	0	0	0	0	0	0	0	0	0	0	0	0	0	0	0	0	0	0	0	0	0	0	0	0	0	0	3	0	0
35	0	0	0	0	0	0	0	0	0	0	0	0	0	0	0	0	0	0	0	0	0	1	0	0	0	0	0	0	2	0
36	0	0	0	0	0	1	0	0	0	0	0	0	0	0	0	0	0	0	0	0	0	0	0	0	0	0	0	0	0	2

Table 3.9: Shape and texture Features: Confusion matrix for Linear Discriminant Analysis.

Comparing Tables 3.6 and 3.9, it is possible to notice that the inclusion of texture features improves discrimination among specimen exhibiting similar shapes but belonging to different plants. For example, the leaf specimen from class 1 wrongly classified by LDA with shape features as belonging to class 4 was now correctly associated with its original class. Although some confusion still exists, most leaves in the test set are being fully recognized.

3.3 Conclusions

Elliptic Fourier Descriptors performed rather poorly in the performed analysis and do not seem to be an adequate technique for the development of an automatic plant recognition system. These results are not in agreement with some literature, although most reviewed papers apply EFD in the context of morphometric analysis with selected databases and far more specific objectives than arbitrary plant recognition.

Shape features performed better than EFD, as they not only yielded better classification results but also provided with qualitatively superior results. Among the biggest advantages of this technique are the interpretability of both the features and the results they provide and the easiness of their computer implementation.

Although commonly accepted as the most discriminating aspect of leaves, shape runs out of discriminative power and the inclusion of other features besides shape improves the results. EFD and shape features were retested in conjunction with statistical based texture variables and it was found out that this combined strategy strongly improves results. The best results were achieved for the combination of shape and texture features with LDA with a cross-validation error of 22.3% and a classification accuracy of 84.3% in the test set.

Two other leaf shape analysis techniques, namely *multiscale distance matrix analysis* [17] and *complex networks analysis* [3] were tested. These techniques were not included in this statistical discussion, as the results obtained were equivalent to those of shape features and these methods require a higher computational expense than shape features and lack their interpretability, bringing therefore no gain in relation to what can be achieved at least in the considered database using simpler techniques.

Chapter 4

Computational tool in Matlab

A computational tool for automatic plant recognition was developed in Matlab R2012b. Figure 4.1 illustrates the main graphic user interface of the programme. This graphic user interface was designed respecting the structure presented in the diagram of Figure 3.1.

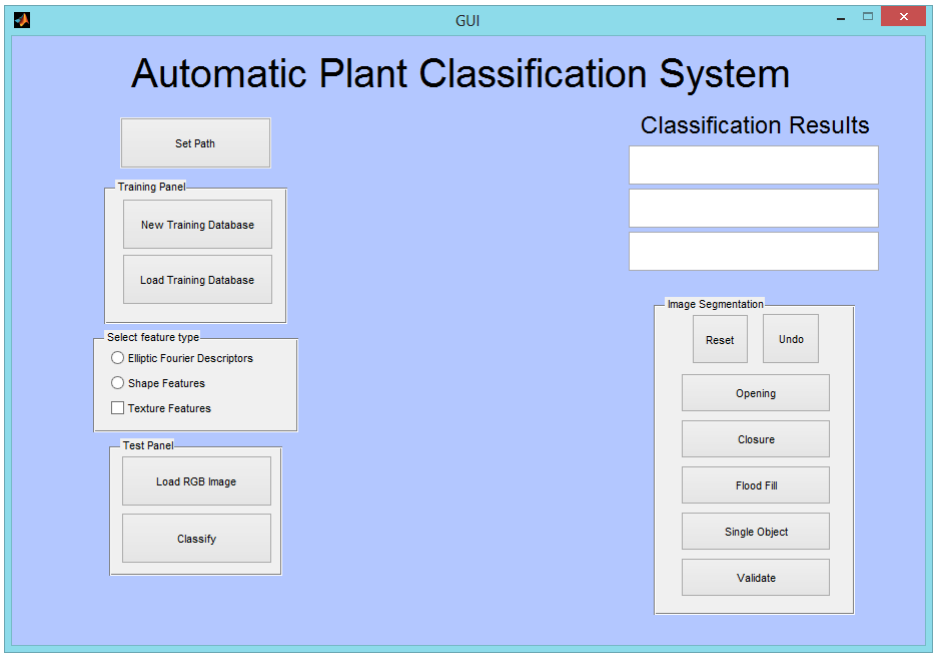

Figure 4.1: Computational Tool: Main Window.

Prior to the utilization of the system, the user must specify the working directory pressing the button *set path*. This button can be used at any time to change the working directory and to indicate a convenient location at each step.

The *training panel* allows the user to either create a new training database or import a previously created training database. The creation of a new feature database is analysed next.

4.1 Creating a new database

Pressing the button *New Training Database* the user gains access to a new window as illustrated in Figure 4.2. This graphic user interface allows the user to automatically segment and extract features from any image database of leaves and save them as a data matrix to the hard drive. For the sake of convenience, original image files should have been labelled according to the rule {*prefix*}_C_{*class number*}_EX{*specimen number*} (for example, iPAD2_C03_EX04.JPG corresponds to an image acquired by the iPAD device, class 3, specimen 4). Both class and specimen number do not need to be sequential.

Clicking on the button *Load RGB Images*, the user may upload to memory all original images to be processed. The imported files are automatically listed in the listbox on the right (cf. Figure 4.2)

The user must indicate at this step which features to extract: either Elliptic Fourier Descriptors or shape features, like previously discussed. The user can furthermore combine any of these shape analysis methods with texture features by clicking on the appropriate checkbox.

Pressing the *Start* button will initiate the sequential processing of the loaded RGB images. On the center of the window both the original RGB image and an automatically obtained binary image are exhibited (cf. Figure 4.2).

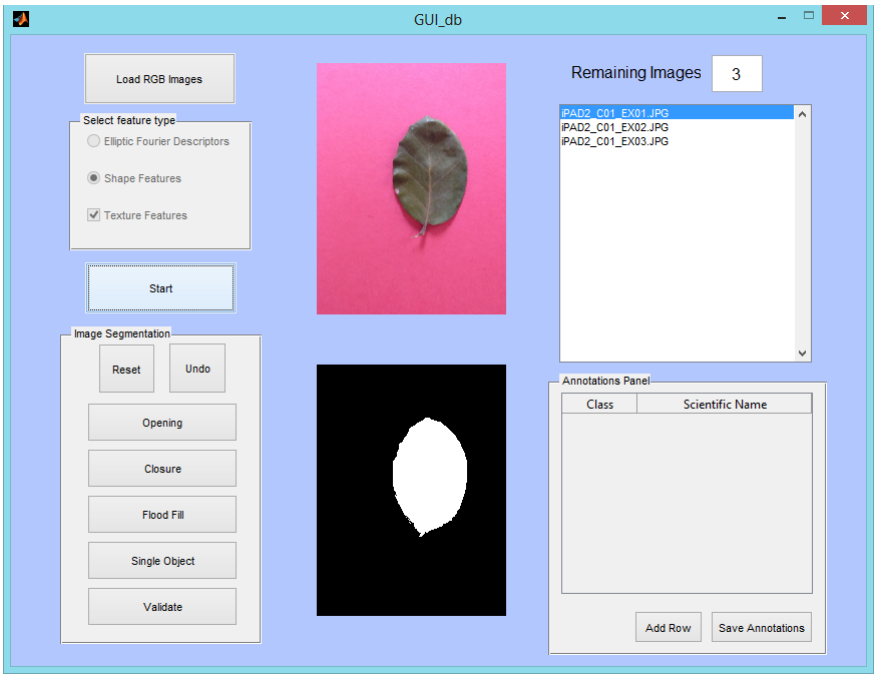

Figure 4.2: Computational Tool: New Database Window.

Before proceeding to feature extraction the user has the opportunity to correct possible problems in the automatic image segmentation process using ordinary morphological operators (opening, closure and flood fill). These include possible problems with particular results of the algorithm but also correction of deformed specimens and petiole removal.

For instance, if a leaf has one or more holes which it would normally not exhibit, the user may correct this problem in the binary image by an application of the flood fill filter. Analogously, some shape deviations on the leaf boundary, which normally would not be present, may also be corrected with morphological operations. As previously remarked, petioles introduce volatility in the classification process and they must be generically removed before feature extraction. The user may achieve this using the morphological operators provided.

The button *Single Object* eliminates any minority connected components possibly existing in the image and ensures that just the largest object (the leaf) remains. This operation is useful for example in the elimination of possible small spots appearing in the image in consequence of uneven illumination in the moment of its acquisition.

When the user is done with the corrections of the segmented image, he/she may press the button *Validate* to continue the process of database construction. If *Single Object* button has not been pressed prior to *Validate*, the programme will automatically eliminate any possible minority connected components and proceed. Pressing *Validate* updates the number of images to be processed and the new file being processed is highlighted in the listbox on the right side. The respective new image as well as its corresponding segmented version are rendered in the window centre.

The segmentation and feature extraction processes continue until all loaded files have been processed. By this time the user is prompted and a name for the developed database must be provided. The system saves the constructed database as a text file in the specified path under this name.

The user may now create an annotations file using the *annotations pannel* at the lower right corner. The annotations file is a convenient way of associating the class number of each considered plant species with its name. This file is used to allow the system to output the plant name instead of the class number.

4.2 Classifying a new observation

To classify an unknown leaf, the user must set the working directory and load a training database and an annotations file. The user must afterwards indicate the original RGB image of the leaf to be processed pressing the button *Load RGB Image* in the *test panel* (cf. Figure 4.1).

Both the original RGB image and its binary version are exhibited in the center of the graphic user interface, as illustrated in Figure 4.2. The user must confirm the results of the segmentation process pressing *Validate*.

The user must indicate afterwards which features to extract (the features used for the construction of the database used as reference). Pressing *classify* after this declaration will initiate the classification process. Inspired by the statistical results discussed along this chapter, linear discriminant analysis with principal component analysis is the classification method chosen for this system.

The system outputs the results of classification in the text boxes at the upper right corner. LDA predicts the class to which a new observation belongs by selecting the class maximizing the posterior probability associated with this new observation. The system uses the posterior probability estimatives computed by LDA to rank the three likeliest classes of origin to the provided new observation. The annotations file is used to convert the predicted classes into the plants names and these are output to the user.

The values of the posterior probabilities are also used as an indicative degree of confidence in the results obtained. A qualitative scale is used to indicate reliability on the predicted class of a given new observation considering the posterior probability estimates of each possible origin class. The system changes the background colours of the text boxes where the results are exhibited according to the following rules: if a given class was predicted with an associated posterior probability below 0.5, the colour red is used; if the probability value was higher than 0.5 and below 0.7, the colour yellow is used; if the posterior probability estimate was higher than 0.7, the colour green is used.

4.3 Limitations

The presentation of this system concludes with the discussion of some of its limitations, using for this effect the test set described in Section 3.2. Figure 4.3 illustrates the result of a successful classification of a leaf specimen of *salix atrocinera* using both shape and texture features.

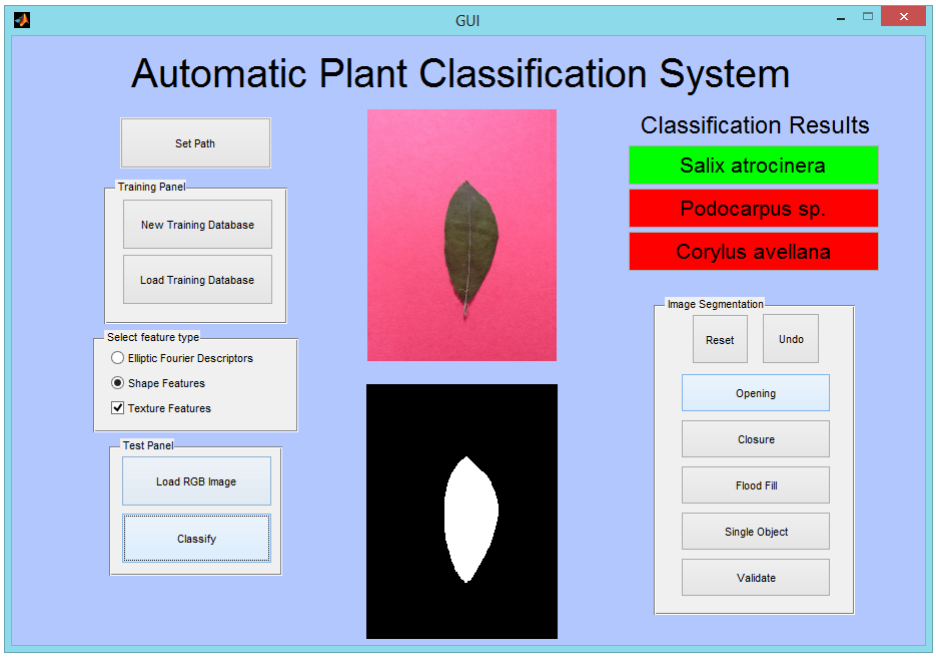

Figure 4.3: Computational Tool: Classifying a new leaf (good result).

The first class suggested corresponds to the real class of origin of the leaf specimen in analysis. The low posterior probability results of the second and third proposed classes are indicated with the red colour. This example illustrates a situation in which the system was able to identify the right plant of origin of the input leaf. This is sometimes not the case and the limitations of the system are those exposed by the statistical results presented in the beginning of this chapter.

Figure 4.4 illustrates the result of an unsuccessful classification of a leaf specimen of *quercus suber* as belonging to the species *corylus avellana*. Notice that the real class is not even proposed by the system.

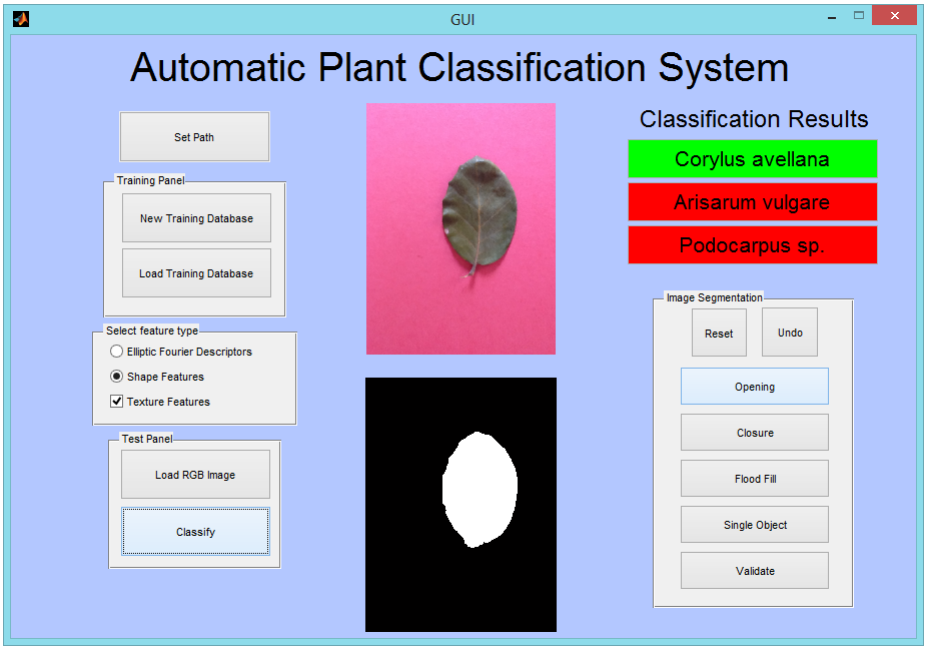

Figure 4.4: Computational Tool: Classifying a new leaf (wrong result).

This case illustrates how the posterior probability can be deceiving and how it should be understood as an indicative result. The false class *corylus avellana* is selected with high posterior probability and the real class *quercus suber* is not even selected as a possible origin class of this observation. Notwithstanding, the leaves of the *corylus avellana* resemble the leaves of the species *quercus suber* to a certain degree. Notice that this situation is not different in terms of output from the successful classification results of Figure 4.3.

Figure 4.5 represents the classification results of the same specimen of *quercus suber* using just shape features. The system indicates new ranked possible plants of origin for this leaf, selecting *ilex perado ssp. azorica* as the most probable source, yet with a low value of posterior probability. The real plant of origin, *quercus suber*, is indicated as the second most probable result but with a low value of posterior probability.

This example illustrates that although the system might sometimes be unable to determine the right class of the given observation, the output results are nonetheless useful, as the user can inspect them and decide whether this leaf could belong to any of the proposed plants.

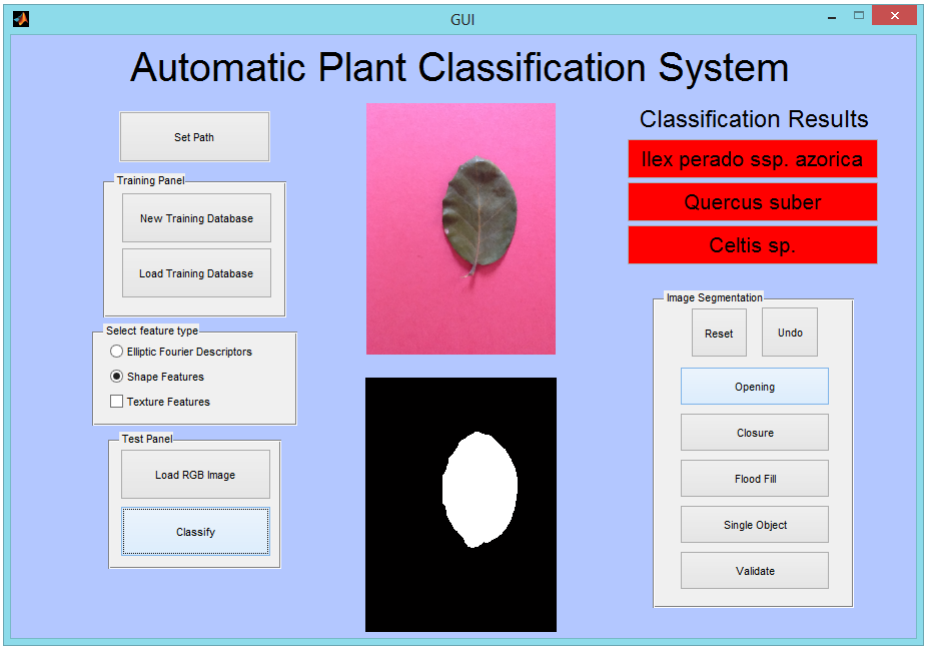

Figure 4.5: Computational Tool: Classifying a new leaf (wrong result).

The success rate of the system is naturally related with the statistical results of the employed analysis methods and features. These depend on several factors such as the number of classes considered and the number of training samples in each class. It is therefore not possible to infer about this system's general success rate. However, both the quantitative results of the classification schemes applied in the test database and the qualitative results of the hierarchical analysis indicate, on average, good classification rates (roughly 80% success).

Hierarchical clustering made clear that shape features could effectively aggregate different leaves according to shape similarity. This means that even if the system is not able to predict the real plant of origin of a given leaf, it is likely able to identify it within the first three options.

This idea is further expanded considering a leaf of a plant not present in the database, namely *physalis*. As this plant is not considered in this database, the system will obviously not be able to identify its origin but it may provide a good approximation in the sense of shape and/or texture resemblance.

Figure 4.6 and Figure 4.7 present the classification results for this new leaf using both shape features and shape features in combination with texture features as analysis methods.

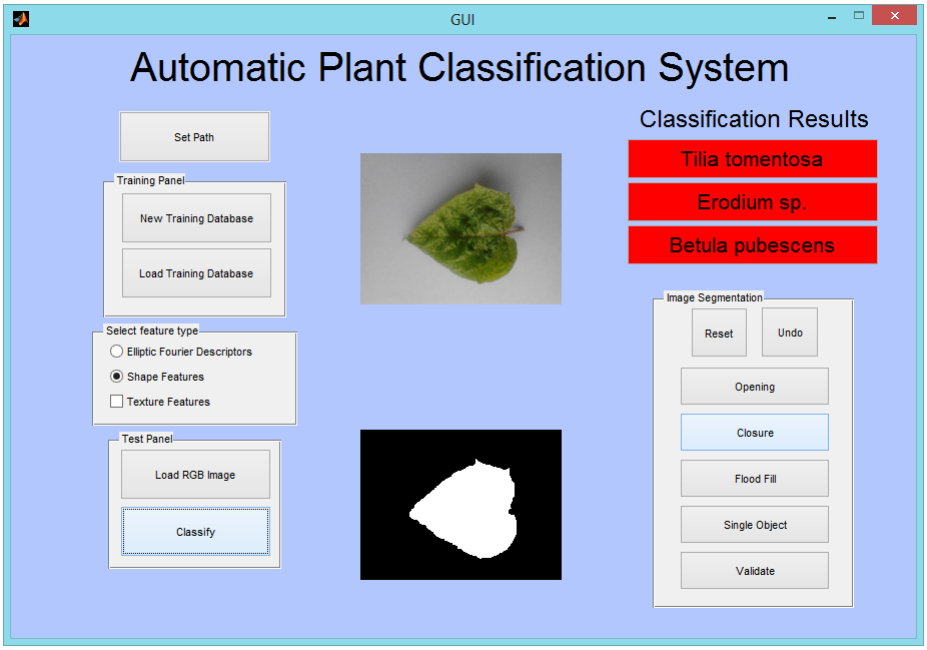

Figure 4.6: Computational Tool: Classifying a leaf of a plant not present in the database.

Considering shape features, *tilia tomentosa*, *erodium sp.* and *betula pubescens* are proposed as the possible plants of origin of the *physalis'* leaf. Notice the shape similarity between this leaf and the leaves of *tilia tomentosa* and *betula pubescens*. *Erodium sp.* does not visually resemble this new leaf. All results were selected with low posterior probability.

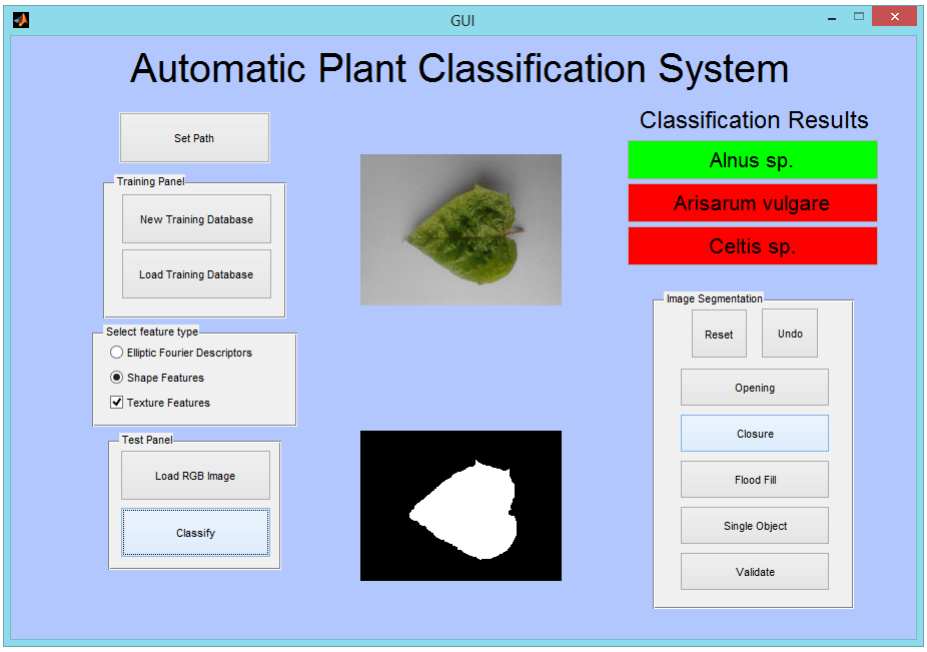

Figure 4.7: Computational Tool: Classifying a leaf of a plant not present in the database.

Considering shape features in conjunction with texture features, *alnus sp.* is proposed with a high result of posterior probability and both *arisarum vulgare* and *celtis sp.* are proposed with low values of posterior probability. The leaves of *alnus sp*, although somewhat different from the leaves of *physalis* in terms of shape, exhibit similar texture and this explains the obtained results.

This example illustrates that in spite of effectively decreasing the misclassification rate for new leaves of plants referenced in the database, the combination of shape and texture features seems to perform worse in providing approximations for the possible origin of leaves which came from plants not referenced in the database.

Shape features may provide the user with good indications of possible plants of origins for a given leaf even if the plant it came from is not referenced and shape features in combination

Altogether, the fragilities of the developed system are the fragilities of the statistical nature of the problem of plant recognition thorough leaf images and the features used for automatic classification.

Although inference is in this case hardly possible, given the huge inter and intra-species variability, the analysis performed in the presented database indicates good possibilities for automatic classification, especially if more than one leaf attribute is taken into consideration.

On the other hand, although the system may often - around 2 in 10 times, considering the cross validation test for the best result - not be able to provide with a single correct answer, the correct answer is tendentiously among the three selected possibilities. The user can use this result to afterwards select the ultimate correct plant by manual inspection. This is already a good achievement both in the case of a user who has no idea of what plant might be the origin of a certain leaf, as well as in the case of a specialist who needs to distinguish from a large number of possibly similar plants.

Chapter 5

Conclusions

In this final chapter, an overview of the work done during the development of this thesis is provided, referring its main contributions and indicating also perspectives of possible future work.

5.1 Contributions

A complete review of the state of the art of image and signal processing techniques as applied to automatic plant recognition with basis in leaf images was provided.

A leaf database considering a wide selection of plants was constructed. A total number of 40 plants with an average number of 10 leaves for each plant was selected and two image databases with a total number of 443 entries were assembled.

A statistical experiment was conducted to test the behaviour of two of the most common shape analysis methods for leaf identification using cross-validation in a randomized training set and a randomized test set, considering the dataset described in Section 3.1. A solution to improve the misclassification rate was proposed through the inclusion of statistical based texture analysis.

A fully functional computer tool was developed for the automatic classification of plants with basis in common images of leaves and a discussion of its limitations was performed. This system was inspired by the statistical analysis carried out and uses simple shape and texture features to identify plants with high accuracy. These results blaze the trail of automatic plant recognition in mobile devices, still further improvements are necessary.

5.2 Future Work

Several possibilities for future work exist, namely:

- expansion of the developed database to contemplate more plants with other types of leaves, and to increase the number of specimens considered for each class;
- development of a classification scheme which could integrate both simple and complex leaves in the same computational application;
- comparison between other techniques not considered in this analysis in order to provide a non-biased evaluation of the classification results;
- development of a classification scheme which could imitate the decisions taxonomers take when classifying leaves.

The developed system could be transformed into a plant disease recognition tool, which is something also very desired in practical applications. This was set as an objective during this thesis but the absence of databases did not allow its fulfilment.

References

[1] Gaurav Agarwal, Peter Belhumeur, Steven Feiner, David Jacobs, W. John Kress, Ravi Ramamoorthi, Norman A. Bourg, Nandan Dixit, Haibin Ling, Dhruv Mahajan, Rusty Russell, Sameer Shirdhonkar, Kalyan Sunkavalli, and Sean White. First steps toward an electronic field guide for plants. *Taxon*, 55(3):597–610, 2006.

[2] I.M. Andrade, S.J. Mayo, D. Kirkup, and C. Berg. Comparative morphology of populations of monstera adans. (araceae) from natural forest fragments in northeast brazil using elliptic fourier analysis of leaf outlines. *Kew Bulletin*, 63(2):193–211, 2008.

[3] André Ricardo Backes, Dalcimar Casanova, and Odemir Martinez Bruno. A complex network-based approach for boundary shape analysis. *Pattern Recognition*, 42(1):54 – 67, 2009.

[4] Odemir Martinez Bruno, Rodrigo de Oliveira Plotze, Mauricio Falvo, and Mário de Castro. Fractal dimension applied to plant identification. *Information Sciences*, 178(12):2722 – 2733, 2008.

[5] James S. Cope, David P. A. Corney, Jonathan Y. Clark, Paolo Remagnino, and Paul Wilkin. Plant species identification using digital morphometrics: A review. *Expert Syst. Appl.*, 39(8):7562–7573, 2012.

[6] Chris Ding and Xiaofeng He. K-means clustering via principal component analysis. In *Proceedings of the twenty-first international conference on Machine learning*, ICML '04, pages 29–, New York, NY, USA, 2004. ACM.

[7] Ji-Xiang Du, De-Shuang Huang, Xiao-Feng Wang, and Xiao Gu. Computer-aided plant species identification (capsi) based on leaf shape matching technique. *Transactions of the Institute of Measurement and Control*, 28(3):275–285, 2006.

[8] Ji-Xiang Du, Xiao-Feng Wang, and Guo-Jun Zhang. Leaf shape based plant species recognition. *Applied Mathematics and Computation*, 185(2):883 – 893, 2007. Special Issue on Intelligent Computing Theory and Methodology.

[9] Ji-Xiang Du, Chuan-Min Zhai, and Qing-Ping Wang. Recognition of plant leaf image based on fractal dimension features. *Neurocomputing*, (0):–, 2012.

[10] Herbert Freeman. Computer processing of line-drawing images. *ACM Comput. Surv.*, 6(1):57–97, March 1974.

[11] Charles R. Giardina and Frank P. Kuhl. Accuracy of curve approximation by harmonically related vectors with elliptical loci. *Computer Graphics and Image Processing*, 6(3):277 – 285, 1977.

[12] Rafael C. Gonzalez and Richard E. Woods. *Digital Image Processing (3rd Edition)*. Prentice-Hall, Inc., Upper Saddle River, NJ, USA, 2006.

[13] A. John Haines and James S. Crampton. Improvements to the method of fourier shape analysis as applied in morphometric studies. *Palaeontology*, 43(4):765–783, 2000.

[14] David J. Hearn. Shape analysis for the automated identification of plants from images of leaves. *Taxon*, 58(3):934–954, 2009.

[15] J. Hemming and T. Rath. Precision agriculture: Computer-vision-based weed identification under field conditions using controlled lighting. *Journal of Agricultural Engineering Research*, 78(3):233 – 243, 2001.

[16] J. Hossain and M.A. Amin. Leaf shape identification based plant biometrics. In *Computer and Information Technology (ICCIT), 2010 13th International Conference on*, pages 458–463, 2010.

[17] Rongxiang Hu, Wei Jia, Haibin Ling, and Deshuang Huang. Multiscale distance matrix for fast plant leaf recognition. *Image Processing, IEEE Transactions on*, 21(11):4667–4672, 2012.

[18] Suckchul Kim, Yoonsik Tak, Yunyoung Nam, and Eenjun Hwang. mclover: mobile content-based leaf image retrieval system. In *Proceedings of the 13th annual ACM international conference on Multimedia*, MULTIMEDIA '05, pages 215–216, New York, NY, USA, 2005. ACM.

[19] Frank P. Kuhl and Charles R. Giardina. Elliptic Fourier features of a closed contour. 18(3):236–258, March 1982.

[20] Tracy McLellan and John A. Endler. The relative success of some methods for measuring and describing the shape of complex objects. *Systematic Biology*, 47(2):264–281, 1998.

[21] F. Mokhtarian and S. Abbasi. Matching shapes with self-intersections:application to leaf classification. *Image Processing, IEEE Transactions on*, 13(5):653–661, 2004.

[22] João Camargo Neto, George E. Meyer, David D. Jones, and Ashok K. Samal. Plant species identification using elliptic fourier leaf shape analysis. *Comput. Electron. Agric.*, 50(2):121–134, February 2006.

[23] Perner P. Image mining: issues, framework, a generic tool and its application to medical-image diagnosis. *Engineering Applications of Artificial Intelligence*, 15(2):205–216, 2002.

[24] Eric J. Pauwels, Paul M. de Zeeuw, and Elena Ranguelova. Computer-assisted tree taxonomy by automated image recognition. *Eng. Appl. of AI*, 22(1):26–31, 2009.

[25] W. Petry and W. Kühbauch. Automatisierte unterscheidung von unkrautarten nach formparametern mit hilfe der quantitativen bildanalyse. *Journal of Agronomy and Crop Science*, 163(5):345–351, 1989.

[26] D.L. Royer. Stomatal density and stomatal index as indicators of paleoatmospheric {CO2} concentration. *Review of Palaeobotany and Palynology*, 114(1-2):1–28, 2001.

[27] Pedro F. B. Silva, Andre R. S. Marcal, and Rubim M. Almeida da Silva. Evaluation of features for leaf discrimination. In Springer Verlag, editor, *Springer Lecture Notes on Computer Science*, volume 7950, pages 197–205, 2013.

[28] Oskar J. O. Söderkvist. Computer vision classification of leaves from swedish trees. Master's thesis, Linköoping University, September 2001.

[29] Xiao-Feng Wang, Ji-Xiang Du, and Guo-Jun Zhang. Recognition of leaf images based on shape features using a hypersphere classifier. In *Proceedings of the 2005 international conference on Advances in Intelligent Computing - Volume Part I*, ICIC'05, pages 87–96, Berlin, Heidelberg, 2005. Springer-Verlag.

[30] Z. Wang, Z. Chi, and D. Feng. Shape based leaf image retrieval. *Vision, Image and Signal Processing, IEE Proceedings* -, 150(1):34–43, 2003.

[31] Zhiyong Wang, Zheru Chi, Dagan Feng, and Qing Wang. Leaf image retrieval with shape features. In *Proceedings of the 4th International Conference on Advances in Visual Information Systems*, VISUAL '00, pages 477–487, London, UK, UK, 2000. Springer-Verlag.

[32] S.G. Wu, F.S. Bao, E.Y. Xu, Yu-Xuan Wang, Yi-Fan Chang, and Qiao-Liang Xiang. A leaf recognition algorithm for plant classification using probabilistic neural network.

In *Signal Processing and Information Technology, 2007 IEEE International Symposium on*, pages 11–16, 2007.

[33] Zheng Xiao-Dong and Wang Xiao-Jie. Feature extraction of plant leaf based on visual consistency. In *Computer Network and Multimedia Technology, 2009. CNMT 2009. International Symposium on*, pages 1–4, 2009.

[34] Lexiang Ye and Eamonn Keogh. Time series shapelets: a new primitive for data mining. In *Proceedings of the 15th ACM SIGKDD international conference on Knowledge discovery and data mining*, KDD '09, pages 947–956, New York, NY, USA, 2009. ACM.

[35] Dengsheng Zhang and Guojun Lu. Study and evaluation of different fourier methods for image retrieval. *Image and Vision Computing*, 23(1):33 – 49, 2005.

[36] Shanwen Zhang and Ying-Ke Lei. Modified locally linear discriminant embedding for plant leaf recognition. *Neurocomput.*, 74(14-15):2284–2290, July 2011.

[37] Shanwen Zhang, Ying-Ke Lei, and Yan-Hua Wu. Semi-supervised locally discriminant projection for classification and recognition. *Know.-Based Syst.*, 24(2):341–346, March 2011.

[38] Shanwen Zhang, Yingke Lei, Tianbao Dong, and Xiao-Ping Zhang. Label propagation based supervised locality projection analysis for plant leaf classification. *Pattern Recogn.*, 46(7):1891–1897, July 2013.

[39] Xiaodong Zheng and Xiaojie Wang. Leaf vein extraction using a combined operation of mathematical morphology. In *Information Engineering and Computer Science (ICIECS), 2010 2nd International Conference on*, pages 1–4, 2010.

Appendix


'iPAD2_C01_EX01.JPG'

'iPAD2_C01_EX02.JPG'

'iPAD2_C01_EX03.JPG'
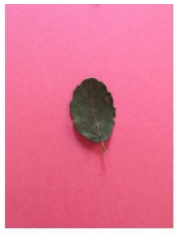
'iPAD2_C01_EX04.JPG'
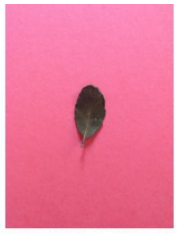
'iPAD2_C01_EX05.JPG'

'iPAD2_C01_EX06.JPG'
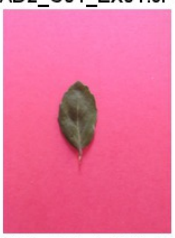
'iPAD2_C01_EX07.JPG'

'iPAD2_C01_EX08.JPG'
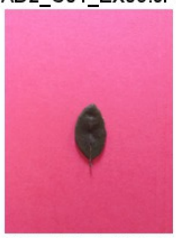
'iPAD2_C01_EX09.JPG'
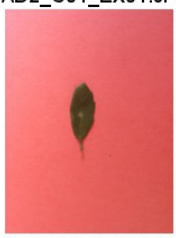
'iPAD2_C01_EX10.JPG'

'iPAD2_C01_EX11.JPG'

'iPAD2_C01_EX12.JPG'

'iPAD2_C02_EX01.JPG'

'iPAD2_C02_EX02.JPG'

'iPAD2_C02_EX03.JPG'

'iPAD2_C02_EX04.JPG'

'iPAD2_C02_EX05.JPG'

'iPAD2_C02_EX06.JPG'

'iPAD2_C02_EX07.JPG'

'iPAD2_C02_EX08.JPG'

'iPAD2_C02_EX09.JPG'

'iPAD2_C02_EX10.JPG'

'iPAD2_C03_EX01.JPG'

'iPAD2_C03_EX02.JPG'

'iPAD2_C03_EX03.JPG'

'iPAD2_C03_EX04.JPG'

'iPAD2_C03_EX05.JPG'

'iPAD2_C03_EX06.JPG'

'iPAD2_C03_EX07.JPG'

'iPAD2_C03_EX08.JPG'

'iPAD2_C03_EX09.JPG'

'iPAD2_C03_EX10.JPG'

'iPAD2_C04_EX01.JPG'

'iPAD2_C04_EX02.JPG'

'iPAD2_C04_EX03.JPG'

'iPAD2_C04_EX04.JPG'

'iPAD2_C04_EX05.JPG'

'iPAD2_C04_EX06.JPG'

'iPAD2_C04_EX07.JPG'

'iPAD2_C04_EX08.JPG'

'iPAD2_C05_EX01.JPG'

'iPAD2_C05_EX02.JPG'

'iPAD2_C05_EX03.JPG'

'iPAD2_C05_EX04.JPG'

'iPAD2_C05_EX05.JPG'

'iPAD2_C05_EX06.JPG'

'iPAD2_C05_EX07.JPG'

'iPAD2_C05_EX08.JPG'

'iPAD2_C05_EX09.JPG' 'iPAD2_C05_EX10.JPG' 'iPAD2_C05_EX11.JPG' 'iPAD2_C05_EX12.JPG' 'iPAD2_C06_EX01.JPG' 'iPAD2_C06_EX02.JPG'

'iPAD2_C06_EX03.JPG' 'iPAD2_C06_EX04.JPG' 'iPAD2_C06_EX05.JPG' 'iPAD2_C06_EX06.JPG' 'iPAD2_C06_EX07.JPG' 'iPAD2_C06_EX08.JPG'

'iPAD2_C07_EX01.JPG' 'iPAD2_C07_EX02.JPG' 'iPAD2_C07_EX03.JPG' 'iPAD2_C07_EX04.JPG' 'iPAD2_C07_EX05.JPG' 'iPAD2_C07_EX06.JPG'

'iPAD2_C07_EX07.JPG' 'iPAD2_C07_EX08.JPG' 'iPAD2_C07_EX09.JPG' 'iPAD2_C07_EX10.JPG' 'iPAD2_C08_EX01.JPG' 'iPAD2_C08_EX02.JPG'

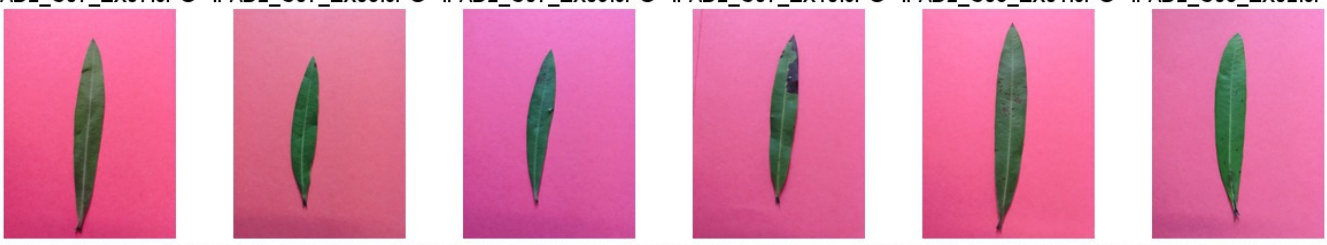

'iPAD2_C08_EX03.JPG' 'iPAD2_C08_EX04.JPG' 'iPAD2_C08_EX05.JPG' 'iPAD2_C08_EX06.JPG' 'iPAD2_C08_EX07.JPG' 'iPAD2_C08_EX08.JPG'

'iPAD2_C08_EX09.JPG' 'iPAD2_C08_EX10.JPG' 'iPAD2_C08_EX11.JPG' 'iPAD2_C09_EX01.JPG' 'iPAD2_C09_EX02.JPG' 'iPAD2_C09_EX03.JPG'

'iPAD2_C09_EX04.JPG' 'iPAD2_C09_EX05.JPG' 'iPAD2_C09_EX06.JPG' 'iPAD2_C09_EX07.JPG' 'iPAD2_C09_EX08.JPG' 'iPAD2_C09_EX09.JPG'

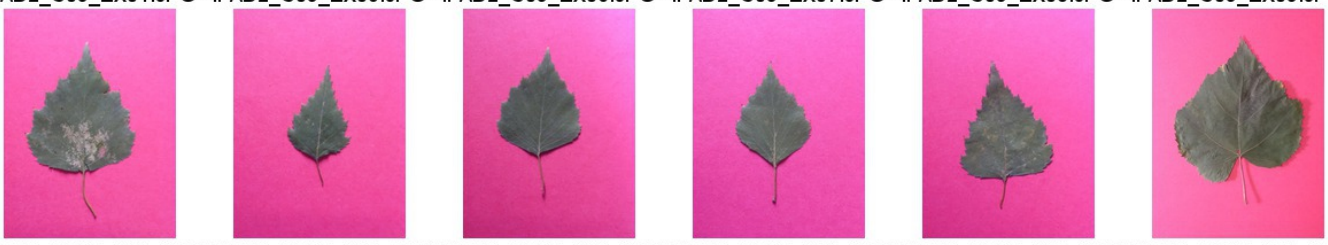

'iPAD2_C09_EX10.JPG' 'iPAD2_C09_EX11.JPG' 'iPAD2_C09_EX12.JPG' 'iPAD2_C09_EX13.JPG' 'iPAD2_C09_EX14.JPG' 'iPAD2_C10_EX01.JPG'

'iPAD2_C10_EX02.JPG' 'iPAD2_C10_EX03.JPG' 'iPAD2_C10_EX04.JPG' 'iPAD2_C10_EX05.JPG' 'iPAD2_C10_EX06.JPG' 'iPAD2_C10_EX07.JPG'

'iPAD2_C10_EX08.JPG' 'iPAD2_C10_EX09.JPG' 'iPAD2_C10_EX10.JPG' 'iPAD2_C10_EX11.JPG' 'iPAD2_C10_EX12.JPG' 'iPAD2_C10_EX13.JPG'

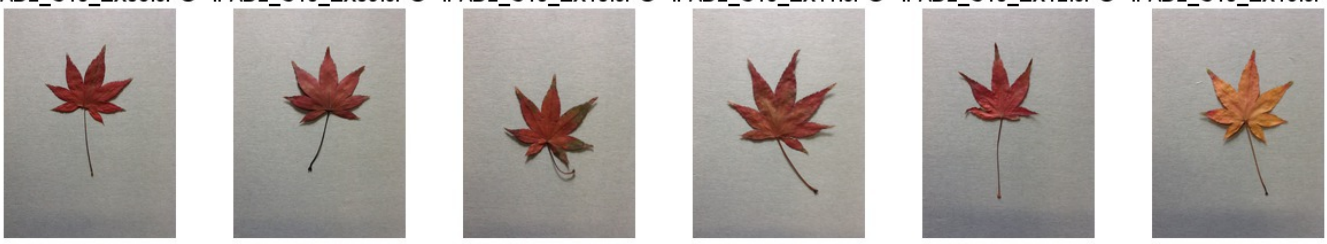

'iPAD2_C11_EX01.JPG' 'iPAD2_C11_EX02.JPG' 'iPAD2_C11_EX03.JPG' 'iPAD2_C11_EX04.JPG' 'iPAD2_C11_EX05.JPG' 'iPAD2_C11_EX06.JPG'

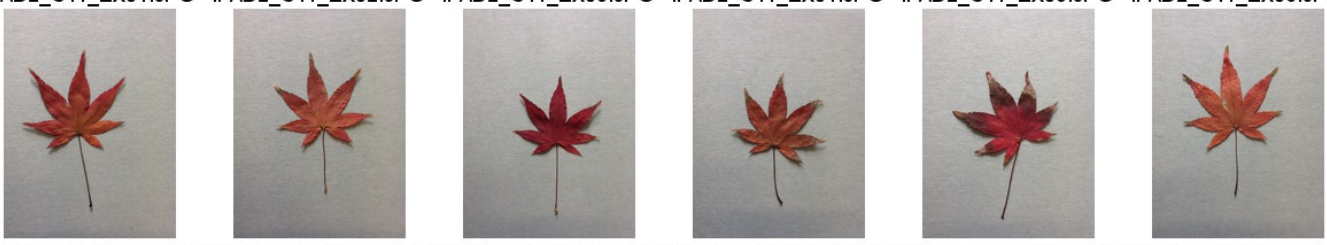

'iPAD2_C11_EX07.JPG' 'iPAD2_C11_EX08.JPG' 'iPAD2_C11_EX09.JPG' 'iPAD2_C11_EX10.JPG' 'iPAD2_C11_EX11.JPG' 'iPAD2_C11_EX12.JPG'

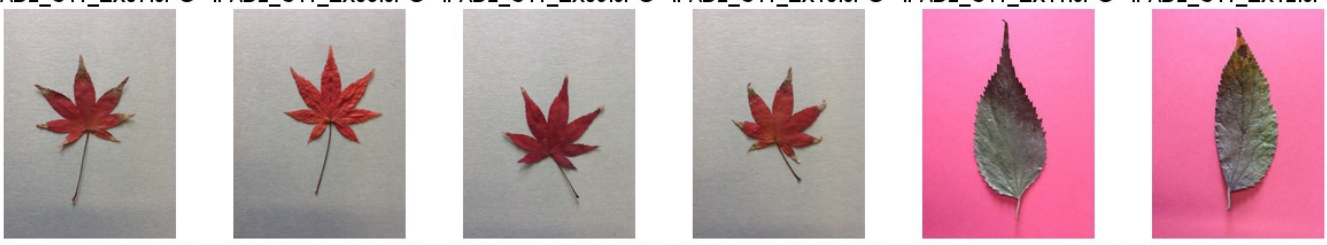

'iPAD2_C11_EX13.JPG' 'iPAD2_C11_EX14.JPG' 'iPAD2_C11_EX15.JPG' 'iPAD2_C11_EX16.JPG' 'iPAD2_C12_EX01.JPG' 'iPAD2_C12_EX02.JPG'

'iPAD2_C12_EX03.JPG' 'iPAD2_C12_EX04.JPG' 'iPAD2_C12_EX05.JPG' 'iPAD2_C12_EX06.JPG' 'iPAD2_C12_EX07.JPG' 'iPAD2_C12_EX08.JPG'

'iPAD2_C12_EX09.JPG' 'iPAD2_C12_EX10.JPG' 'iPAD2_C12_EX11.JPG' 'iPAD2_C12_EX12.JPG' 'iPAD2_C13_EX01.JPG' 'iPAD2_C13_EX02.JPG'

'iPAD2_C13_EX03.JPG' 'iPAD2_C13_EX04.JPG' 'iPAD2_C13_EX05.JPG' 'iPAD2_C13_EX06.JPG' 'iPAD2_C13_EX07.JPG' 'iPAD2_C13_EX08.JPG'

'iPAD2_C13_EX09.JPG' 'iPAD2_C13_EX10.JPG' 'iPAD2_C13_EX11.JPG' 'iPAD2_C13_EX12.JPG' 'iPAD2_C13_EX13.JPG' 'iPAD2_C14_EX01.JPG'

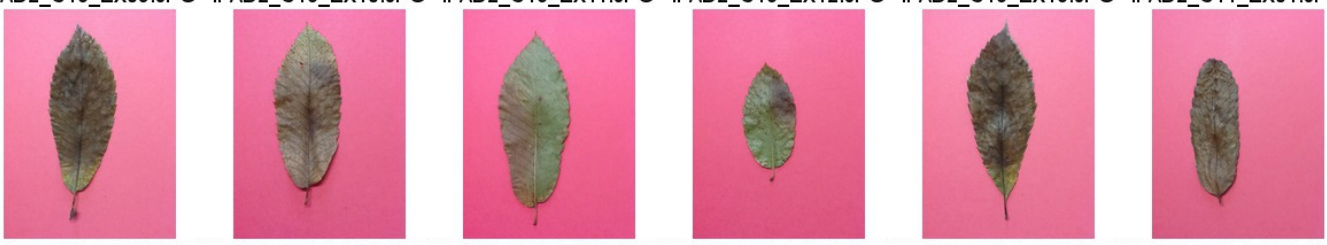

'iPAD2_C14_EX02.JPG' 'iPAD2_C14_EX03.JPG' 'iPAD2_C14_EX04.JPG' 'iPAD2_C14_EX05.JPG' 'iPAD2_C14_EX06.JPG' 'iPAD2_C14_EX07.JPG'

'iPAD2_C14_EX08.JPG' 'iPAD2_C14_EX09.JPG' 'iPAD2_C14_EX10.JPG' 'iPAD2_C14_EX11.JPG' 'iPAD2_C14_EX12.JPG' 'iPAD2_C15_EX01.JPG'

'iPAD2_C15_EX02.JPG' 'iPAD2_C15_EX03.JPG' 'iPAD2_C15_EX04.JPG' 'iPAD2_C15_EX05.JPG' 'iPAD2_C15_EX06.JPG' 'iPAD2_C15_EX07.JPG'

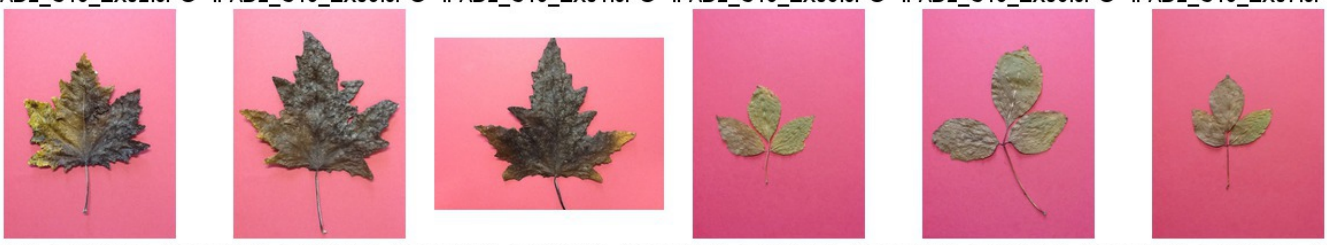

'iPAD2_C15_EX08.JPG' 'iPAD2_C15_EX09.JPG' 'iPAD2_C15_EX10.JPG' 'iPAD2_C16_EX01.JPG' 'iPAD2_C16_EX02.JPG' 'iPAD2_C16_EX03.JPG'

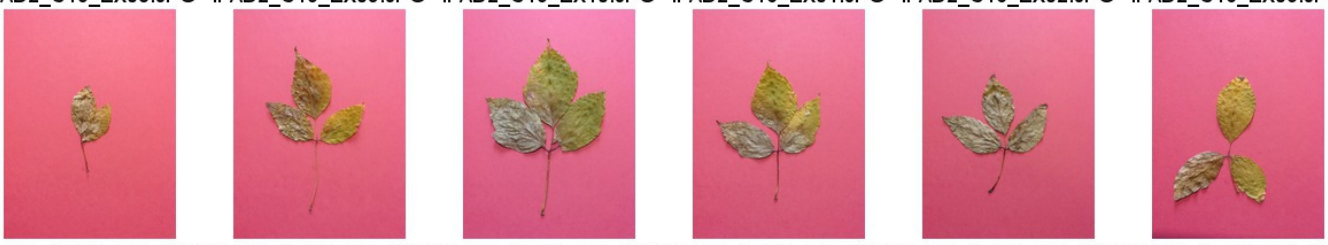

'iPAD2_C16_EX04.JPG' 'iPAD2_C16_EX05.JPG' 'iPAD2_C16_EX06.JPG' 'iPAD2_C16_EX07.JPG' 'iPAD2_C16_EX08.JPG' 'iPAD2_C16_EX09.JPG'

'iPAD2_C16_EX10.JPG' 'iPAD2_C17_EX01.JPG' 'iPAD2_C17_EX02.JPG' 'iPAD2_C17_EX03.JPG' 'iPAD2_C17_EX04.JPG' 'iPAD2_C17_EX05.JPG'

'iPAD2_C18_EX01.JPG' 'iPAD2_C18_EX02.JPG' 'iPAD2_C18_EX03.JPG' 'iPAD2_C18_EX04.JPG' 'iPAD2_C18_EX05.JPG' 'iPAD2_C18_EX06.JPG'

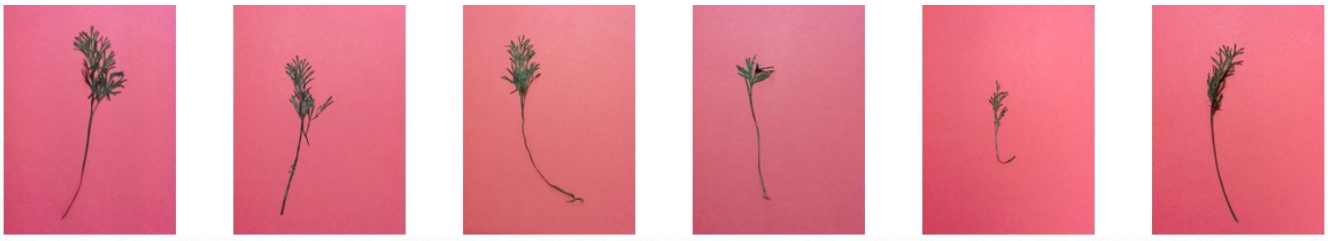

'iPAD2_C18_EX07.JPG' 'iPAD2_C18_EX08.JPG' 'iPAD2_C18_EX09.JPG' 'iPAD2_C18_EX10.JPG' 'iPAD2_C18_EX11.JPG' 'iPAD2_C18_EX12.JPG'

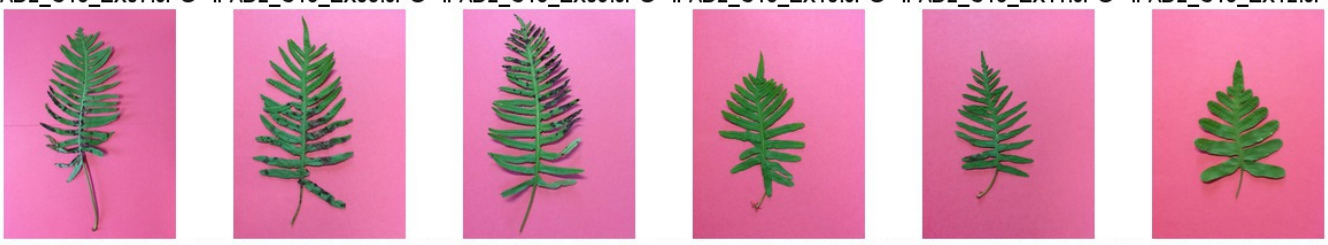

'iPAD2_C19_EX01.JPG' 'iPAD2_C19_EX02.JPG' 'iPAD2_C19_EX03.JPG' 'iPAD2_C19_EX04.JPG' 'iPAD2_C19_EX05.JPG' 'iPAD2_C19_EX06.JPG'

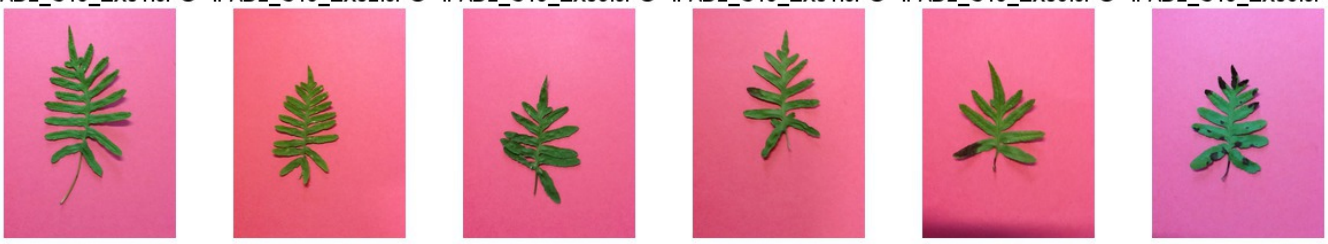

'iPAD2_C19_EX07.JPG' 'iPAD2_C19_EX08.JPG' 'iPAD2_C19_EX09.JPG' 'iPAD2_C19_EX10.JPG' 'iPAD2_C19_EX11.JPG' 'iPAD2_C19_EX12.JPG'

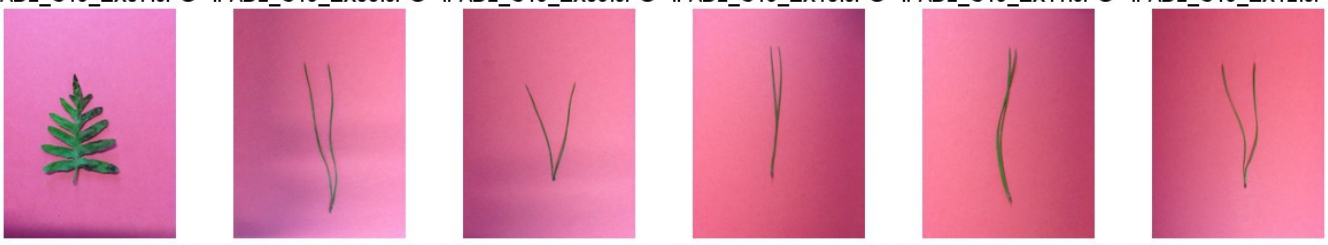

'iPAD2_C19_EX13.JPG' 'iPAD2_C20_EX01.JPG' 'iPAD2_C20_EX02.JPG' 'iPAD2_C20_EX03.JPG' 'iPAD2_C20_EX04.JPG' 'iPAD2_C20_EX05.JPG'

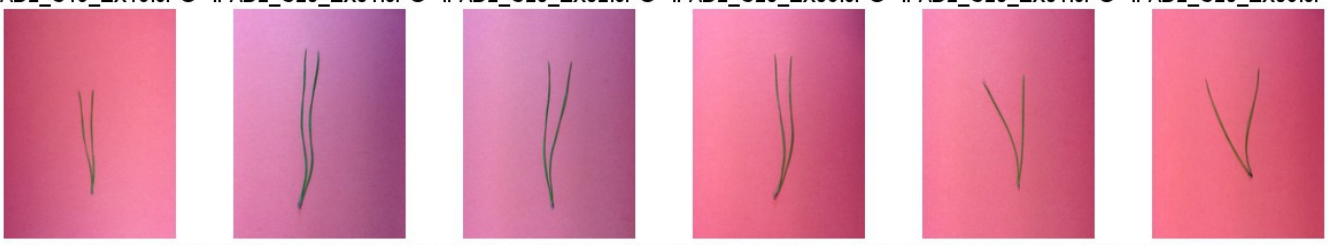

'iPAD2_C20_EX06.JPG' 'iPAD2_C20_EX07.JPG' 'iPAD2_C20_EX08.JPG' 'iPAD2_C20_EX09.JPG' 'iPAD2_C20_EX10.JPG' 'iPAD2_C20_EX11.JPG'

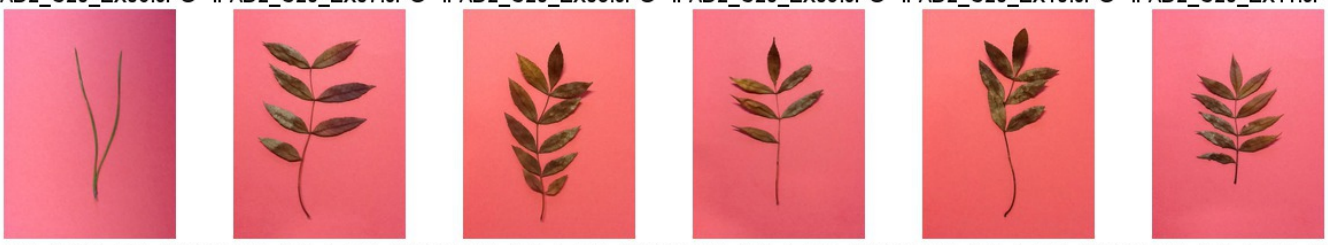

'iPAD2_C20_EX12.JPG' 'iPAD2_C21_EX01.JPG' 'iPAD2_C21_EX02.JPG' 'iPAD2_C21_EX03.JPG' 'iPAD2_C21_EX04.JPG' 'iPAD2_C21_EX05.JPG'

'iPAD2_C21_EX06.JPG' 'iPAD2_C21_EX07.JPG' 'iPAD2_C21_EX08.JPG' 'iPAD2_C21_EX09.JPG' 'iPAD2_C21_EX10.JPG' 'iPAD2_C22_EX01.JPG'

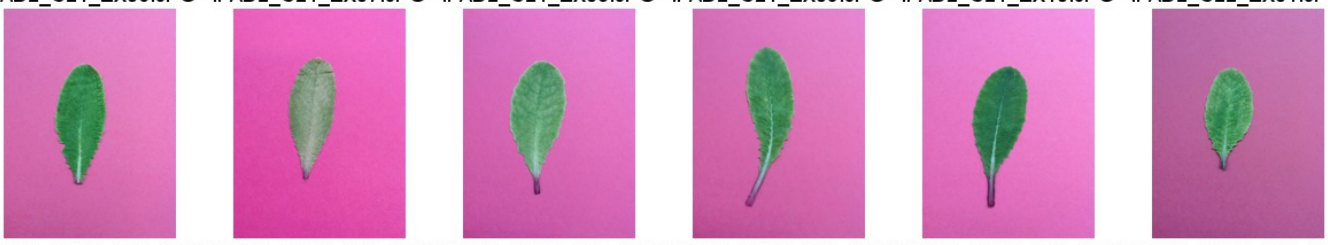

'iPAD2_C22_EX02.JPG' 'iPAD2_C22_EX03.JPG' 'iPAD2_C22_EX04.JPG' 'iPAD2_C22_EX05.JPG' 'iPAD2_C22_EX06.JPG' 'iPAD2_C22_EX07.JPG'

'iPAD2_C22_EX08.JPG' 'iPAD2_C22_EX09.JPG' 'iPAD2_C22_EX10.JPG' 'iPAD2_C22_EX11.JPG' 'iPAD2_C22_EX12.JPG' 'iPAD2_C23_EX01.JPG'

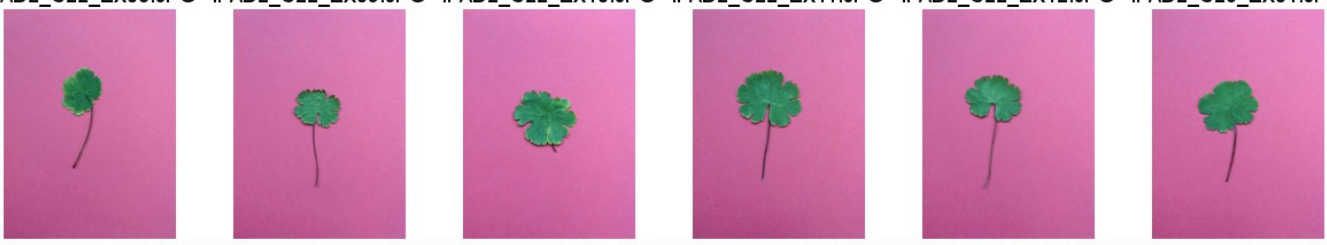

'iPAD2_C23_EX02.JPG' 'iPAD2_C23_EX03.JPG' 'iPAD2_C23_EX04.JPG' 'iPAD2_C23_EX05.JPG' 'iPAD2_C23_EX06.JPG' 'iPAD2_C23_EX07.JPG'

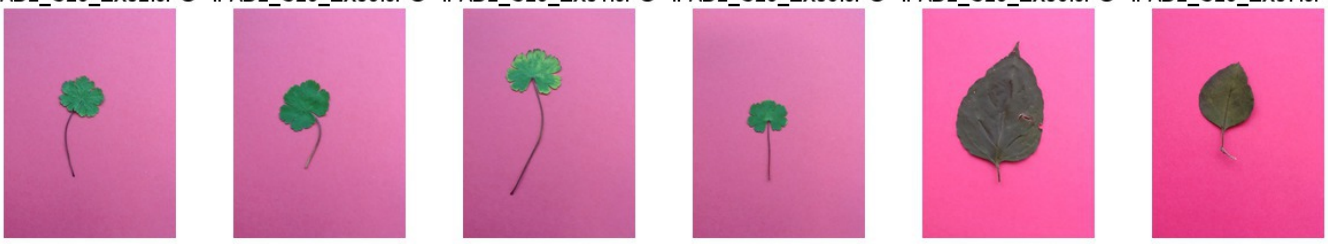

'iPAD2_C23_EX08.JPG' 'iPAD2_C23_EX09.JPG' 'iPAD2_C23_EX10.JPG' 'iPAD2_C23_EX11.JPG' 'iPAD2_C24_EX01.JPG' 'iPAD2_C24_EX02.JPG'

'iPAD2_C24_EX03.JPG' 'iPAD2_C24_EX04.JPG' 'iPAD2_C24_EX05.JPG' 'iPAD2_C24_EX06.JPG' 'iPAD2_C24_EX07.JPG' 'iPAD2_C24_EX08.JPG'

'iPAD2_C24_EX09.JPG' 'iPAD2_C24_EX10.JPG' 'iPAD2_C24_EX11.JPG' 'iPAD2_C24_EX12.JPG' 'iPAD2_C24_EX13.JPG' 'iPAD2_C25_EX01.JPG'

'iPAD2_C25_EX02.JPG' 'iPAD2_C25_EX03.JPG' 'iPAD2_C25_EX04.JPG' 'iPAD2_C25_EX05.JPG' 'iPAD2_C25_EX06.JPG' 'iPAD2_C25_EX07.JPG'

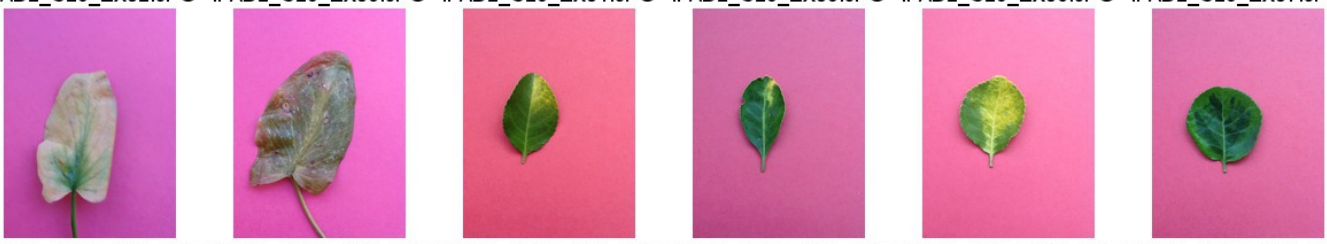

'iPAD2_C25_EX08.JPG' 'iPAD2_C25_EX09.JPG' 'iPAD2_C26_EX01.JPG' 'iPAD2_C26_EX02.JPG' 'iPAD2_C26_EX03.JPG' 'iPAD2_C26_EX04.JPG'

'iPAD2_C26_EX05.JPG' 'iPAD2_C26_EX06.JPG' 'iPAD2_C26_EX07.JPG' 'iPAD2_C26_EX08.JPG' 'iPAD2_C26_EX09.JPG' 'iPAD2_C26_EX10.JPG'

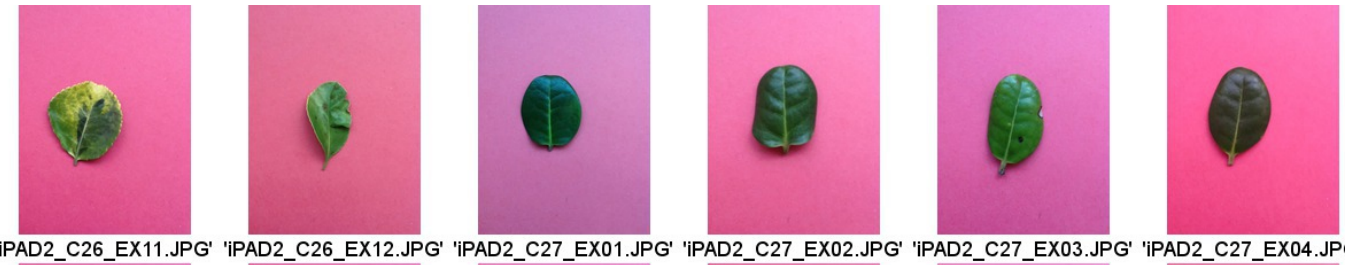
'iPAD2_C26_EX11.JPG' 'iPAD2_C26_EX12.JPG' 'iPAD2_C27_EX01.JPG' 'iPAD2_C27_EX02.JPG' 'iPAD2_C27_EX03.JPG' 'iPAD2_C27_EX04.JPG'


'iPAD2_C27_EX05.JPG' 'iPAD2_C27_EX06.JPG' 'iPAD2_C27_EX07.JPG' 'iPAD2_C27_EX08.JPG' 'iPAD2_C27_EX09.JPG' 'iPAD2_C27_EX10.JPG'


'iPAD2_C27_EX11.JPG' 'iPAD2_C28_EX01.JPG' 'iPAD2_C28_EX02.JPG' 'iPAD2_C28_EX03.JPG' 'iPAD2_C28_EX04.JPG' 'iPAD2_C28_EX05.JPG'


'iPAD2_C28_EX06.JPG' 'iPAD2_C28_EX07.JPG' 'iPAD2_C28_EX08.JPG' 'iPAD2_C28_EX09.JPG' 'iPAD2_C28_EX10.JPG' 'iPAD2_C28_EX11.JPG'

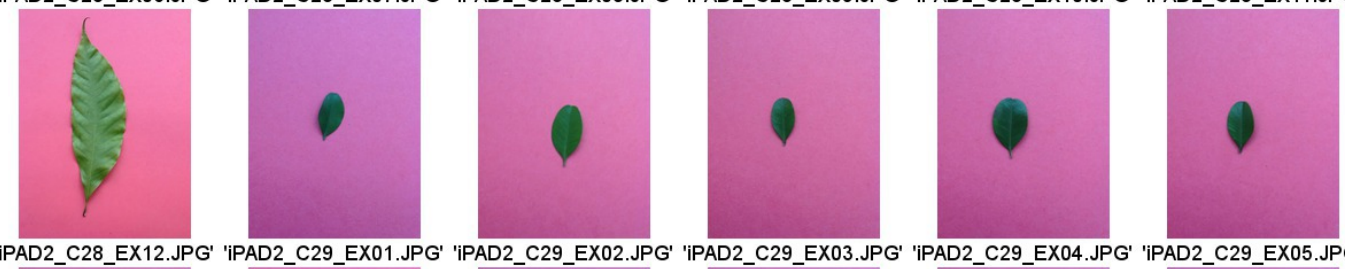
'iPAD2_C28_EX12.JPG' 'iPAD2_C29_EX01.JPG' 'iPAD2_C29_EX02.JPG' 'iPAD2_C29_EX03.JPG' 'iPAD2_C29_EX04.JPG' 'iPAD2_C29_EX05.JPG'

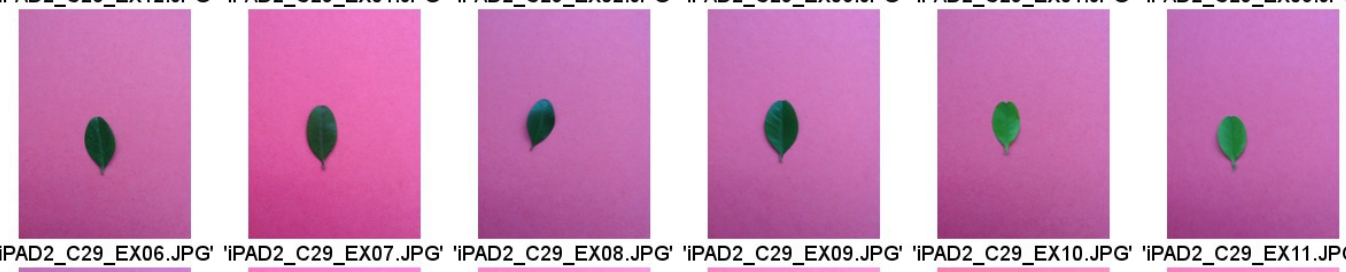
'iPAD2_C29_EX06.JPG' 'iPAD2_C29_EX07.JPG' 'iPAD2_C29_EX08.JPG' 'iPAD2_C29_EX09.JPG' 'iPAD2_C29_EX10.JPG' 'iPAD2_C29_EX11.JPG'


'iPAD2_C29_EX12.JPG' 'iPAD2_C30_EX01.JPG' 'iPAD2_C30_EX02.JPG' 'iPAD2_C30_EX03.JPG' 'iPAD2_C30_EX04.JPG' 'iPAD2_C30_EX05.JPG'


'iPAD2_C30_EX06.JPG' 'iPAD2_C30_EX07.JPG' 'iPAD2_C30_EX08.JPG' 'iPAD2_C30_EX09.JPG' 'iPAD2_C30_EX10.JPG' 'iPAD2_C30_EX11.JPG'

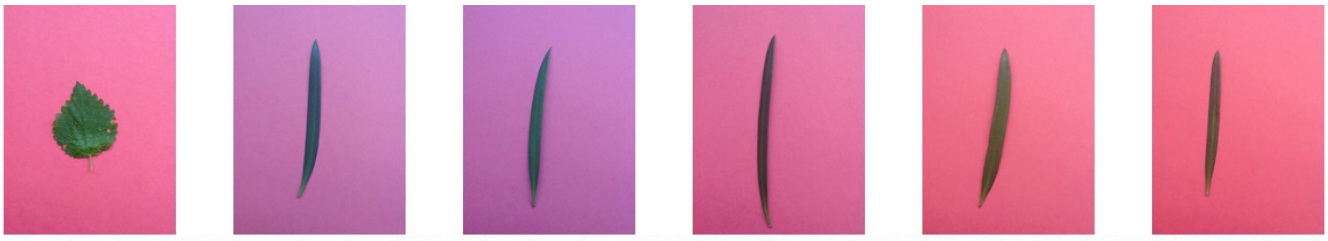

'iPAD2_C30_EX12.JPG' 'iPAD2_C31_EX01.JPG' 'iPAD2_C31_EX02.JPG' 'iPAD2_C31_EX03.JPG' 'iPAD2_C31_EX04.JPG' 'iPAD2_C31_EX05.JPG'

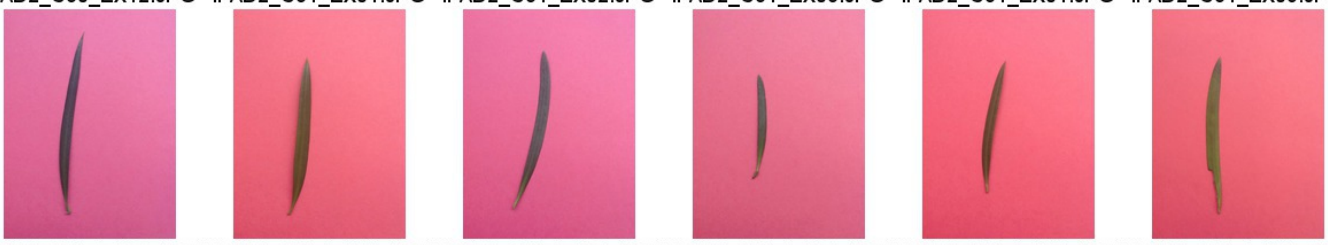

'iPAD2_C31_EX06.JPG' 'iPAD2_C31_EX07.JPG' 'iPAD2_C31_EX08.JPG' 'iPAD2_C31_EX09.JPG' 'iPAD2_C31_EX10.JPG' 'iPAD2_C31_EX11.JPG'

'iPAD2_C32_EX01.JPG' 'iPAD2_C32_EX02.JPG' 'iPAD2_C32_EX03.JPG' 'iPAD2_C32_EX04.JPG' 'iPAD2_C32_EX05.JPG' 'iPAD2_C32_EX06.JPG'

'iPAD2_C32_EX07.JPG' 'iPAD2_C32_EX08.JPG' 'iPAD2_C32_EX09.JPG' 'iPAD2_C32_EX10.JPG' 'iPAD2_C32_EX11.JPG' 'iPAD2_C33_EX01.JPG'

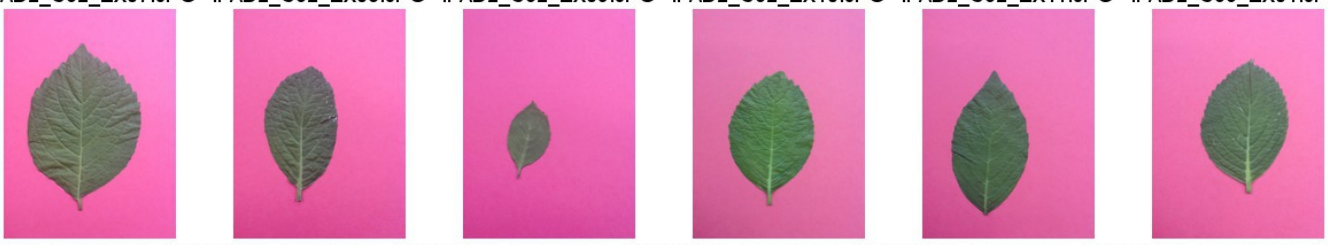

'iPAD2_C33_EX02.JPG' 'iPAD2_C33_EX03.JPG' 'iPAD2_C33_EX04.JPG' 'iPAD2_C33_EX05.JPG' 'iPAD2_C33_EX06.JPG' 'iPAD2_C33_EX07.JPG'

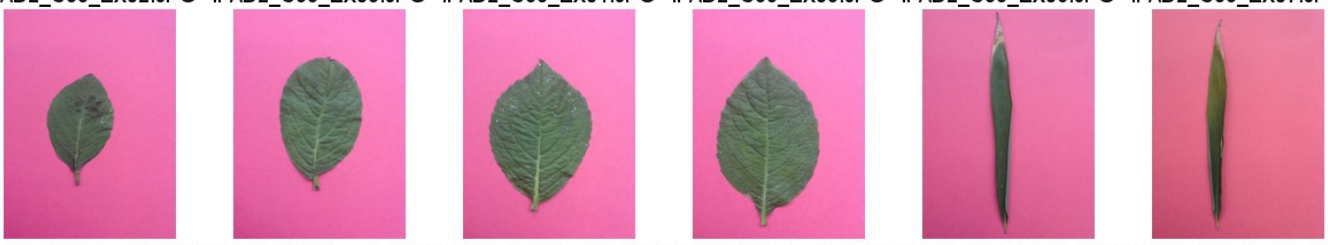

'iPAD2_C33_EX08.JPG' 'iPAD2_C33_EX09.JPG' 'iPAD2_C33_EX10.JPG' 'iPAD2_C33_EX11.JPG' 'iPAD2_C34_EX01.JPG' 'iPAD2_C34_EX02.JPG'

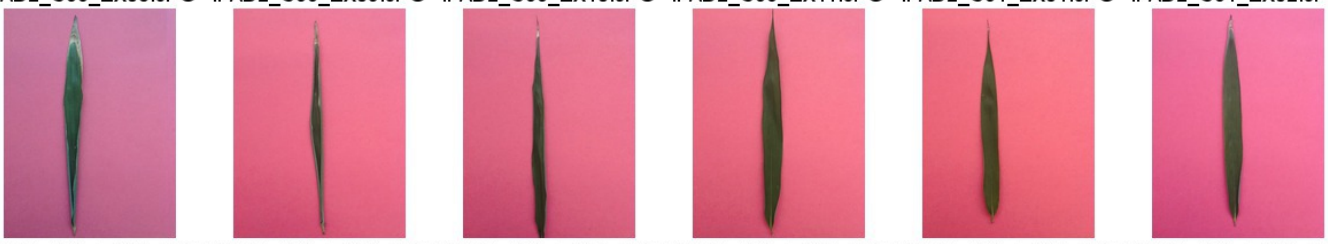

'iPAD2_C34_EX03.JPG' 'iPAD2_C34_EX04.JPG' 'iPAD2_C34_EX05.JPG' 'iPAD2_C34_EX06.JPG' 'iPAD2_C34_EX07.JPG' 'iPAD2_C34_EX08.JPG'

'iPAD2_C34_EX09.JPG' 'iPAD2_C34_EX10.JPG' 'iPAD2_C34_EX11.JPG' 'iPAD2_C35_EX01.JPG' 'iPAD2_C35_EX02.JPG' 'iPAD2_C35_EX03.JPG'

'iPAD2_C35_EX04.JPG' 'iPAD2_C35_EX05.JPG' 'iPAD2_C35_EX06.JPG' 'iPAD2_C35_EX07.JPG' 'iPAD2_C35_EX08.JPG' 'iPAD2_C35_EX09.JPG'

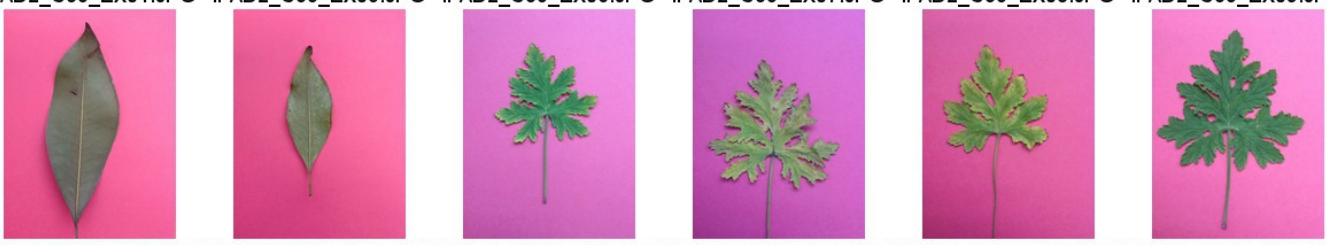

'iPAD2_C35_EX10.JPG' 'iPAD2_C35_EX11.JPG' 'iPAD2_C36_EX01.JPG' 'iPAD2_C36_EX02.JPG' 'iPAD2_C36_EX03.JPG' 'iPAD2_C36_EX04.JPG'

'iPAD2_C36_EX05.JPG' 'iPAD2_C36_EX06.JPG' 'iPAD2_C36_EX07.JPG' 'iPAD2_C36_EX08.JPG' 'iPAD2_C36_EX09.JPG' 'iPAD2_C36_EX10.JPG'

'iPAD2_C37_EX01.JPG' 'iPAD2_C37_EX02.JPG' 'iPAD2_C37_EX03.JPG' 'iPAD2_C37_EX04.JPG' 'iPAD2_C37_EX05.JPG' 'iPAD2_C37_EX06.JPG'

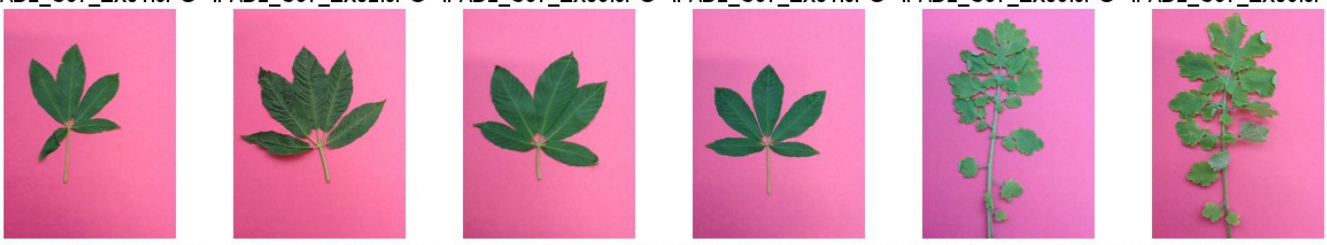

'iPAD2_C37_EX07.JPG' 'iPAD2_C37_EX08.JPG' 'iPAD2_C37_EX09.JPG' 'iPAD2_C37_EX10.JPG' 'iPAD2_C38_EX01.JPG' 'iPAD2_C38_EX02.JPG'

'iPAD2_C38_EX03.JPG' 'iPAD2_C38_EX04.JPG' 'iPAD2_C38_EX05.JPG' 'iPAD2_C38_EX06.JPG' 'iPAD2_C38_EX07.JPG' 'iPAD2_C38_EX08.JPG'

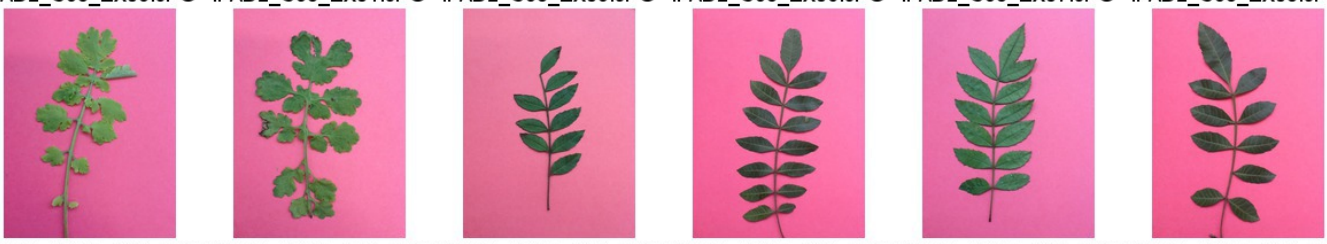

'iPAD2_C38_EX09.JPG' 'iPAD2_C38_EX10.JPG' 'iPAD2_C39_EX01.JPG' 'iPAD2_C39_EX02.JPG' 'iPAD2_C39_EX03.JPG' 'iPAD2_C39_EX04.JPG'

'iPAD2_C39_EX05.JPG' 'iPAD2_C39_EX06.JPG' 'iPAD2_C39_EX07.JPG' 'iPAD2_C39_EX08.JPG' 'iPAD2_C39_EX09.JPG' 'iPAD2_C39_EX10.JPG'


'iPAD2_C40_EX01.JPG'

'iPAD2_C40_EX02.JPG'

'iPAD2_C40_EX03.JPG'

'iPAD2_C40_EX04.JPG'
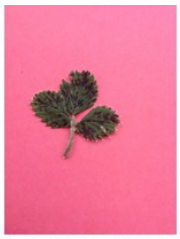
'iPAD2_C40_EX05.JPG'

'iPAD2_C40_EX06.JPG'

'iPAD2_C40_EX07.JPG'

'iPAD2_C40_EX08.JPG'

'iPAD2_C40_EX09.JPG'

'iPAD2_C40_EX10.JPG'

'iPAD2_C40_EX11.JPG'